2015

Mammary Glands Possess Intrinsic Molecular Laterality and Respond Left-Right Differently to Genetic and Pharmacological Manipulation

Jacqulyne Michelle Ponville-Robichaux
Medical University of South Carolina

Mammary Glands Possess Intrinsic Molecular Laterality and Respond Left-Right Differently to Genetic and Pharmacological Manipulation

by

Jacqulyne Michelle Ponville Robichaux

A dissertation submitted to the faculty of the Medical University of South Carolina in partial fulfillment of the requirements for the degree of Doctor of Philosophy in the College of Graduate Studies

Department of Regenerative Medicine and Cell Biology

2015

Approved by:

Chairman, Advisory Committee — Ann F. Ramsdell

_____

Advisory Committee — Steven W. Kubalak

_____

Carola A. Neumann

_____

Bryan P. Toole

_____

Dennis K. Watson

_____

ABSTRACT

JACQULYNE PONVILLE ROBICHAUX. Mammary Glands Possess Intrinsic Molecular Laterality and Respond Left-Right Differently to Genetic and Pharmacological Manipulation. (Under the direction of Ann Ramsdell)

More tumors form in the left (L) breast and tumors in the right (R) breast may be more aggressive. These epidemiological findings suggest L-R differences in overall tumor biology depending on the side of tumor origin, leading to the hypothesis that **mammary glands are L-R different and have discordant responses to neoplastic risk factors**. Here we show that normal mammary glands are molecularly L-R different, and have more mammary stem cells (MaSCs) in the L thoracic mammary gland (TMG). In addition, MaSCs from the L and R TMGs are molecularly and functionally different *in vitro* and *in vivo*. MaSCs respond to ErbB2 and EGFR inhibition via Lapatinib treatment asymmetrically. L-side MaSCs are inhibited by Lapatinib whereas R-side MaSCs increase in self-renewal with Lapatinib treatment. MMTV-Neu$^{Tg/Tg}$ mice overexpress the oncogene Neu also known as ErbB2 or HER2 and model HER2+ breast cancer. MMTV-Neu$^{Tg/Tg}$ mouse TMGs respond L-R discordantly to oncogene overexpression resulting in asymmetric ductal network formation and discordant gene regulation. Furthermore, MaSCs are increased asymmetrically enhancing L-side enrichment of MaSCs, and MaSC *in vitro* function was asynchronously effected. Additionally, when gene expression is inverted in the MMTV-Neu$^{Tg/Tg}$ model, MaSC *in vitro* growth, self-renewal, and response to Lapatinib is also inverted. Inguinal mammary glands (IMGs) of the MMTV-Neu$^{Tg/Tg}$ model show delayed molecular laterality and are less sensitive to oncogene over-expression. When WT mice are

exposed to estrogen (E2) neonatally, E2 induces asymmetric ductal morphogenesis, asymmetrically reduces luminal cell differentiation, and induces an asymmetric increase in MaSCs in TMGs. IMGs of E2 treated mice have no detectable L-R differences in morphology, suggesting IMGs are not as sensitive to early E2 exposure. Lastly, L-R differences in TMG development are shown to have an embryonic origin. RXRα$^{+/-}$ mice with altered embryonic development have asymmetric TMG development but not IMG development. Taken together these data show that L-R differences in TMGs originate embryonically, TMGs are lateralized organs that respond to stimulus L-R differently, and TMGs are more sensitive to perturbation than IMGs. These L-R differences in MaSC populations during normal development allow for L-R different responses to neoplasia, as well as correlate with L-R differences in patient outcome and response to therapy.

TABLE OF CONTENTS

LIST OF TABLES AND FIGURES

Chapter 1

Chapter 2

Chapter 3.1

Chapter 3.2

Chapter 4

Chapter 5

Chapter 6

List of Abbreviations

Aldh3a1	Aldehyde dehydrogenase 3 family, member A1
A-P	Anterior-posterior
BPA	Bisphenol A
CD24	Cluster of differentiation 24 or heat stable antigen
CD29	Integrin beta-1
CD49b	Cluster of differentiation 49b
CD49f	Integrin alpha-6
Ct value	Cycle threshold value
D	Fractal dimension
DES	Diethylstilbestrol
DKK1	Dickkopf-related protein 1
DLC	Differentiated luminal Cell
DMSO	Dimethyl Sulfoxide
DNA	Deoxyribonucleic acid
E	Embryonic day
E2	17-β estradiol
ECM	Extracellular matrix
EGF	Epidermal growth factor
EGFR	Epidermal growth factor receptor
Elf-5	Ets domain transcription factor -5
EpCAm	Epithelial cell adhesion molecule
ER+ LP	Estrogen receptor positive luminal progenitor
ERa	Estrogen receptor alpha
ErbB2	v-erb-b2 avian erythroblastic leukemia viral oncogene homolog
ER-LP	Estrogen receptor negative luminal progenitor
FACS	Fluorescence-activated cell sorting
FGF	Fibroblast growth factor
FoxM1	Forkhead box protein M1
GAPDH	Glyceraldehyde 3-phosphate dehydrogenase
Gata3	Trans-acting T-cell-specific transcription factor
GH	Growth hormone
GPRc5d	G-protein coupled receptor family C group 5 member D
Hb-EGF	Heparin binding - epidermal growth factor
HER2-	human epidermal growth factor receptor negative
Her2+	human epidermal growth factor receptor positive
IGF	Insulin like growth factor
IMG	Inguinal Mammary gland
IOD	Integrated optical density
IOD/A	Integrated optical density / Area
K14	Cytokeratin 14

K5	Cytokeratin 5
K8/18	Cytokeratin 8/18
L	Left
Lef1	Lymphoid enhancer-binding factor 1
LP	Luminal Progenitor
MaSC	Mammary stem cell
MMTV	Mouse mammary tumor virus
mRNA	Messenger ribonucleic acid
Neu	Proto-oncogene form of Receptor tyrosine-protein kinase erbB-2
P63	Transformation-related protein 63
PCR	Polymerase chain reaction
Pitx2	Paired like homeodomain 2
PR	Progesterone receptor
R	Right
RA	Retinoic acid
RANK-L	Receptor activator of nuclear factor kappa-B ligand
RNA	Ribonucleic acid
ROI	Region of Interest
RT-PCR	Reverse transcriptase - polymerase chain reaction
RXRα	Retinoid X receptor alpha
Sca-1	Stem-cell antigen-1
SEM	Standard error of the mean
SMA	Smooth muscle actin
Stmn1	Stathmin-1
Tbx3	T-box transcription factor-3
TEBs	Terminal end buds
TMG	Thoracic mammary gland
WNT	Wingless-type MMTV integration site family
WT	Wild type

ACKNOWLEDGEMENTS

There are so many people who have played a part in getting me through graduate school, but my grandmother was the one who always knew I'd "be a doctor so I could take care of her". She may be gone, but she was right, I'm studying breast cancer to help those who come after her.

I want to thank my family who didn't question why or feel resentment when I left at such an inconvenient time to pursue my PhD. To my mom who has listened to probably every presentation I've ever had to give in grad school, my dad who taught me the real meaning of never giving up when things seem impossible, my sister who showed me it's never too late pursue education, and my brother who picked up the slack when I couldn't be there and for always knowing how to make me laugh when I need it. Also to my awesome in-laws, thanks for understanding when I took your son half-way across the country and for always being so supportive.

I want to thank my mentor, Dr. Ann Ramsdell, for her guidance and for always believing in me when sometimes I didn't. Thanks for letting me learn how fun science can be even in the face of difficulties. You taught me through example not only how to ask great questions and always question status quo, but also how to not let things knock me down. To my committee thanks for guiding me through a great project, reining me in when it was necessary, and for being a sounding board when things were tough.

I want to thank the non-committee faculty members who have also been there for me as a support system along the way. Dr. Joe Blumer, thanks for

understanding your grad student came with an add-on, always allowing me to work in your lab when I just needed to find some quiet, and for always being so supportive. Dr. Jen Isaacs, thanks for always checking in that I'm on track and that things are okay. Dr. Adam Soloff, thanks for making FACS fun and letting me vent when grad school was trying. Also, I'd like to thank Dr. Steve Ethier for allowing me to work in his space for the last six months and the many lab members of the Ethier group who were there when I needed help with things.

To my Charleston friends, thanks for being a family for me when I was so desperately home sick. You've gotten me through this more than you know.

Last, but definitely not least, I want to thank my husband and classmate, (almost) Dr. William Robichaux, for his support through grad school and what has been the most trying part of our lives. You have been my study partner, my sounding board, my harshest critic, my greatest supporter, and my sparring partner when I really needed it. I guess this is the last time we get to graduate from somewhere together but they always say the third time is the best. I'm so proud of your accomplishments, and I'm pretty sure if not for you I'd have never made it through this. Words can't express how grateful I am to have you by my side through this ride. Just remember I would go with you anywhere, and I think it's time for our next adventure.

CHAPTER ONE

REVIEW OF LITERATURE, SPECIFIC AIMS, AND SIGNIFICANCE

REVIEW OF LITERATURE

Mammary Gland Development: Embryonic Through Lactation

Mammary gland development is unique because mammary glands undergo several phases of development throughout the lifespan of the organism, with the majority of development being post-natal. In addition, mammary gland development is not complete until pregnancy and lactation, which means that for some, the organ never reaches full developmental potential. Murine mammary gland development closely models human mammary gland development with few species specific differences in development (Veltmaat, Mailleux et al. 2003). The most obvious species specific difference between human and murine mammary gland development is that mice have 5 pairs of mammary glands. These glands are bilaterally paired and spaced along the anterior to posterior (A-P) axis (Figure 1). This section will review in detail each of the stages of mammary gland development: embryonic development, pubescent development, pregnancy and lactation, and, briefly, involution, focusing on murine and human development.

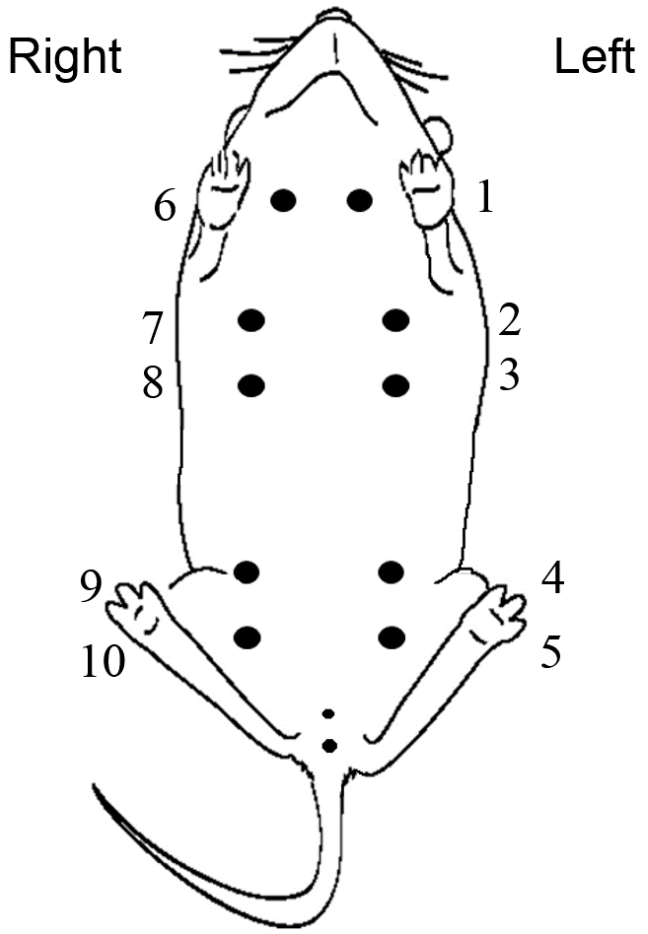

Figure 1. Schematic of Anatomical Location of Mouse Mammary Glands. The 5 pairs of mammary glands are bilaterally paired and spaced along the anterior to posterior (A-P) axis numbered 1-10 left to right and anteriorly to posteriorly. Glands 1 and 6 are cervical mammary glands, glands 2/7 and 3/8 are thoracic mammary glands (TMGs), and glands 4/8 and 5/10 are inguinal mammary glands (IMGs).

Embryonic development

Embryonic development of the mammary glands exists in several steps with slight variations across species. The first step of embryonic development of the mammary gland is hypothesized to be the formation of the mammary line or milk line (Howard and Gusterson 2000). The mammary line has been observed by scanning electron microscope (SEM) in rabbit, rat, pig, cat and human embryos, but reports have not established a clear observation of the mammary line in mouse embryos although reports show molecular hints of a mammary line also existing in mice (Howard and Gusterson 2000, Veltmaat, Van Veelen et al. 2004, Howard 2012). Formation of the mammary line initiates about embryonic day 10.5 (E10.5) – E11.0 in mice and is located between the fore and hind limbs (Veltmaat, Mailleux et al. 2003, Howard 2012). The bilateral structures span the location of the future mammary glands running along the A-P axis and appear to be a raised line of epidermal cells (Howard and Gusterson 2000, Veltmaat, Mailleux et al. 2003, Veltmaat, Van Veelen et al. 2004, Howard 2012).

Although the mammary lines exist as the first structures in the anatomical location of the mammary glands and exist before further development, the mammary placodes, the structures from which mammary glands derive, may not actually be derived directly from the mammary line. Mammary placodes do not arise simultaneously or in order along the A-P axis, but instead glands 3 and 8 form, then glands 4 and 9, then glands 1 and 6 as well as 5 and 10, and lastly, glands 2 and 7 form (Mailleux, Spencer-Dene et al. 2002, Veltmaat, Mailleux et al. 2003, Veltmaat, Van Veelen et al. 2004, Veltmaat, Ramsdell et al. 2013).

Additionally, mammary placode induction appears to begin before the completion of the mammary line overlapping on E11.0 and continuing to E11.5, suggesting the mammary line may not actually be directly involved in mammary placode induction (Veltmaat, Van Veelen et al. 2004). The mammary placodes are oblong shaped layered structures consisting of epithelial cells rising above the ectoderm (Veltmaat, Mailleux et al. 2003, Howard 2012).Over the next 3 days (E12.5 - E14.5), the placode increases in size through what is hypothesized to be cell migration, with only limited proliferation (Balinsky 1950, Propper and Gomot 1967, Propper 1978, Howard 2012). Unlike human mammary gland development, at this time (approximately E13.0-14.5), the murine male mammary gland will undergo an androgen dependent breakdown of the mammary rudiment (Kratochwil 1969, Kratochwil 1977, Durnberger and Kratochwil 1980, Heuberger, Fitzka et al. 1982). At E13.5 the female mammary gland will continue development forming a partially committed and specified mammary mesenchyme that is derived from the dermal mesenchyme and surrounds the mammary placode (Kratochwil 1969, Sakakura, Nishizuka et al. 1976, Sakakura, Sakagami et al. 1979, Durnberger and Kratochwil 1980, Chiquet-Ehrismann, Mackie et al. 1986, Inaguma, Kusakabe et al. 1988). At E13.5 - 14.5, the developing mammary placode invaginates into the surrounding mammary and dermal mesenchyme and is no longer a raised epithelial structure, but now is beginning the formation of the primary mammary rudiment (Veltmaat, Mailleux et al. 2003). Additionally, at E14.5, the first signs of a mammary fat pad arise: pre-adipocytes, vasculature, and nerve cells accumulate at the most distal

part of the invaginating mammary rudiment (Sakakura, Sakagami et al. 1982, Sakakura, Kusano et al. 1987, Sakakura 1991).

In the next step of mammary gland development, E15.5, the fat pad becomes less compact due to pre-adipocyte differentiation; additionally, the vasculature forms small capillary networks among differentiating fat cells (Sakakura, Sakagami et al. 1982, Sakakura, Kusano et al. 1987, Sakakura 1991). At E16.5, the invaginated mammary epithelium begins the first rounds of rapid proliferation and ductal morphogenesis, infiltrating the developing fat pad at the distal end, and growing to a few bifurcated branches forming the primary mammary duct or rudiment (Sakakura, Kusano et al. 1987, Sakakura 1991, Veltmaat, Ramsdell et al. 2013). After formation of the mammary duct/rudiment, the gland will only grow isometrically with the organism until puberty. At the proximal end of the mammary rudiment, early nipple formation initiates with epidermal and keratinized cells migrating to form a funnel shaped depression called the nipple sheath (Sakakura, Kusano et al. 1987, Veltmaat, Mailleux et al. 2003). At E18.5, only days before birth, the epidermis from the nipple sheath will rise up from the proximal end of the mammary rudiment to form the nipple anlage, the last step of embryonic mammogenesis (Sakakura, Kusano et al. 1987). A schematic of embryonic development can be seen in Figure 2.

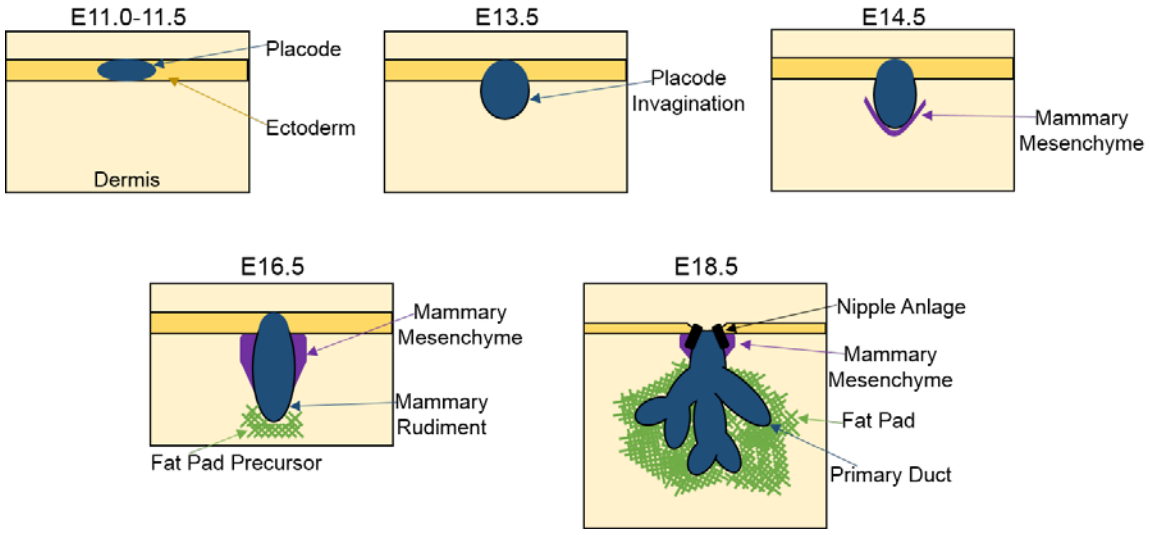

Figure 2. Schematic of Embryonic Development Timeline. Placode induction takes place at E11.0-11.5. At E13.5 the placode invaginates into the dermal mesenchyme. The mammary mesenchyme can be first seen at E14.5. At E16.5 the primary mammary rudiment forms and begins to undergo ductal elongation, and by E18.5 forms the primary duct. Lastly, at E18.5 the nipple anlage can be seen.

Molecular patterning of embryonic mammogenesis

Throughout embryonic mammogenesis, molecular patterning is responsible for not only the initiation of the gland, but also for the position of each of the glands both left and right as well as anteriorly and posteriorly. The complete molecular mechanism of mammary gland induction is not entirely known but begins around the formation of the milk line in mice. Using wingless-type mouse mammary tumor virus integration site (WNT) signaling reporter mice (DasGupta and Fuchs 1999), the mouse mammary line can be seen to form at E10.5, and can be eliminated by the WNT inhibitor, Dickkopf-related protein 1 (DKK1), showing the necessity of WNT signaling for the formation of the mammary line (Chu, Hens et al. 2004, Veltmaat, Van Veelen et al. 2004, Hens and Wysolmerski 2005). Cells reporting WNT signaling migrate and merge at each of the anatomical locations of future mammary gland development forming the placodes (Veltmaat, Mailleux et al. 2003, Hens and Wysolmerski 2005). WNT signaling (specifically Wnt2b and Wnt16) was shown to be necessary and sufficient for inducing placode formation by Chu et al. (Chu, Hens et al. 2004). Briefly, when embryos were cultured in the presence of WNT signaling inducers, placode induction was enhanced; in addition, when embryos were cultured with DKK1 or DKK1 was transgenically expressed, mammary gland development was completely inhibited (Chu, Hens et al. 2004). In addition to WNT signaling, T-Box transcription factor 3 (Tbx3) is required for mammary pairs 1, 3, 4, and 5, but not mammary pair 2 (Davenport, Jerome-Majewska et al. 2003, Eblaghie, Song et al. 2004). However, other than its mesenchymal expression, little is known about the role of TBX2/3 during mammary

gland development other than it is hypothesized to be the link between retinoic acid and Lef1 induction (Cho, Kwon et al. 2012).

In addition to WNT and Tbx signaling, Fibroblast Growth Factor (FGF) family signaling is essential in mammary placode induction for four out of five mammary pairs (Mailleux, Spencer-Dene et al. 2002, Veltmaat, Relaix et al. 2006). Knockout of Fgf10 and Fgf2b results in complete inhibition of growth for mammary pairs 1, 2, 3, and 5 whereas inguinal mammary pair 4 develops normally, suggesting a Fgf dependent mechanism of placode induction for all pairs of mammary glands except pair 4 (Mailleux, Spencer-Dene et al. 2002). This evidence suggests that the use of mammary pair number 4 for experimental analysis may be flawed, since human mammary glands exist in the thoracic cavity and would be hypothesized to have an Fgf dependent induction. In addition, mammary placode 3, the first pair of mammary glands to form, requires somitic Fgf10 signaling from the thoracic somites. At E10.5, in the thoracic cavity, somites 17-18 which are located beneath mammary glands 3 and 8 express Fgf10; however, by E11.0, the time of mammary pair 3 initiation, somites 11-24 express Fgf10 (Veltmaat, Relaix et al. 2006). Mammary pairs 1, 2 and 5 receive Fgf10 signaling from older somites at E11.25 where the Fgf10 gradient extends to all 45 somites (Veltmaat, Relaix et al. 2006). This again suggests that the mammary gland pair number 3 within the thoracic cavity requires accurate somitic gradients of Fgf signaling for proper spatial arrangement. Additionally, mammary gland pair 3 is more sensitive to perturbations and reduction of somitic Fgf10 compared to pairs 1, 2, and 5 (Mailleux, Spencer-Dene et al. 2002, Veltmaat, Relaix et al. 2006).

Due to the anatomical location of mammary pair 3, and the strong dependence of mammary pair 3 on somitic signals, we hypothesize that mammary pair 3, and not mammary pair 4, more closely models human mammary gland development and therefore will be the focus of our studies.

In addition to A-P differences in mammary gland development, L-R differences are hypothesized to occur. Mammary line and placode induction appear to be enhanced on the left side of the embryo (Veltmaat, Ramsdell et al. 2013), and underlying somites contributing Fgf10 for mammary induction are molecularly L-R different (Golding, Partridge et al. 2004, Golding, Tsoni et al. 2004). Specifically, left side somites have elevated heparin-binding Epidermal Growth Factor-like growth factor (hb-EGF) (Golding, Tsoni et al. 2004), during the window of mammary glands 3 and 8 initiation (Veltmaat, Ramsdell et al. 2013). Furthermore, hb-EGF is a ligand for erythroblastic leukemia viral oncogene (ErbB) family members 1 and 4 (Olayioye, Neve et al. 2000). ErbB family members are required during distinct stages of mammary gland development (Troyer and Lee 2001) and often overexpressed in breast cancer (Korkaya, Paulson et al. 2008, McDermott and Wicha 2010, Reichman, Altekruse et al. 2010, Ithimakin, Day et al. 2013). Moreover, retinoic acid (RA) signaling is essential to proper spatial arrangement of the somites (Vermot, Gallego Llamas et al. 2005, Brend and Holley 2009, Vilhais-Neto, Maruhashi et al. 2010), as well as mammary gland development (Cohn, Ossowski et al. 2010, Cho, Kwon et al. 2012). Under normal conditions, RA signaling results in bilaterally paired somite formation, however, altered RA signaling leads to asynchronous somite formation of the somites

underlying mammary placode pairs 2 and 3 (Mailleux, Spencer-Dene et al. 2002, Veltmaat, Mailleux et al. 2003, Kawakami, Raya et al. 2005, Vermot, Gallego Llamas et al. 2005, Veltmaat, Relaix et al. 2006, Vilhais-Neto, Maruhashi et al. 2010, Cho, Kwon et al. 2012). Therefore, if mammary gland laterality originates from somitic signals during mammary placode formation, altered RA signaling will result in asymmetric somites, and therefore, asymmetric mammary gland morphogenesis. Thus we hypothesize that *mammary glands are lateralized structures with L-R differences originating embryonically*. This hypothesis will be tested in chapter 5.

Pubescent Development

The most extensive stage of mammary gland ductal elongation occurs during pubescent development. Early pubescent development in mice begins at approximately 28 days of age (Colby and Vandenberg 1974) with the first estrous cycle occurring at approximately 30-35 days of age. Pubescent ductal elongation initiates when ovarian hormones and growth factors signal from the adipocytes, fibroblasts, and immune cells comprising the tissue stroma in a paracrine fashion to the surrounding duct to initiate growth and differentiation of the epithelial cells within the primary duct (Lu and Werb 2008, Polyak and Kalluri 2010) . In addition, complicated paracrine cross-talk exists between mammary epithelial sub-populations to regulate hormonally driven epithelial cell differentiation during mammary gland development (Joshi, Jackson et al. 2010, Lydon 2010, Aupperlee, Leipprandt et al. 2013). During puberty, the primary duct or rudiment undergoes

rapid proliferation and differentiation, and, by the end of puberty, approximately 8 weeks of age, the ductal network branches into a web-like structure encompassing the entire fat pad.

There are two distinct epithelial cell types that exist within the mammary ductal network: luminal cells and basal cells. Each cell type contains subpopulations of cells that vary in the state of differentiation. The luminal compartment is comprised of cytokeratin 8/18 (K8/18) positive cells, consisting of estrogen receptor alpha (ERα) positive luminal progenitor cells (ER+ LPs), ERα negative luminal progenitor cells (ER- LPs), and differentiated luminal cells (DLCs) (Kouros-Mehr, Slorach et al. 2006, Asselin-Labat, Vaillant et al. 2008, Visvader and Smith 2011, Carr, Kiefer et al. 2012, Shehata, Teschendorff et al. 2012, Rios, Fu et al. 2014). The basal compartment is comprised of K14 positive cells consisting of mammary stem cells (MaSCs), a hypothesized myoepithelial progenitor cell, and differentiated myoepithelial cells (Guo, Keckesova et al. 2012, Zhao, Malhotra et al. 2012, Rios, Fu et al. 2014). The mammary ducts are organized with basal cells encapsulating a single layer of luminal cells surrounding the mammary lumen (Figure 3). In between the luminal and basal layers as well as at the end of ducts within the terminal end buds, stem and progenitor cells are enriched (Kenney, Smith et al. 2001, Booth, Boulanger et al. 2008, Park, Raafat et al. 2013, Sale, Lafkas et al. 2013, Rios, Fu et al. 2014) (Figure 3). Terminal end buds (TEBs) are club-shaped structures at the leading edge of the ductal network where there is increased proliferation and ductal elongation (Richert, Schwertfeger et al. 2000, Silberstein 2001).

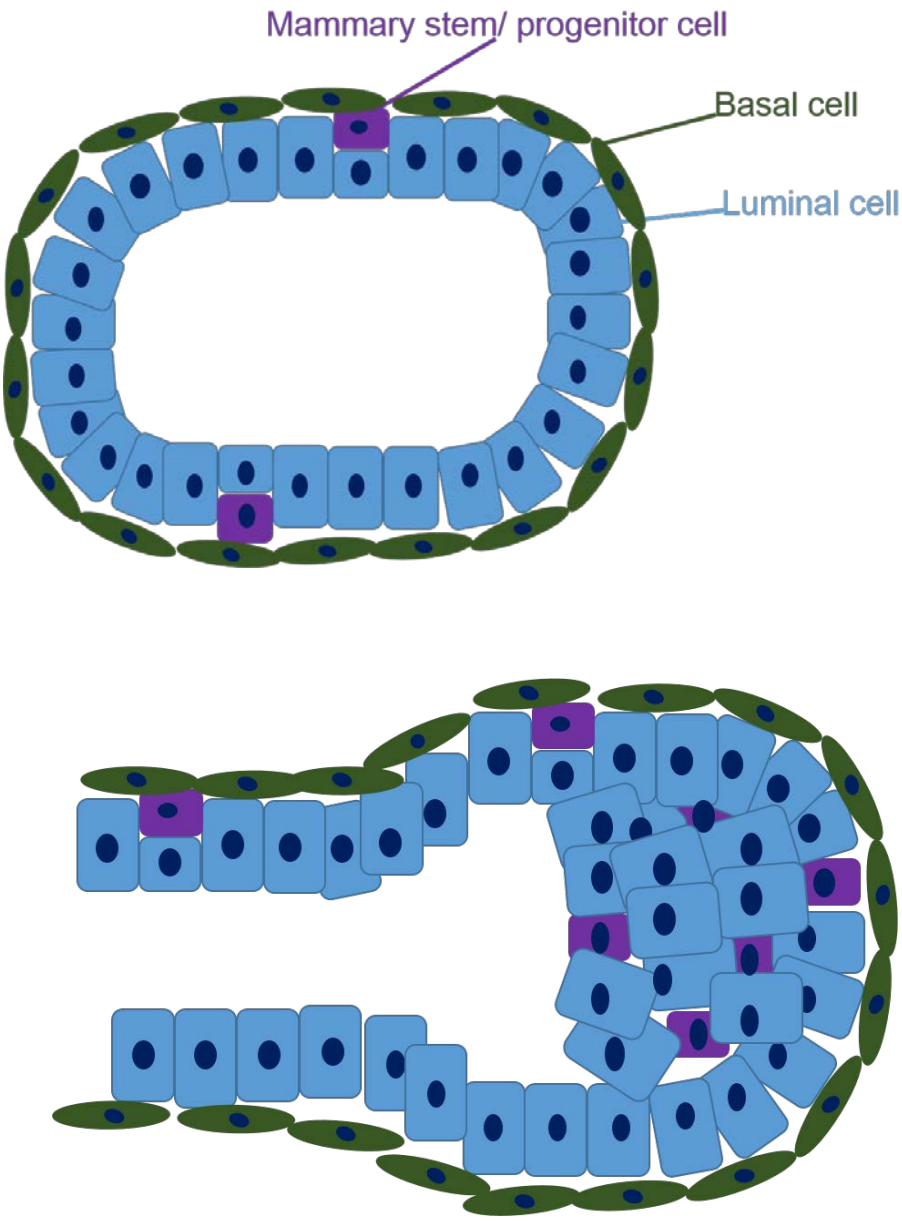

Figure 3. Schematic of Cross-Section of Mammary Duct and terminal end bud. The mammary ducts are organized with basal cells surrounding luminal cells around the mammary lumen. In between the luminal and basal layers as well as at the end of ducts, within the terminal end buds, stem and progenitor cells are enriched. Figure adapted from Tiede and Kang 2011.

Hormones and Pubescent Mammary Ductal Mammogenesis

Ovarian hormones, estrogen and progesterone, as well as other hormones such as growth hormone (GH) and its downstream target insulin-like growth factor (IGF), play an essential role during pubescent ductal mammogenesis. Estrogen and progesterone have been shown to regulate mammary stem cell number and cell differentiation regulating the size of the ductal network (Asselin-Labat, Vaillant et al. 2010, Joshi, Jackson et al. 2010, Diaz-Guerra, Lillo et al. 2012). IGF has been shown to increase cell proliferation and reduce apoptosis within TEBs and works concurrently with estrogen and progesterone to increase the number of TEBs (Ruan, Newman et al. 1992, Bonnette and Hadsell 2001, Stull, Richert et al. 2002, Lee, Zhang et al. 2003, Stull, Rowzee et al. 2004).

The most important hormone during pubertal mammary ductal morphogenesis is estrogen, whereas progesterone has been shown to effect ductal morphogenesis to a lesser extent (Brisken, Park et al. 1998, Asselin-Labat, Vaillant et al. 2010, Aupperlee, Leipprandt et al. 2013). Ovariectomy or genetic knockout of ERα results in ablation of pubescent ductal elongation (Feng, Manka et al. 2007). In addition, estrogen rescues development of the mammary glands in ovariectomized mice (Daniel, Silberstein et al. 1987). ERα is expressed in the stroma but not in all mammary epithelial cell types. ERα+ LPs, and DLCs express ERα, but MaSCs, ERα- LPs, and myoepithelial cells do not express ERα (Kouros-Mehr, Slorach et al. 2006, Asselin-Labat, Vaillant et al. 2008, Visvader and Smith 2011, Carr, Kiefer et al. 2012, Shehata, Teschendorff et al. 2012, Rios, Fu et al. 2014). Although the major role of progesterone action occurs during pregnancy,

progesterone has been shown to increase TEB formation and increase proliferation throughout the ducts through amphiregulin signaling during puberty (Aupperlee, Leipprandt et al. 2013). Interestingly, progesterone receptor knockout mice undergo ductal morphogenesis at puberty but fail to undergo side branching and alveolargenesis during pregnancy (Lydon, DeMayo et al. 1995, Brisken, Park et al. 1998); however, both estrogen and progesterone have been shown to play a role in regulation of MaSC proliferation and differentiation (Asselin-Labat, Vaillant et al. 2010, Joshi, Jackson et al. 2010, Simoes, Piva et al. 2011). Mechanistically, the way in which estrogen signals to ERα- MaSCs is unclear, but estrogen has been shown to expand breast cancer stem-like cells that are ERα- through the FGF/Tbx3 pathway (Fillmore, Gupta et al. 2010). In addition, progesterone has been shown to signal to progesterone receptor negative (PR-) MaSCs via PR+ luminal cells releasing Receptor activator of nuclear factor kappa-B ligand (RANK-L) which stimulates MaSCs (Asselin-Labat, Vaillant et al. 2010, Joshi, Jackson et al. 2010).

Puberty as a critical time point for determining future breast cancer risks

Both estrogen and progesterone signaling during puberty play an essential role in setting up the mammary gland for adulthood through mechanisms that closely resemble tumorigenesis (Mori, Bern et al. 1976, Warner 1976, Hilakivi-Clarke, Cho et al. 1997, Fenton 2006, Incassati, Chandramouli et al. 2010, Biro and Deardorff 2013). Perinatal exposure to estrogen or estrogen mimetics like diethylstilbestrol (DES) or Bisphenol A (BPA) results in increased tumor formation

in mice (Walker 1984, Lopez, Ogren et al. 1988, Walker 1990, Hilakivi-Clarke, Onojafe et al. 1996, Markey, Luque et al. 2001). These changes to normal ductal morphogenesis induced by early estrogen exposures were observed as early as 4 weeks of age, the beginning of puberty (Hilakivi-Clarke, Cho et al. 1997, Markey, Luque et al. 2001). In addition, a recent study shows that not only does early menarche in humans increases later breast cancer risk, but the timing of several pubescent developmental time points correlates with increased breast cancer risk (Bodicoat, Schoemaker et al. 2014). These studies and others show that breast cancer risks may be determined as early as puberty.

In addition to determining future breast cancer risks, puberty may also be a time point of vulnerability to outside perturbations due to the rapid ductal expansion during puberty. Reactivation of the hypothalamic-pituitary-gonadal axis takes place to allow breast development as well as the initiation of fertility (Biro and Deardorff 2013). Rapid expansion of MaSCs, progenitors, and differentiated cells leave glands susceptible to environmental influences (Okasha, McCarron et al. 2003). In addition, studies of early estrogen exposure show that mice exposed to exogenous estrogens in utero become more sensitive to endogenous estrogen signaling during puberty (Wadia, Vandenberg et al. 2007). Both the increased vulnerability, and early determination of future breast cancer risk make puberty a potential time point for early intervention and breast cancer prevention. However, very few preventative methods exist, and development of early intervention is not possible without exhaustive knowledge of normal development.

Pregnancy, Lactation, and Involution

Lastly, a mammary gland has not fully undergone complete development until pregnancy and subsequent lactation. During pregnancy, mammary glands undergo terminal differentiation in the remaining TEBs to form secretory lobuloalveolar units that later fill with milk (Oakes, Hilton et al. 2006). Rapid proliferation and differentiation are initiated by increases in prolactin and progesterone levels (Brisken 2002). If levels of progesterone do not increase, side branching and alveolargenesis do not occur (Lydon, DeMayo et al. 1995, Brisken, Park et al. 1998). Alveolar sacs are surrounded by myoepithelial cells, but unlike the pubescent mammary gland, sections of luminal cells are not be covered by myoepithelial basal cells, but instead have contact with the basement membrane, indicating completing differentiation of the mammary gland (Fata, Werb et al. 2004, Oakes, Hilton et al. 2006). Before parturition, milk and colostrum proteins enter the alveolar lumen (Fata, Werb et al. 2004, Anderson, Rudolph et al. 2007). Milk production reaches maximum at 12-13 days post-partum and continues for 3 to 4 weeks (Anderson, Rudolph et al. 2007). Upon the weaning of pups, lactation ceases and involution begins. Involution takes place in two steps: 1.) apoptosis of the secretory epithelium within alveolar sacs, and 2.) proliferation and remodeling of adipocytes to fill in the space left after removal of the lobulaoalveolar sacs (Watson 2006). The first step of involution is reversible and due to accumulation of milk within the ducts, not systemic hormones (Li, Liu et al. 1997, Marti, Feng et al. 1997) whereas the second step is not reversible until subsequent pregnancy

and is triggered by matrix metalloproteinases (MMPs), phagocytosis, and autophagy (Monks, Rosner et al. 2005, Watson 2006).

Mammary Stem Cells and Cell Differentiation

The National Institutes of Health defines stem cells by two unique properties: 1.) stem cells are unspecialized cells capable of self- renewal even after quiescence, and 2.) stem cells have the ability to become functional and specialized cells within a tissue or organ (National Institutes of Health 2002). MaSCs exist at the top of the mammary epithelial cell hierarchy (Figure 4). The existence of a bona fide MaSC was found in 2006 when Shackleton and colleges were able to reconstruct a functional mammary gland from a single cell (Shackleton, Vaillant et al. 2006). This discovery not only found a single cell that could give rise to both lineages of mammary epithelial cells *in vivo*, but also gave us definitive cell surface markers of MaSCs. A more recent report by Rios and colleges in 2014 showed through lineage tracing experiments *in vivo* the bi-potent MaSC truly does exist and contributes to ductal morphogenesis at puberty and maintenance of the duct throughout adulthood (Rios, Fu et al. 2014). Additionally, a fetal MaSC, that functionally and molecularly differs from the adult MaSC has been identified and has been shown to be able to give rise to both lineages of mammary epithelial cells, have a higher regenerative potential *in vitro* and *in vivo* when transplanted into cleared mammary fat pads, and potentially give rise to a population of adult MaSCs (Spike, Engle et al. 2012, Boras-Granic, Dann et al. 2014). It has become evident through these studies that the pool of mammary stem

cells is both heterogeneous and dynamic depending on the developmental needs of the gland.

The fetal MaSC taken from E18.5 rudiments has been shown to express high levels of heat stable antigen (CD24) and α6 integrin (CD49f), distinct gene expression unique from the adult MaSC including upregulated ErbB family members 2, 3, and 4 (but not ErbB1/EGFR), and a strong reliance on growth factors EGF and FGF (Spike, Engle et al. 2012). Fetal MaSCs stain positive for both the luminal and basal lineages (Spike, Engle et al. 2012, Boras-Granic, Dann et al. 2014). In addition, long-label retaining experiments have shown that a population of fetal MaSCs persist through puberty into adulthood, are responsive to ovarian hormones such as estrogen and progesterone, and are active during times of ductal remodeling such as puberty, pregnancy, and involution (Boras-Granic, Dann et al. 2014). These long lived fetal MaSCs, although only recently discovered, appear to play an essential role in the mammary epithelial cell hierarchy and dynamic developmental capabilities of the mammary gland; however, the fetal MaSC is only a small compartment of the heterogeneous stem cell pool.

The adult MaSC, although better characterized than the fetal MaSC, is not completely understood. Adult MaSCs express $CD24^{med}$ or Epithelial Cell Adhesion Molecule $(EpCAM)^{med}$, and $CD49f^{high}$ or integrin β1 $(CD29)^{high}$ (Smalley, Titley et al. 2005, Smalley 2010, Shehata, Teschendorff et al. 2012, Smalley, Kendrick et al. 2012, Nautiyal, Steel et al. 2013). Adult MaSCs are capable of growing in anchorage independent assays such as the mammosphere assay as well as the

3D matrigel assay (Stingl, Eirew et al. 2006, Shaw, Harrison et al. 2012). Similar to fetal MaSCs, adult MaSCs stain positive for both lineages, and give rise to both luminal and basal cell progenitors (Stingl, Eirew et al. 2006). MaSCs have been shown to respond to ovarian hormones, epidermal growth factor (EGF), FGF, as well as other ligands (Korkaya, Paulson et al. 2008, Asselin-Labat, Vaillant et al. 2010, Fillmore, Gupta et al. 2010, Joshi, Jackson et al. 2010, Simoes, Piva et al. 2011, Spike, Engle et al. 2012). Adult MaSCs have been shown to express EGFR (ErbB1), ErbB2 ErbB3, but not ErbB4. Lineage tracking experiments show that adult MaSCs play an essential role during pubescent ductal morphogenesis, maintenance of the adult duct, pregnancy, and remain after involution (Rios, Fu et al. 2014). At the top of the mammary epithelial cell hierarchy, the fetal and adult MaSCs are long lived and hypothesized to play a role in tumor initiation due to increased risk for accumulation of mutations over time; however, both cell types are essential to the dynamic developmental potential of the gland.

MaSCs give rise to both luminal progenitor cells as well as hypothesized basal progenitor cells (Visvader and Stingl 2014) (Figure 4). Although a basal progenitor cell has yet to be definitively isolated by fluorescence-activated cell sorting (FACS), non-MaSC basal cells have a sub-population of cells with higher regenerative potential *in vitro* and *in vivo* (Shackleton, Vaillant et al. 2006). In addition, Zhao and colleges found an intermediate step between immortalized human stem cells expressing high levels of tumor protein 63 (p63), a basal linage marker, and differentiated myoepithelial cells (Zhao, Malhotra et al. 2012). These hypothesized myoepithelial progenitors express low levels of p63 and moderate

levels of smooth muscle actin (SMA), a marker of differentiated myoepithelial cells (Zhao, Malhotra et al. 2012). The proposed myoepithelial progenitor cell gives rise to the differentiated myoepithelial cell which is characterized by high levels of SMA, K14 and K5 staining (Makarem, Spike et al. 2013). Differentiated myoepithelial cells have many functions including paracrine signaling to luminal cells during ductal morphogenesis during puberty, contraction of myoepithelial cells during lactation driving milk towards the nipple, and secreting proteins needed by the extracellular matrix (ECM) (Sopel 2010). Differentiated myoepithelial cells are not thought to play a major role in invasive mammary tumorigenesis (Sopel 2010, Visvader and Stingl 2014); however, studies show an ability of differentiated myoepithelial cells to convert back to MaSCs which are believed to play a critical role in mammary tumorigenesis (Guo, Keckesova et al. 2012).

The luminal lineage of mammary epithelial cells is more complex and consists of several different types of cells (Figure 4). The luminal lineage is K8 positive and regulated by Notch signaling (Bouras, Pal et al. 2008, Sale, Lafkas et al. 2013). Cell types include the bi-potent luminal progenitor, the ER+ LP, the ER- LP and the differentiated ductal and alveolar cells (Figure 4) (Visvader and Stingl 2014). The ER+ and ER- LP cells have several cell surface markers including $CD24^{high}$, $EpCAM^{high}$, $CD49f^{med}$, and $CD49b^{high}$. The major cell surface antigen difference besides ERα expression, is stem cell antigen-1 (Sca-1), ER+ LPs are Sca-1+ whereas the ER- LP cells are Sca-1- (Shehata, Teschendorff et al. 2012, Visvader and Stingl 2014). Both the ER+ and ER- LP cells express Forkhead box protein-M1 (FoxM1), aldehyde dehydrogenase-1a3 (Aldh1a3), E74-like factor-5

(Elf5); however, ER+ LP cells have a slightly higher in vivo regenerative potential than ER- LP cells (Carr, Kiefer et al. 2012, Shehata, Teschendorff et al. 2012).

FoxM1 and Notch signaling play an essential role in lineage determination for luminal cells (Bouras, Pal et al. 2008, Carr, Kiefer et al. 2012, Chakrabarti, Wei et al. 2012, Sale, Lafkas et al. 2013). Up-regulation of Notch signaling increases MaSC differentiation into LP cells, whereas inhibition of Notch signaling enriches the MaSC pool (Bouras, Pal et al. 2008). Up-regulation of FoxM1 results in an increase in LP cells preventing differentiation into mature luminal cells, whereas inhibition of FoxM1 increases luminal cell differentiation (Carr, Kiefer et al. 2012). FoxM1 prevents differentiation of luminal progenitors through down-regulation of GATA binding protein 3 (GATA-3) (Carr, Kiefer et al. 2012). GATA-3 plays an essential role in the differentiation of LPs, and is most highly enriched during pubescent development (Kouros-Mehr, Slorach et al. 2006, Asselin-Labat, Sutherland et al. 2007). Inhibition of GATA-3 results in a lack of TEB formation and defective ductal morphogenesis during puberty, inhibition of alveolargenesis and lactation during pregnancy, and an increase in LPs (Kouros-Mehr, Slorach et al. 2006, Asselin-Labat, Sutherland et al. 2007). Elf-5 plays an essential role in differentiation of ER- LPs into alveolar cells during pregnancy (Chakrabarti, Wei et al. 2012). Up-regulation of Elf-5 in virgin mice causes an aberrant increase in alveolar differentiation; whereas mice with decreased Elf-5 expression fail to lactate and have defective alveolar differentiation (Oakes, Naylor et al. 2008). Differentiated alveolar cells are CD24+, EpCAM^{high}, Sca-1^{lo}, and CD49b- (Shehata, Teschendorff et al. 2012, Visvader and Stingl 2014). These cells are

responsible for milk production during lactation and are initiated during pregnancy by up-regulation of Elf-5 via RANK-L activation from progesterone signaling (Lee, Gallego-Ortega et al. 2013) and up-regulation of prolactin and Signal Transducer and Activator of Transcription 5a (Stat5a) (Liu, Robinson et al. 1997).

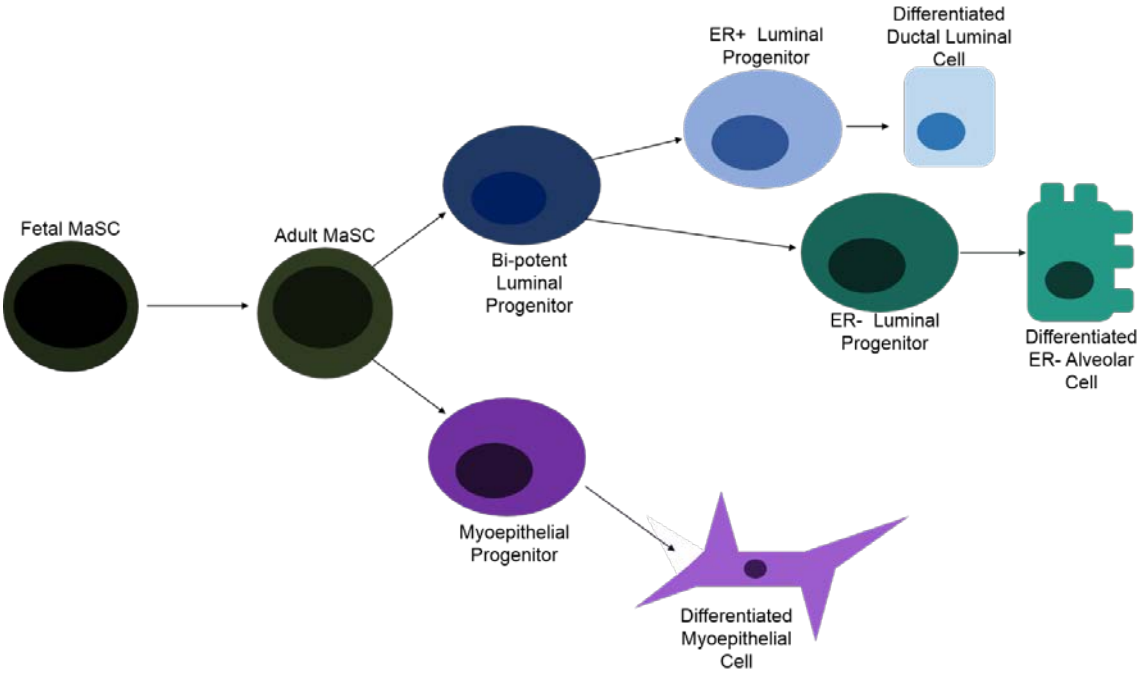

Figure 4. Schematic of Mammary Epithelial Cell Hierarchy. Fetal MaSCs are thought to give rise to adult MaSCs as well as persist into adulthood. Adult MaSCs give rise to both a bi-potent luminal progenitor and a proposed myoepithelial progenitor. The myoepithelial progenitor gives rise to differentiated myoepithelial cells. The bi-potent luminal progenitor gives rise to both an ER+ luminal progenitor and an ER- luminal progenitor. The ER+ luminal progenitor gives rise to the differentiated luminal ductal cell that can be either ER+ or ER-. The ER- luminal progenitor gives rise to ER- alveolar cells during pregnancy (Visvader and Stingl 2014). Figure adapted from Visvader and Stingl 2014.

Mammary Stem Cells, Breast Cancer, and Laterality

Originally, many believed that the heterogeneity of tumors and cancer originated from embryonic remnants that upon reactivation of embryonic processes became teratomas (Sell 2010). Later this theory was revised with the hypothesis that tumors arise from adult stem cells, and normal cell differentiation is disrupted resulting in tumor formation (Sell 2010). However in recent years, the cancer stem cell theory has evolved into a hypothesis separated from the tumor initiating cells, but into a study of the cells that propagate the tumor after the tumor is formed and the search for the tumor initiating cells has become the focus of many labs (Visvader 2011). Mammary stem and progenitor cells play a critical role in breast cancer initiation and progression (Prat and Perou 2009, Regan, Kendrick et al. 2012, Shehata, Teschendorff et al. 2012). However, there is a great debate whether different types of mutations of MaSCs are responsible for variability in mammary tumorigenesis, or if mutations of each subpopulation of stem and progenitor cells gives rise to the various subtypes of breast cancer. Directly testing these two hypotheses has proven difficult, with data suggesting that both hypotheses may indeed be partially correct as it pertains to breast cancer (Clarke, Anderson et al. 2003, Dontu, Al-Hajj et al. 2003, Dontu, El-Ashry et al. 2004, Bouras, Pal et al. 2008, Lim, Vaillant et al. 2009, Prat and Perou 2009, Molyneux, Geyer et al. 2010, Shehata, Teschendorff et al. 2012, Spike, Engle et al. 2012, Makarem, Kannan et al. 2013, Sale, Lafkas et al. 2013, Zvelebil, Oliemuller et al. 2013),

Breast cancer like many cancers is heterogeneous in the types of tumors formed; breast cancers vary cellularlly and molecularly and therefore vary in response to treatments (Prat and Perou 2009, Eroles, Bosch et al. 2012). Breast cancer is broken down into six subtypes: Luminal A, Luminal B, Her2+, basal–like, normal-like, and claudin-low (Eroles, Bosch et al. 2012). Researchers have found that certain molecular pathways enriched in each of these breast cancer subtypes are also enriched in subtypes of mammary epithelium (Bouras, Pal et al. 2008, Lim, Vaillant et al. 2009, Prat and Perou 2009, Molyneux, Geyer et al. 2010, Shehata, Teschendorff et al. 2012, Sale, Lafkas et al. 2013, Zvelebil, Oliemuller et al. 2013), supporting the cell of origin hypothesis in breast cancer. However, others believe that adult stem and/or fetal stem cells are responsible for breast tumors through various acquired mutations accumulated over time, and the heterogeneity of breast cancer is due to heterogeneity of mutations of the adult and/or fetal stem cells (Dontu, Al-Hajj et al. 2003, Dontu, El-Ashry et al. 2004, Spike, Engle et al. 2012, Makarem, Kannan et al. 2013). In support of the MaSC being the tumor initiating cell, discovery of ERα+ stem like cells have been identified and were hypothesized to be the cells that become mutated in steroid hormone positive breast cancers (Zeps, Dawkins et al. 1996, Zeps, Bentel et al. 1999, Alvi, Clayton et al. 2003, Clarke, Anderson et al. 2003, Dontu, El-Ashry et al. 2004). Although these two hypotheses seem to differ greatly, it appears that both hypotheses could contribute to the vast differences seen in patients especially when stem cell heterogeneity is taken into consideration. But only, further investigation into mammary stem cell differentiation throughout development can give us important

insights to the cells responsible for tumor initiation opening a novel window of breast cancer prevention.

In addition to breast cancer heterogeneity within each breast, breast cancer also appears to be lateralized. More tumors form in the left breast (55% L vs. 45% R) (Perkins, Hotes et al. 2004, Roychoudhuri, Putcha et al. 2006, Saleh and Abdeen 2007, Arkoob, Al-Nsour et al. 2010, Wilting and Hagedorn 2011, Fatima, Zaman et al. 2013, Veltmaat, Ramsdell et al. 2013, Zeeneldin, Ramadan et al. 2013). In addition, epidemiological studies have shown that aggressive breast cancer subtypes occur more often in the right breast and right sided tumors metastasize quicker and more frequently (Saleh and Abdeen 2007, Fatima, Zaman et al. 2013, Zeeneldin, Ramadan et al. 2013). Furthermore, these L-R differences may affect overall patient survival; however, due to deficient data sets this relationship requires additional investigation (Hartveit, Tangen et al. 1984, Borisenkov 2001, Roychoudhuri, Putcha et al. 2006, Zeeneldin, Ramadan et al. 2013). These epidemiological findings indicate L-R differences in overall tumor biology depending on the side of origin, suggesting L-R differences in mammary glands from which those tumors arise; however, no previous studies exist to determine the molecular cause of these left-right (L-R) differences in tumor biology or normal development.

SPECIFIC AIMS

We have developed four specific aims to characterize mammary gland development and laterality under both normal conditions and pre-neoplastic conditions. Our aims are: 1.) *Determine if fractal dimension analysis is a sensitive and quantitative approach to determine differences in thoracic mammary glands; 2.) Determine if WT mammary glands are symmetric and the effect of ErbB2 signaling on mammary gland ductal morphogenesis, cell populations, and stem cell self-renewal; 3.) Determine if mammary glands are differentially susceptible to neonatal estrogen exposure; and 4.) Determine if mammary gland laterality originates during embryonic development.*

Currently, no standardized method of quantifying ductal morphogenesis exists in the field of mammary gland biology; therefore, specific aim one will test the hypothesis that fractal dimension analysis is an objective and sensitive method to quantify ductal morphogenesis. To this end, fractal dimension analysis, in combination with conventional morphometric analysis, will be used to quantify pubescent thoracic mammary glands of WT and MMTV-Neu$^{Tg/+}$ mice.

Specific aim two will test the hypothesis that WT mammary glands are lateralized and due to intrinsic L-R differences will have an asymmetric response to changes in ErbB2 signaling. To test this hypothesis morphology, cell signaling, and mammary stem cell populations and self-renewal will be examined in both WT and MMTV-Neu$^{Tg/Tg}$ mammary glands. Fractal dimension and conventional morphometrics will be used to examine L vs. R morphology, microarray and/or RT-

PCR will be used to examine L-R differences in cell signaling, FACS will be used to examine L-R differences in epithelial cell populations, and the mammosphere assay will be used to detect L-R differences in stem-cell self-renewal.

Specific aim three will test the hypothesis that mammary glands respond L-R differently to early neonatal estrogen exposure. To test this hypothesis, a murine model of high dose, neonatal estrogen exposure was generated. Briefly, mice were injected with high dose estrogen for five days after birth, then allowed to reach puberty. At 28 days of age, mice were euthanized, and mammary glands were extracted. To determine if high dose estrogen results in L-R differences, glands will be examined by fractal dimension and conventional morphometrics to survey for L-R changes in morphology, glands will be studied for L-R changes in cell signaling by RT-PCR, and lastly, glands will be examined by long label retaining experiments, FACS, and mammosphere assays to survey for L-R differences in mammary cell populations.

Lastly, specific aim four will test the hypothesis that mammary gland laterality originates embryonically. To test this hypothesis, the Retinoid X Receptor alpha (RXRα) knockout mouse was used. The RXRα mouse has altered RA signaling which may lead to asynchronous somite formation of the somites prior to thoracic mammary gland initiation (Mailleux, Spencer-Dene et al. 2002, Veltmaat, Mailleux et al. 2003, Kawakami, Raya et al. 2005, Vermot, Gallego Llamas et al. 2005, Veltmaat, Relaix et al. 2006, Vilhais-Neto, Maruhashi et al. 2010, Cho, Kwon et al. 2012). Therefore, mammary glands will be examined by fractal dimension and conventional morphometrics to survey for L-R changes in morphology.

SIGNIFICANCE

Currently, no standardized method of quantifying ductal morphogenesis exists in the field of mammary gland biology; therefore, the second chapter will determine an objective and sensitive method to quantify ductal morphogenesis. Fractal dimension analysis is a technique which allows for quantification of differences in complex and irregular shapes, such as the ductal epithelium of a mammary gland. Thus, chapter two will determine if fractal dimension analysis in conjunction with traditional morphogenesis can detect quantifiable differences between normal mammary gland development and the development of mammary glands from a murine model of breast cancer. If sensitive enough, this technique may not only be useful in the field of mammary gland biology, but may also lead to a more sensitive technique for examining mammography increasing early detection and possibly prevention of invasive breast cancer in women.

Higher tumor incidence in the left breast, more aggressive tumors in the right breast and possible L-R differences in survival are virtually unstudied features of breast cancer (Perkins, Hotes et al. 2004, Roychoudhuri, Putcha et al. 2006, Saleh and Abdeen 2007, Arkoob, Al-Nsour et al. 2010, Wilting and Hagedorn 2011, Fatima, Zaman et al. 2013, Veltmaat, Ramsdell et al. 2013, Zeeneldin, Ramadan et al. 2013). These epidemiological findings suggest L-R differences in overall tumor biology depending on the side of origin, suggesting L-R differences in mammary glands from which those tumors arise; however, no previous studies have addressed the question of baseline L-R differences during normal

development. Puberty is a good developmental time-point to probe for L-R differences during development, because the rapid ductal expansion leaves the glands vulnerable to outside perturbations (Warner 1976, Hilakivi-Clarke, Cho et al. 1997, Fenton 2006), as well as mimics the signaling pathways that often become reactivated during early neoplasia (Incassati, Chandramouli et al. 2010). Chapter three will demonstrate that there are L-R differences during normal pubescent development.

HER2/ErbB2/Neu is amplified in 20-30% of breast cancers and is associated with aggressive tumor phenotype and early drug resistance (Korkaya, Paulson et al. 2008, McDermott and Wicha 2010, Reichman, Altekruse et al. 2010, Ithimakin, Day et al. 2013); additionally, a recent study reports HER2 is amplified in the right breast more often (Fatima, Zaman et al. 2013). Furthermore, studies suggest that HER2 increases stem/progenitor cell populations (Ithimakin, Day et al. 2013, Korkaya and Wicha 2013). MMTV-Neu$^{Tg/Tg}$ mice are a well-accepted model of HER2+ breast cancer (Guy, Webster et al. 1992, Muller, Arteaga et al. 1996). Preliminary data reveal that the L and R TMGs from MMTV-Neu$^{Tg/Tg}$ mice, have asymmetric ductal morphogenesis at puberty and that the asymmetry is sustained after puberty is complete. These data suggest that HER2/ErbB2/Neu affect the L and R mammary glands differently resulting L-R different morphology, gene expression, and cell populations. Chapter 3 will demonstrate that ErbB2 signaling effects the L and R mammary glands discordantly both on a morphological and cellular level. Understanding the normally occurring L-R differences and the asymmetric response to the HER2 oncogene will be important

in understanding L-R differences in tumor biology and stem/progenitor cell regulation during breast cancer which is essential to better clinical treatment of breast cancer patients. Additionally, these studies are the first to demonstrate a differential response to a drug used clinically for patients with HER2 positive breast tumors on normal mammary stem cells. Understanding how drugs used in the clinic effect normal mammary tissue is critical in the long-term care of a breast cancer patient. Additionally, an L-R difference in normal tissue to a drug used clinically would suggest that tumor cells may also have an L-R difference in response to therapy.

At puberty, ovarian hormones and growth factors signal from the tissue stroma in a paracrine fashion; signaling occurs from the stroma surrounding the duct to initiate growth and differentiation of the epithelial cells. Within the duct early estrogen (E2) exposure has been correlated to increased risk of gynecological cancers later in life (Warner 1976, Hilakivi-Clarke, Cho et al. 1997, Fenton 2006). In addition, early E2 exposure has also been designated a risk factor for breast cancer by the National Cancer Institute (NCI) (Warner 1976, Hilakivi-Clarke, Cho et al. 1997, Fenton 2006). However; studies examining the effects of postnatal E2 exposure have not examined the long term effects of estrogen exposure during pubescent ductal morphogenesis nor the distribution of cell populations that leave the mammary glands more vulnerable for breast cancer later in life. Chapter 4 demonstrates that the mammary glands respond L-R differently to neonatal estrogen which suggests patients receiving endocrine therapy, may have a differential response to therapy depending on the side of origin, and increased

estrogen exposure may elevate the risk for breast cancer asymmetrically.

The origin of mammary gland laterality is unknown; however, laterality of other well characterized organs begins embryonically with L-R patterning (Stalsberg 1969, Patterson, Drysdale et al. 2000, Levin 2005, Raya and Izpisua Belmonte 2006, Shiratori and Hamada 2006). As discussed earlier, thoracic mammary glands 3 and 8 require somitic FGF signaling for placode initiation (Mailleux, Spencer-Dene et al. 2002, Veltmaat, Relaix et al. 2006, Veltmaat, Ramsdell et al. 2013). Retinoic acid (RA) signaling plays an essential role in somite formation [30-32] and mammary gland development (Wang, Shen et al. 2005, Cohn, Ossowski et al. 2010, Cho, Kwon et al. 2012). Altered RA signaling leads to asynchronous somite formation during the time window of mammary placode initiation (Mailleux, Spencer-Dene et al. 2002, Veltmaat, Mailleux et al. 2003, Kawakami, Raya et al. 2005, Vermot, Gallego Llamas et al. 2005, Veltmaat, Relaix et al. 2006, Vilhais-Neto, Maruhashi et al. 2010, Cho, Kwon et al. 2012). Therefore if mammary gland laterality originates from somitic signals during mammary placode formation, altered RA signaling will result in asymmetric somites and therefore asymmetric mammary gland morphogenesis. Therefore to determine the origin of mammary gland laterality, the Retinoid X Receptor alpha (RXRα) knockout mouse model was used. The homozygous RXRα knockout mouse is embryonic lethal (Sucov, Dyson et al. 1994), subsequently RXRα mice heterozygous for RXRα knockout ($RXR\alpha^{+/-}$) was employed. Chapter 5 demonstrates that $RXR\alpha^{+/-}$ mice display asymmetric ductal morphogenesis in thoracic mammary glands but not inguinal mammary glands. In addition left

thoracic mammary glands are more sensitive to RXRα$^{+/-}$ knockout. These data suggest an embryonic origin for L-R mammary gland asymmetry.

CHAPTER TWO

CHAPTER 2: MORPHOMETRIC AND FRACTAL DIMENSION ANALYSIS IDENTIFIES EARLY NEOPLASTIC CHANGES IN MAMMARY EPITHELIUM OF MMTV-CNEU MICE

Note: This chapter contains a published paper in its entirety with changes only in formatting:

Anticancer Research 2014; volume 34, pages 1171-1178

Morphometric and Fractal Dimension Analysis Identifies Early Neoplastic Changes in Mammary Epithelium of MMTV-cNeu Mice

John W. Fuseler*, Jacqulyne P. Robichaux*, Huda Atiya, and Ann F. Ramsdell
* These authors contributed equally to the study.

INTRODUCTION

Breast cancer is the most common type of cancer that occurs in women and is the second leading cause of women's cancer-related deaths (Group 2013). Diagnosis, prognostication, and therapeutic decisions in the management of breast cancer are guided by disease staging and other criteria, including hormone receptor expression, Her-2/Neu amplification, and histological tumor type (Saez, McGuire et al. 1989, Lonning 2007). While incorporation of these parameters has been useful in identifying patients who stand to benefit from targeted biological and endocrine therapies, the utility of histological tumor grading in assessing chemotherapeutic benefit has been shown to be relatively less predictive, in part due to its semi-quantitative nature (Tambasco, Eliasziw et al. 2010). In an attempt to overcome this limitation, fractal dimension analysis has emerged as an alternative approach to assess tumor morphology for breast and other cancer types (Losa and Nonnenmacher 1996, Cross 1997).

Fractal dimension is a quantitative tool for objective measurement of complex structures that cannot be readily described and quantified by application of Euclidian geometry. The ductal epithelial network of the mammary gland, the site where breast tumors originate, can be considered a fractal object and its topological dimension, or fractal dimension (D), is expressed by a non-integer number lying between the Euclidian integers 1 and 2 for a two-dimensional object.

Computation of the fractal dimension allows for quantification of the complexity, or chaos, and space-filling properties associated with the structure of interest, *i.e.* the ductal epithelium. The greater the value of the fractal dimension of the object, the greater is its irregularity and complexity (chaos).

Fractal analysis has been applied to delineating the growth and complex architecture associated with a variety of tumors (Bizzarri, Giuliani et al. 2011), including breast ductal carcinomas in images generated by optical coherence tomography (Sullivan, Hunt et al. 2011), mammography (Raguso, Ancona et al. 2010, Rashidnasab, Elangovan et al. 2013), magnetic resonance (Kontos, Ikejimba et al. 2011, Di Giovanni, Ahearn et al. 2012), needle biopsy smears (Cross, Bury et al. 1997, Dey and Mohanty 2003) and histological methods (Tambasco and Magliocco 2008, Tambasco, Eliasziw et al. 2010). It moreover has been used to distinguish benign from malignant tissues in resected specimens from breast conserving surgeries (Nyirenda, Farkas et al. 2011, Laughney, Krishnaswamy et al. 2012). Increased fractal dimension is significantly associated with higher tumor grade (*i.e.* loss of differentiated structure), larger tumor size, and positive lymph node status, all of which are indicators of more aggressive disease (Tambasco and Magliocco 2008, Braverman and Tambasco 2013). Consistent with this, increased fractal dimension also has been shown to be significantly associated with lower disease-specific and overall survival of breast cancer patients (Tambasco, Eliasziw et al. 2010).

Given the clinical utility of fractal dimension, we have investigated whether fractal analysis can be applied in morphological assessments in pre-clinical breast

cancer mouse models. For the present study we conducted fractal and conventional morphometric analysis in a widely used breast cancer mouse model, MMTV-cNeu. MMTV-cNeu$^{Tg/+}$ mice overexpress the *ErbB2/Neu* oncogene, which models Her-2+ breast cancer, and develop mammary tumors relatively rapidly, *i.e.* by approximately four months of age (Guy, Webster et al. 1992, Hutchinson and Muller 2000). Using combined fractal dimension and morphometric analyses, we found that this approach detected quantitative changes in mammary ductal epithelial growth and complexity that preceded overt tumor formation. Moreover, when analyzed independently, our results showed that left-side mammary glands were more labile to oncogene-driven changes in ductal morphology compared to right-side glands, a difference that is consistent with elevated left-side tumor incidence that occurs in breast cancer patients (Veltmaat, Ramsdell et al. 2013). Together, these results indicate that fractal dimension analysis can be applied in conjunction with conventional morphometric measurements in a murine breast cancer model to quantify changes in the ductal epithelium that occur during early neoplasia. This combined methodological approach is highly sensitive and has provided the first documentation that lateralized morphological alterations initiate early in the neoplastic process.

MATERIALS AND METHODS

Mice

All experiments were performed in accordance with the regulations of the Medical University of South Carolina Institutional Animal Care and Use Committee. FVB/N wild-type and FVB/N-TgN (MMTVNeu) 202Mul) mice were obtained from Taconic (Germantown, NY, USA) and JAX® Mice and Services (Bar Harbor, ME, USA). Wild-type and single-copy MMTV-cNeu$^{Tg/+}$ mice were used for all experiments and fed Harlan Teklad rodent diet 2918 and provided water *ad libitum*.

Histology and image collection

Carmine red stained whole mounts (de Assis, Warri et al. 2010) prepared from #3 and #8 thoracic mammary glands of day-28 mice (Veltmaat, Ramsdell et al. 2013) were imaged on an Olympus SZX12 stereomicroscope equipped with a Spot camera. Overlapping images of each whole mount were processed into a single composite image with Adobe Photoshop®.

Image analysis.

The color images of the mammary glands were converted to 8-bit monochrome images for image and fractal analysis. The mammary gland within an image was outlined and isolated from the background tissue and defined as a Region of Interest (ROI) (Figure 5). The isolated image of the mammary gland was thresholded using the set threshold subroutine of MetaMorph Image analysis

software (ver. 6.1). The area (A) and integrated optical density (IOD) of the ductal epithelial networks were measured using the integrated morphometry analysis sub-routine of MetaMorph. The fractal dimension (**D**), was determined by the box counting method using HarFA software (Nezadal, Zemeskal et al. 2001) [http://www.fch.vutbr.cz/lectures/imagesci]) applied to the isolated image of the mammary gland using the same threshold values.

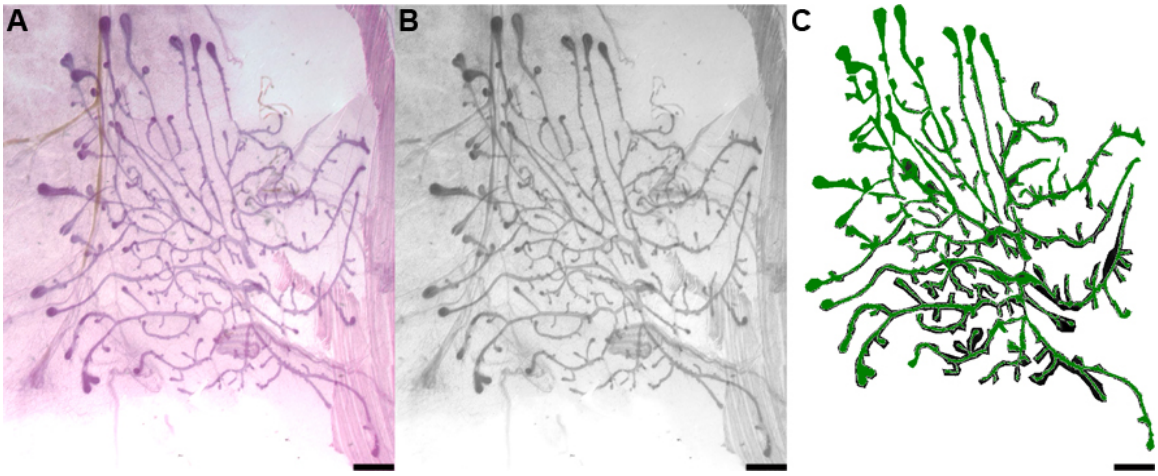

Figure 5. Stepwise example of 8 bit monochrome image conversion. (A) A composite image of a carmine red stained whole mount prepared from wild type (WT) mouse TMG. (B) 8-bit gray scale image of TMG. (C) Manually traced and isolated TMG used for analysis with MetaMorph® image analysis software. (scale bar in all figures = 1mm)

Integrated optical density (IOD).

The IOD of the mammary gland ROI delineated by the thresholded boundaries is considered to be the “mass” of the ROI and a measurement of the total amount of labeled material in the region (Walter and Berns 1986, Fuseler, Merrill et al. 2006, Fuseler, Millette et al. 2007, Rogers and Fuseler 2007, Fuseler and Valarmathi 2012). The IOD of a selected region can be expressed as the weighted sum of the image histogram in which each term in the histogram is multiplied by the gray value it represents. When applied to thresholded boundaries the IOD is defined by the following expression:

$$IOD(T1, T2) = \sum_{GV=T1}^{T2} H(GV) \times GV$$

Where the upper and lower thresholds defining the ROI in the histogram are given by T1 and T2. GV is the gray value of each pixel and H (GV) is the gray level histogram.

Application of the fractal dimension (D)

The thoracic mammary glands in the wild type and MMTV-cNeu mice appear as irregular and complex objects composed of parts at different levels of resolution (ducts of different bore sizes) which are functionally and physiologically similar (self-similar) to the whole object. Under the conditions of these properties, the thoracic mammary glands can be considered fractal objects and their topological dimension, the fractal dimension (**D**), be expressed by a non-integer number lying

between two Euclidian integer topological dimensions (Grizzi, Russo et al. 2005). The values of **D** characterizing the thoracic mammary glands are therefore fractional. Since the thoracic mammary gland is essentially a 2-dimensional object, the **D** values will lie between 1 and 2. As the mammary gland becomes more complex and irregular, its **D** value becomes greater approaching 2. In applying fractal analysis, the **D** value of the mammary gland is determined by applying the box-counting method (Fernandez and Jelinek 2001, Grizzi, Russo et al. 2005). The box-counting method has been the most widely used and general model for applying fractal analysis to biological and non-biological systems. The box-counting method consists of a grid of boxes of size e superimposed over the image of the structure, and the number of boxes containing any part of the structure recorded as ***N(e)***. A fractal object expresses a straight line when Log[***N(e)***] is plotted against Log(***1/e***). The box fractal dimension **D** can be determined from the slope of the regression line. That is: **D**= Log[***N(e)***] / Log(***1/e***). The **D** values of the thoracic mammary glands were determined using HarFA software (Nezadal, Zemeskal et al. 2001) [http://www.fch.vutbr.cz/lectures/imagesci]. The HarFA software assigned mesh sizes of boxes with **e** values ranging from 2 to 207 pixels and 30 steps within this range were calculated to generate the Log[***N(e)***] versus Log(***1/e*)** lines to determined .

Branch points and terminal end buds (TEBs)

Branch points and TEBs were quantified by manual counting from the images.

RESULTS

Whereas the mammary gland begins its development during embryonic mid-gestation stages, the majority of its growth and development takes place post-natally, with the first substantial expansion of the ductal epithelial network occurring during puberty. Genetic, hormonal, and environmental factors that perturb the ductal architecture during puberty or other periods of growth and morphogenesis also increase risk of developing breast cancer later in life (Fenton 2006, Fenton, Reed et al. 2012, Biro and Deardorff 2013). Mammary ductal epithelial branching and elongation are driven by bifurcation of specialized invasive structures located at the ends of the rudimentary ducts, termed terminal end buds (TEBs) (Sternlicht 2006). Shorter (secondary) side branches also arise as lateral sprouts from trailing ducts, increasing the area of the ductal tree with each successive ovarian cycle (Sternlicht, Kouros-Mehr et al. 2006). The pattern of mammary branching morphogenesis is non-stereotypical (*i.e.* it varies from individual to individual), and is controlled by paracrine-derived signals within the local microenvironment (Lu, Sternlicht et al. 2006, Sternlicht, Kouros-Mehr et al. 2006).

In order to determine if changes in ductal epithelial growth and complexity can be identified during early neoplasia, several morphological and fractal parameters of ductal epithelial networks were quantified and compared between thoracic mammary glands (TMG) of pubertal stage wild type and MMTV-cNeu mice (Figure 6). We chose to focus specifically on TMGs for two reasons. Firstly, the

vast majority of tumors in MMTV-cNeu mice develop in the thoracic glands compared to the cervical or inguinal glands; and second, based on differences amongst signaling pathways that regulate induction of the five pairs of mouse mammary glands, as well as their anterior-posterior anatomical locations, it appears that TMGs most closely model human breast development (Veltmaat, Ramsdell et al. 2013). Thus, we reasoned that if early neoplastic changes were present, they would be detectable in the TMGs.

Consistent with a previous report (Mukherjee, Louie et al. 2000), we found that the area occupied by the ductal epithelial network in TMGs in wild-type mice is significantly greater than the area of the ductal epithelial network in TMGs in the MMTV-cNeu mice (Figure 6). This indicates that the ductal epithelial networks in TMGs in the MMTV-cNeu mice are smaller, but not necessarily morphologically different from the TMGs present in the controls. To assess potential morphological differences, fractal dimension, branch points, TEBs, and IOD were quantified. Application of the fractal dimension (**D**) is a measure of disorder, or chaos, of the epithelial network. The **D** for MMTV-cNeu TMGs is significantly greater than D for the wild type TMGs (Figure 6). This indicates that the ductal epithelial networks of MMTV-cNeu TMGs are more complex and more space-filling despite smaller size (Area) than those in wild-type mice. Interestingly, the increase in **D** for MMTV-cNeu TMGs does not appear to be the result of an increase in branch points or TEBs, which are the same or decreased, respectively (Fig. 2). This indicates that the increase in D of the MMTV-cNeu TMGs results from an overall lack of order of the

entire network structure, suggesting that the ErbB2/Neu oncogene promotes disorganized pattern during epithelial network development.

Although determination of **D** can quantify an object, a value of **D** does not uniquely specify a particular morphology. In other words, objects of vastly different morphology can have the same or similar fractal dimensions. To adequately describe the morphology of an object, an additional measurement in conjunction with D is required to provide a unique identifier, which quantifies the object. Ideally, such an additional measurement would be determinant of the structure or distribution of material within the thresholded boundary of the region of interest. In this study, we apply the concept that the IOD is a measure of the mass of the ductal network within the ROI (Walter and Berns 1986, Fuseler, Merrill et al. 2006, Fuseler, Millette et al. 2007, Rogers and Fuseler 2007, Fuseler and Valarmathi 2012). Mass measurement deals with this distribution of material within the ROI and leads to the concept of relative density, here defined as IOD/Area. Thus, application of the term IOD/A provides additional information on the concept of mass density or relative density of the mammary ductal network (Smith, Lange et al. 1996). Taken together, these two measurements, D and IOD/A, improve the quantitative description and provide unique characterization and quantitation of the epithelial network morphology of MMTV-cNeu TMGs compared to WT TMGs.

As shown in Figure 6, the relative density of the TMG epithelial network, measured as the IOD/A, is significantly greater in the MMTV-cNeu mice compared to wild type mice. This indicates that there is more physical material content (Carmine alum-stained epithelium) in the TMGs of MMTV-cNeu mice. Since the

MMTV-cNeu TMG networks have smaller area with a larger D, the expression of the greater IOD/A suggests that the ductal walls may be thicker and contain smaller lumens than the ducts in the wild type controls. Taken together, these results indicate that the overexpression of the ErbB2/Neu oncogene results in delayed epithelial growth with an overall concomitant increase in chaos that is consistent with ductal hyperplasia.

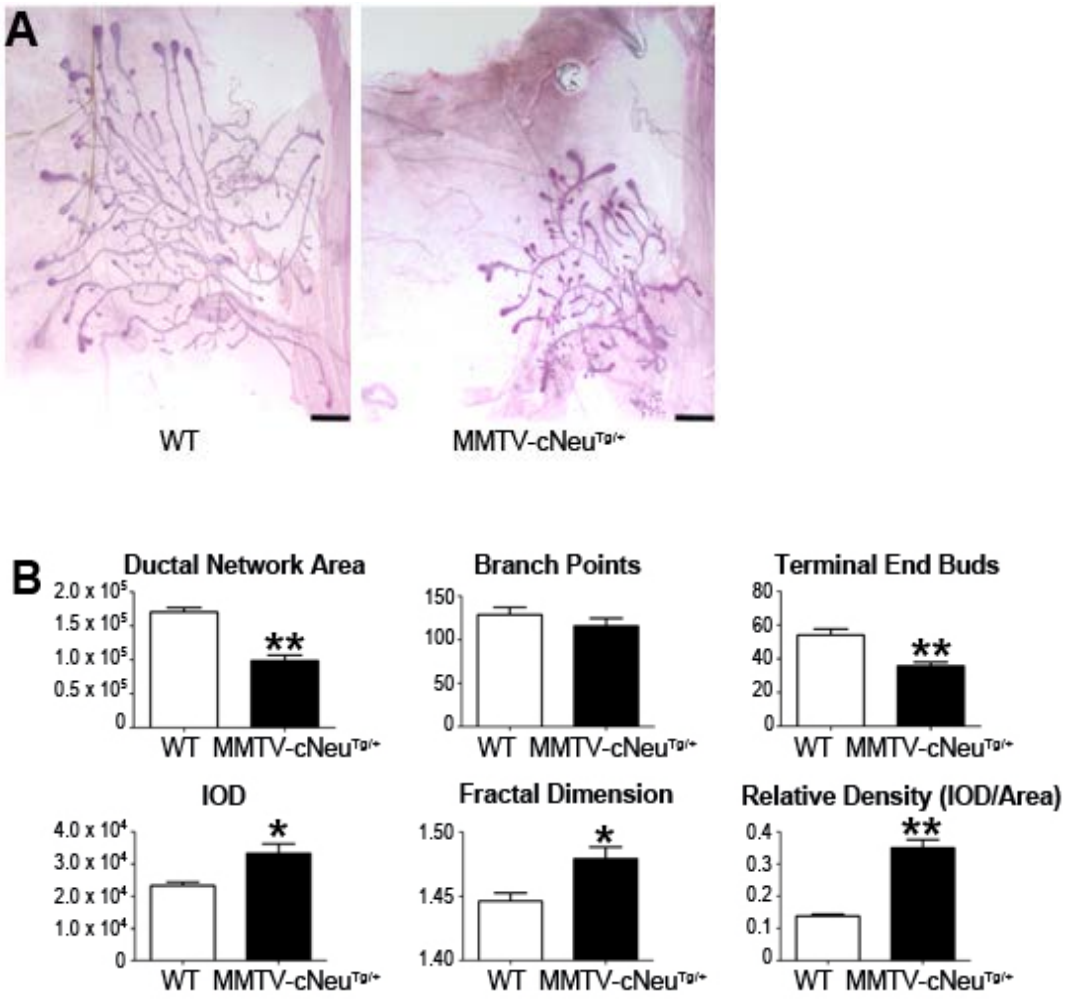

Figure 6. **Morphometric and fractal analysis of ductal networks of wild type versus MMTV-cNeu mice.** (A) Representative images of carmine red stained TMGs from wild type (WT) and MMTV-cNeu$^{Tg/+}$ mice. (B) Morphometric analysis of #3/8 TMGs of WT versus MMTV-cNeu$^{Tg/+}$ mice. Bars are representative of mean ± SEM (WT N = 16 MMTV-cNeu$^{Tg/+}$ N= 26). Unpaired student's t-test, * $p<0.01$, ** $p<0.0001$.

Because epidemiological studies of breast cancer patients indicate that significantly more tumors arise in the left breast compared to the right (Veltmaat, Ramsdell et al. 2013), we next investigated whether the morphological defects in MMTV-cNeu mice were present to the same extent in both the left and right TMGs. Comparing the left TMG ductal networks in the MMTV-cNeu mice to those in the left TMGs of wild type mice indicated significant differences in all measurable parameters except branch points (Figure 7D). By contrast, the right-side ductal epithelial networks of MMTV-cNeu mice expressed a more normal morphometric pattern (Figure 7E). Whereas right side MMTV-cNeu networks had decreased area and number of terminal end buds, there was no difference in the D values of the right TMGs of the MMTV-cNeu mice compared to the right TMGs of controls. This indicates that although the right side TMGs of MMTV-cNeu mice are smaller, they nevertheless exhibit a normal degree of tissue organization and space-filling properties that are the same as wild-type controls. Additionally no difference was detected in the IOD of the right networks of the MMTV-cNeu mice relative to the right-side wild-type TMGs. However, the relative density (IOD/A) of the right side MMTV-cNeu TMGs was greater than relative density of wild type right side TMGs. Together, this suggests that ductal epithelium on the left side is more susceptible to ErbB2/Neu-mediated effects on ductal morphology than is the right side epithelium. Thus, fractal image analysis may be useful in defining tissue of risk (pre-neoplastic tissue or tissue initially undergoing neoplastic transformation) to cancer before the appearance of the tumor.

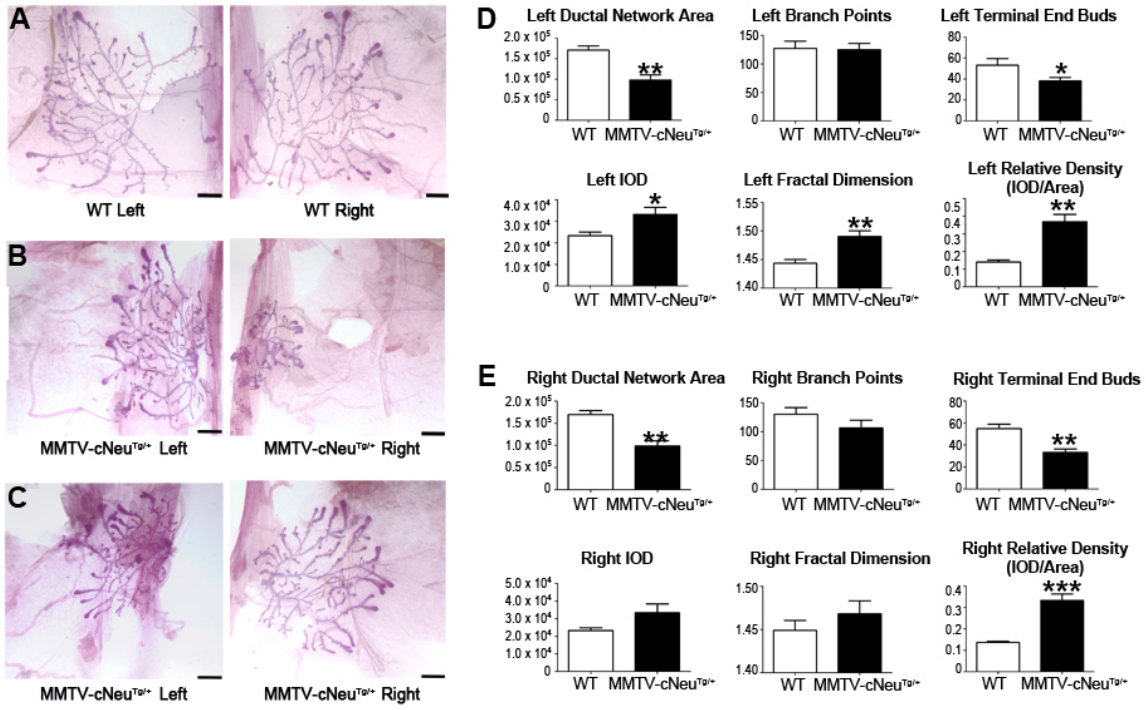

Figure 7. **Independent left and right side analysis of ductal networks in wild type versus MMTV-cNeu mice.** (A) Representative images of a carmine red stained pair of TMGs of wild type (WT) mice. (B,C) Representative images of two different pairs of carmine red stained TMGs of MMTV-cNeu$^{Tg/+}$ mice. (D) Morphometric analysis of #3 left TMGs of WT versus MMTV-cNeu$^{Tg/+}$ mice. (E) Morphometric analysis of #8 right TMGs of WT versus MMTV-cNeu$^{Tg/+}$ mice. Bars are representative of mean ± SEM (WT N = 8 MMTV-cNeu$^{Tg/+}$ N= 13). Unpaired student's t-test, * $p<0.05$, ** $p<0.001$, *** $p<0.0001$.

DISCUSSION

Our results demonstrate that when combined with conventional morphometric analysis, fractal dimension is a highly sensitive and quantitative tool by which one is able to evaluate and compare murine ductal epithelial growth and morphology. This combined approach facilitates precise morphological description which is independent of landmarks such as the lymph node (typically used in semi-quantitative inguinal gland analysis) and permits for inclusion of regions of epithelium that may otherwise be obscured by contaminating muscle tissue (which frequently occurs with cervical and thoracic gland dissections). Similar to its clinical utility, application of fractal dimension to the Her-2+ breast cancer mouse model demonstrates that fractal dimension can identify aberrations in tissue architecture that are not necessarily obvious nor easily appreciated by conventional, semi-quantitative image inspection. The objective nature of fractal analysis and the ease of use of this method position it as a tool that can be used to standardize morphological assessment of mammary epithelial growth and differentiation in both normal and neoplastic development. Because the combined image and fractal analysis used in this study utilizes commercially available software and can be applied to archived specimens (*i.e.* coverslipped mammary whole mounts), this approach offers a means by which results may be reproducibly and quantitatively compared across existing mouse mammary models, as well as in breast cancer mouse models that may be developed in the future.

In addition to its diagnostic and therapeutic decision making utility for breast cancer patients, fractal dimension may also be useful to identify women at heightened risk for developing breast cancer. Fractal dimension analysis of mammographic images has been used for retrospective identification of hormone-associated changes in breast tissue linked with women who were later diagnosed with breast cancer (Daye, Keller et al. 2013). In another retrospective study, fractal dimension analysis detected architectural distortions that were present in screening mammograms taken on average 15 months prior to clinical breast cancer diagnosis (Rangayyan, Banik et al. 2010, Rangayyan, Banik et al. 2013). In our study we found that fractal dimension can also be effectively used in a pre-clinical breast cancer mouse model to similarly detect changes in tissue organization that arise during early oncogenesis. By applying combined fractal/morphometric analysis to MMTV-cNeu mice, we found that numerous aberrances develop in the growth and branching pattern of ductal epithelium during early neoplasia, well in advance of appreciable tumor formation. A particularly intriguing finding was that in addition to overall decreased ductal network area and alterations in other morphologic parameters, the epithelial networks of MMTV-cNeu mice showed more pronounced abnormalities in ductal epithelial network organization and complexity in the left side glands than did the right side glands. This finding suggests that MMTV-cNeu mice may be an appropriate model to investigate left-right differences in neoplastic development, an area that has yet to be addressed at the cellular or molecular level, despite the fact that epidemiological studies consistently find increased tumor incidence on the left side

in breast cancer patients (Wilting and Hagedorn 2011, Veltmaat, Ramsdell et al. 2013).

In summary, the results of our study demonstrate that combined fractal and conventional morphometric analysis is an objective, quantitative method to document early neoplastic changes in ductal epithelial morphology occurring prior to mammary carcinoma development. The sensitivity of this approach in a pre-clinical breast cancer mouse model yields results comparable to those in clinical studies of human breast cancer patients and offers opportunity for investigators to standardize analyses made across the many murine models that are currently in use in studies of both normal and neoplastic mammary gland development.

CHAPTER THREE

CHAPTER 3.1: MAMMARY GLANDS EXHIBIT MOLECULAR LATERALITY AND UNDERGO LEFT-RIGHT ASYMMETRIC DUCTAL EPITHELIAL GROWTH IN MMTV-CNEU MICE

Note: This chapter contains a published paper in its entirety with changes only in formatting:

Oncogene, advance online publication, 9 June 2014; doi:10.1038/onc.2014.149

Mammary glands exhibit molecular laterality and undergo left-right asymmetric ductal epithelial growth in MMTV-cNeu mice

Jacqulyne P. Robichaux, Robin M. Hallet, John W. Fuseler, John A. Hassel, and Ann F. Ramsdell

INTRODUCTION

Cancers that initiate in paired organs and other bilaterally symmetric tissues exhibit an unusual feature, which is that tumors occur with non-equivalent incidence on the left versus right sides (Delahunt, Bethwaite et al. 1994, Roychoudhuri, Putcha et al. 2006, Yoruk, Karasen et al. 2009, Wilting and Hagedorn 2011, Veltmaat, Ramsdell et al. 2013). The basis for this laterality has not been addressed at the cellular or molecular level, an oversight that may be significant because patient survival is reported to differ according to primary tumor situs (Delahunt, Bethwaite et al. 1994, Roychoudhuri, Putcha et al. 2006). The side with elevated tumor incidence is organ-dependent and not necessarily the same side that is associated with poorer disease outcome. For breast cancer, the majority of occurrences are unilateral, with higher tumor incidence on the left (Veltmaat, Ramsdell et al. 2013). Left-side predominance also occurs in bilateral cases, in which more tumors develop first in the left breast or are larger than those on the right (Veltmaat, Ramsdell et al. 2013). Yet, despite the increased incidence and larger average tumor size of left-sided breast cancer, right-sided breast cancer may be associated with worse prognosis. Right-sided breast tumors are prone to earlier onset of bone metastasis and give rise to higher numbers of sites with metastatic involvement (Fatima, Zaman et al. 2013). This suggests that disease progression is related to the side of tumor formation, which could result in

differential patient survival. Although studies directly addressing breast cancer patient survival relative to tumor laterality are limited and have generated contradictory findings (Veltmaat, Ramsdell et al. 2013), there is some indication that lower survival rates occur in patients with right-sided disease (Hartveit, Tangen et al. 1984).

The left-sided excess of breast cancer and potential relationship between tumor laterality and patient prognosis suggests that mammary tissues harbor L-R differences that are relevant to oncogenesis. To address this we have used normal and neoplastic MMTV-cNeu$^{Tg/Tg}$ mice to probe for L-R differences at the beginning and end of puberty--a period when the rapidly growing ductal epithelium (Watson and Khaled 2008) is vulnerable to genetic, hormonal, and other environmental perturbations that heighten risk for developing breast cancer later in life (Fenton 2006, Fenton, Reed et al. 2012, Biro and Deardorff 2013). Here we provide evidence that mouse mammary glands have baseline L-R differences in gene expression that are L-R discordantly altered by *HER2*/*Neu* and that are accompanied by asymmetric ductal epithelial growth and patterning. Furthermore, we used comparative genomic analysis to show that the L-R differences in gene expression that we identified in mouse mammary glands are predictive of breast cancer patient outcome, with right-side expression profiles associated with significantly poorer long-term patient survival.

MATERIALS AND METHODS

Mice

All experiments were performed in accordance with the regulations of the Medical University of South Carolina Institutional Animal Care and Use Committee. FVB/N wild-type and FVB/N-TgN (MMTVNeu) 202Mul) mice were obtained from Taconic (Germantown, NY, USA) and JAX® Mice and Services (Bar Harbor, ME, USA). Wild-type and MMTV-cNeu$^{Tg/Tg}$ mice were used for all experiments and fed Harlan Teklad rodent diet 2918 and provided water *ad libitum*.

Histology and image collection

Carmine red stained whole mounts (de Assis, Warri et al. 2010) prepared from #3 and #8 thoracic mammary glands of day-28 mice (Veltmaat, Ramsdell et al. 2013) were imaged on an Olympus SZX12 stereomicroscope equipped with a Spot camera. Overlapping images of each whole mount were processed into a single composite image with Adobe Photoshop®.

Image analysis.

The color images of the mammary glands were converted to 8-bit monochrome images for image and fractal analysis. The mammary gland within an image was outlined and isolated from the background tissue and defined as a Region of Interest (ROI) (Figure 5). The isolated image of the mammary gland was thresholded using the set threshold subroutine of MetaMorph Image analysis

software (ver. 6.1). The area (A) and integrated optical density (IOD) of the ductal epithelial networks were measured using the integrated morphometry analysis sub-routine of MetaMorph. The fractal dimension (**D**), was determined by the box counting method using HarFA software (Nezadal, Zemeskal et al. 2001) [http://www.fch.vutbr.cz/lectures/imagesci]) applied to the isolated image of the mammary gland using the same threshold values.

Integrated optical density (IOD).

The IOD of the mammary gland ROI delineated by the thresholded boundaries is considered to be the "mass" of the ROI and a measurement of the total amount of labeled material in the region (Walter and Berns 1986, Fuseler, Merrill et al. 2006, Fuseler, Millette et al. 2007, Rogers and Fuseler 2007, Fuseler and Valarmathi 2012). The IOD of a selected region can be expressed as the weighted sum of the image histogram in which each term in the histogram is multiplied by the gray value it represents. When applied to thresholded boundaries the IOD is defined by the following expression:

$$IOD(T1, T2) = \sum_{GV=T1}^{T2} H(GV) \times GV$$

Where the upper and lower thresholds defining the ROI in the histogram are given by T1 and T2. GV is the gray value of each pixel and H (GV) is the gray level histogram.

Application of the fractal dimension (D)

The thoracic mammary glands in the wild type and MMTV-cNeu mice appear as irregular and complex objects composed of parts at different levels of resolution (ducts of different bore sizes) which are functionally and physiologically similar (self-similar) to the whole object. Under the conditions of these properties, the thoracic mammary glands can be considered fractal objects and their topological dimension, the fractal dimension (**D**), be expressed by a non-integer number lying between two Euclidian integer topological dimensions (Grizzi, Russo et al. 2005). The values of **D** characterizing the thoracic mammary glands are therefore fractional. Since the thoracic mammary gland is essentially a 2-dimensional object, the **D** values will lie between 1 and 2. As the mammary gland becomes more complex and irregular, its **D** value becomes greater approaching 2. In applying fractal analysis, the **D** value of the mammary gland is determined by applying the box-counting method (Fernandez and Jelinek 2001, Grizzi, Russo et al. 2005). The box-counting method has been the most widely used and general model for applying fractal analysis to biological and non-biological systems. The box-counting method consists of a grid of boxes of size e superimposed over the image of the structure, and the number of boxes containing any part of the structure recorded as ***N(e)***. A fractal object expresses a straight line when Log[***N(e)***] is plotted against Log(***1/e***). The box fractal dimension **D** can be determined from the slope of the regression line. That is: **D=** Log[***N(e)***] / Log(***1/e***). The **D** values of the thoracic mammary glands were determined using HarFA software (Nezadal, Zemeskal et al. 2001) [http://www.fch.vutbr.cz/lectures/imagesci]. The HarFA

software assigned mesh sizes of boxes with **e** values ranging from 2 to 207 pixels and 30 steps within this range were calculated to generate the Log[***N(e)***] versus Log(***1/e*****)** lines to determined .

Branch points and terminal end buds (TEBs)

Branch points and TEBs were quantified by manual counting from the images.

Microarray Analysis

Microarray analysis of left versus right TMGs using left as the baseline reference was performed using RNA pooled from 3-4 intact 4-week TMGs [#3 and #8 glands as diagrammed in Veltmaat *et al* (Veltmaat, Relaix et al. 2006)] for cDNA synthesis and hybridization to Affymetrix GeneChip Mouse Genome 430 2.0 Arrays. The arrays were preprocessed and normalized using RMA (Irizarry, Hobbs et al. 2003). Each array experiment was completed in biological and technical triplicate. Differentially expressed probesets were identified based on a fold-change (increase or decrease in right side compared to left) of at least 1.2, and a q-value of less than 0.05. Pathway analysis was carried out for each set of laterality associated genes (left or right) by probing the NCI Pathway interaction database (Schaefer, Anthony et al. 2009).

RT-PCR

SYBR Green-based RT-PCR of select array candidates was performed with primers listed in Table 2. Real-time PCR miner was used to calculate Ct values

and replication efficiency(Zhao and Fernald 2005) and fold changes relative to GAPDH mRNA were determined by delta-delta Ct.

Immunoprecipitation

Total ErbB2/Neu protein was immunoprecipitated from left or right TMGs (Antibody #4290, Cell Signaling), immunoblotted, and probed with anti-phospho-ErbB2/Neu (Antibody #2243, Cell Signaling). Densitometry of triplicate results was performed using NIH ImageJ software.

Comparative genomic analysis

Compilation of a large cohort of breast cancer patients from multiple studies available through the Gene Expression Omnibus (http://www.ncbi.nlm.nih.gov/geo/) was compared to the microarray in - to test the association between laterality associated genes and patient survival. Our combined cohort comprised patients from the GSE2034 (Wang, Klijn et al. 2005), GSE7390 (Desmedt, Piette et al. 2007), GSE4922(Ivshina, George et al. 2006), GSE25055 (Hatzis, Pusztai et al.), and GSE3494 (Miller, Smeds et al. 2005) cohorts (n=1334). For all patients, clinical outcome data as well as the gene expression profile of their respective tumors was available. Whenever possible we used 10-yr disease free survival as the clinical endpoint in our study; however, when disease free survival was not available we alternatively used either distant metastasis free or overall survival as the clinical endpoint. The arrays for each separate cohort were preprocessed and normalized using RMA(Irizarry, Hobbs et

al. 2003). ER status was assigned based on the clinical annotation files, and HER2 status was assigned based on the mean ERBB2 transcript levels (probe set ID 216836_s_at) within each study cohort independently. Affymetrix GeneChip Mouse Genome 430 2.0 Arrays probe sets were mapped to their human counterpart genes by Unigene IDs. When multiple probe sets recognized the same gene transcripts, only the probe with the highest mean intensity was used. To assign signature scores to patients, the expression values for each gene were standardized such that the mean and standard deviation were set to 0 and 1 in each individual patient cohort, respectively. Subsequently, we calculated signature scores for each patient as previously described (Hallett, Dvorkin-Gheva et al. 2012, Hallett, Pond et al. 2012), where positive scores were considered to indicate that a tumor had ‘right-sided’ gene expression and negative scores were considered to indicate that a tumor had ‘left-sided’ gene expression. Survival curves were graphed using Graphpad Prism® 5 and statistical tests were completed in R.

RESULTS

Thoracic mammary glands are molecularly L-R asymmetric

Ductal epithelial networks in thoracic mammary glands (TMGs) of early pubertal (4-week) and post-pubertal (10-week) wild type (WT) mice (Figure 8A, B) were quantified by image and fractal analysis as described previously (Fuseler, Robichaux et al. 2014). Despite increases in network area and number of branch points between weeks 4 and 10, as well as changes in TEBs, which decrease in number and initiate regression by week 10 (Richert, Schwertfeger et al. 2000), all of these morphological parameters were statistically equivalent for left and right TMGs at both timepoints, indicative of L-R symmetry (Figure 8C). By contrast, microarray analysis yielded approximately 161 transcripts that were L-R differentially expressed (i.e., up-regulated or down-regulated) with >1.2 fold change (q-value<0.05, Figure 8D), including genes and pathways that have established roles in oncogenesis and/or therapeutic sensitivity (Table 1). Several of the transcripts identified in the array were examined by RT-PCR (Figure 8E), which confirmed that relative to left-side expression, some genes were increased and others were decreased in expression levels on the right side. For example, *Gata-3* and *FoxM1*, which regulate luminal progenitor cell differentiation and renewal (Asselin-Labat, Sutherland et al. 2007, Carr, Kiefer et al. 2012), and which also have opposing protective and causative roles in tumorigenesis in the breast and other organs (Chou, Provot et al. 2010, Teh 2012), were more highly expressed on the left side (Figure 8E). By the end of puberty, both genes were

down-regulated; however, the fold decrease was significantly greater for left-side glands which resulted in net symmetric expression (Figure 8E). Asymmetric expression also was found for *notch-1*, another regulator of mammary luminal progenitor cell commitment (Bouras, Pal et al. 2008) that is involved in breast tumorigenesis (Farnie and Clarke 2007) (Figure 8E). *Notch-1* was right-side elevated, and by 10-weeks it showed slightly higher fold decrease in right-side glands compared to left (Figure 8E). To determine if asymmetric expression of genes with dual roles in ductal growth and tumorigenesis is a general property of TMGs, we examined *estrogen receptor alpha* (*ER*α). *ER*α was L-R equivalently expressed at both the start and end of puberty, consistent with it not being identified as a candidate by microarray (Figure 8E). We also examined *CD24*, a pan-epithelial marker in mouse mammary glands (Visvader 2009), which showed modest left-side elevation in 4-week TMGs, but not in 10-week TMGs (Figure 8E), raising the possibility that subtle differences in epithelial cell number could be present during early puberty, despite equivalent ductal network growth and morphology.

Genes involved in therapeutic sensitivity also were represented in the microarray. Elevated right-side expression was detected for *retinoic acid-inducible G-protein coupled receptor 5D* (*GPRC5D*), a gene that enhances sensitivity to an estrogen receptor antagonist, tamoxifen, in MCF7 breast cancer cells (Mendes-Pereira, Sims et al. 2012) and that was decreased by the end of puberty (Figure 8E). In addition, *stathmin-1* (*Stmn-1*), a microtubule destabilizing protein that confers chemoresistance in breast and other tumor types (Su, Smith et al. 2009,

Baquero, Hanna et al. 2012, Meng, Su et al. 2012, Han, Wang et al. 2013, Miceli, Tejada et al. 2013), was modestly left-side elevated in 4-week TMGs, followed by inversion to modest right-side elevated expression in 10-week TMGs (Figure 8E). Given the many L-R differences in gene expression in TMGs, it was surprising that microarray analysis did not uncover connections to any known laterality genes (Table 1), including *nodal* and *Pitx2,* regulators of embryonic L-R patterning that also are expressed in breast cancer and other tumor types (Wilting and Hagedorn 2011). Thus, we assessed these genes by RT-PCR, which confirmed symmetric expression (Figure 8E). Together, these findings demonstrate that despite symmetric *nodal* and *Pitx2* expression, the left and right TMGs of WT mice are molecularly lateralized with asymmetric expression of other genes that may impart differential predisposition to oncogenesis.

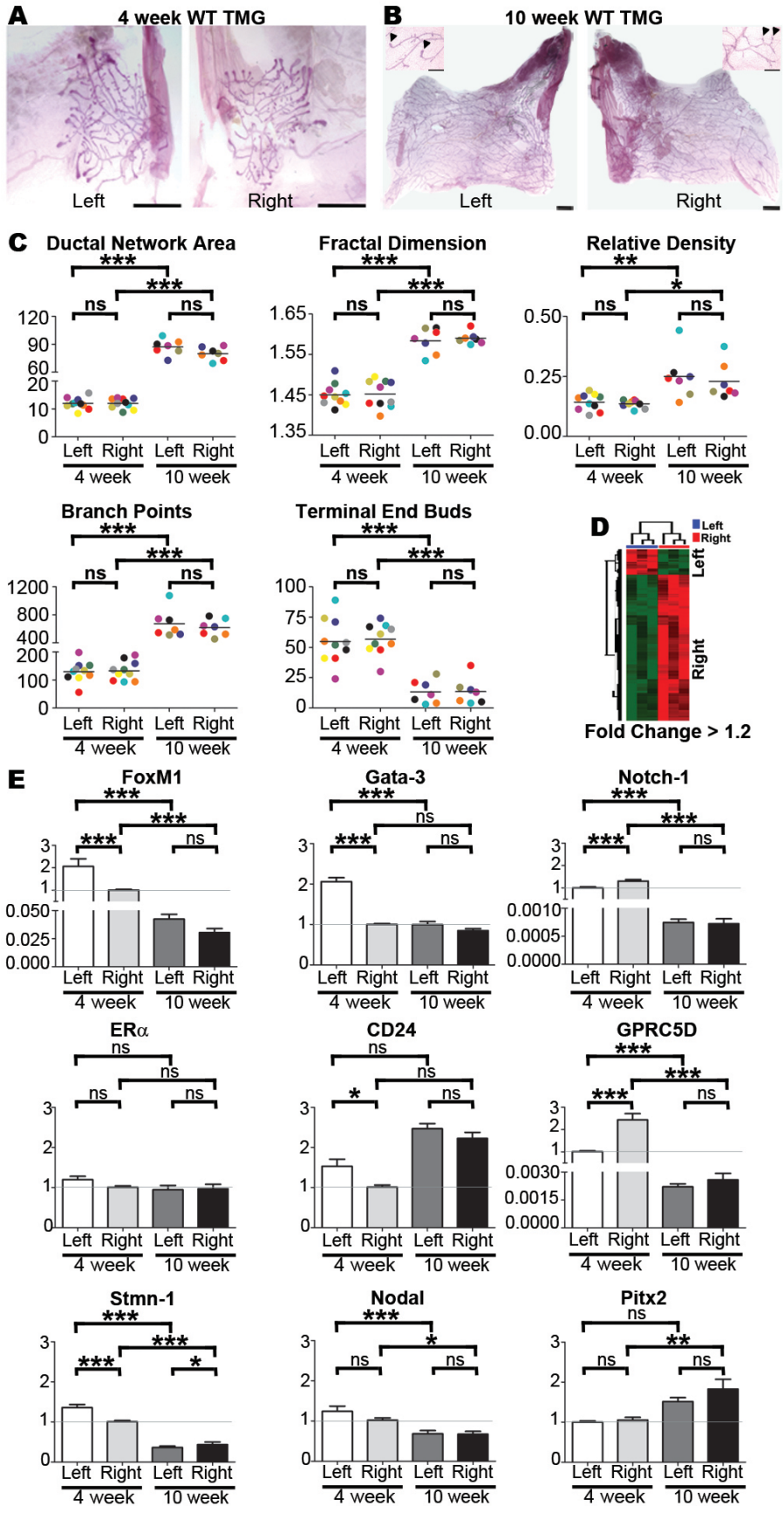
A
4 week WT TMG
Left
Right
B
10 week WT TMG
Left
Right
C
Ductal Network Area
Fractal Dimension
Relative Density
Branch Points
Terminal End Buds
Left Right Left Right
4 week 10 week
D
Left
Right
Fold Change > 1.2
E
FoxM1
Gata-3
Notch-1
ERα
CD24
GPRC5D
Stmn-1
Nodal
Pitx2

Figure 8. Morphological and molecular analysis of TMGs. Wild type mouse TMGs such as the representative L-R matched pairs are shown at 4-weeks (A) and 10-weeks (B) (scale bar = 1mm). Branch points and terminal end buds (TEBs), are shown in higher magnification insets for 10-week glands (arrowheads indicate TEBs; scale bar = 5 μm. Color-coding can be used to follow matched L-R pairs harvested from the same mouse in all graphs. No significant L-R differences (C) were found in ductal network area, fractal dimension, relative density, branch points or TEBs at 4 or 10 weeks as determined by one-tailed paired student's t-test. Microarray analysis of left versus right TMGs using left as the baseline reference (D). SYBR Green-based RT-PCR of select array candidates was performed with primers listed in Table 2 (E). Fold changes across groups were determined using the lower level of 4-week expression as baseline as indicated by the horizontal grey line. Bars represent mean ± SEM of $\geq$5 mice; *p<0.05, **p<0.01; *** p<0.001 (two-tailed paired student's t-tests).

Table 1: Microarray analysis. Transcripts identified in the L-R mouse TMG microarray are listed and the side with elevated expression is indicated (A). Results from pathway analysis of microarray data also are indicated (B).

A. Left and Right gene signature

Gene	Side
NPY2R	Left
DEFB4	Left
ICAM4	Left
AFM	Left
TMEM59	Left
CAMK2A	Left
NPY5R	Left
RYR2	Left
EHHADH	Left
IFT122	Left
GLP1R	Left
TG	Left
GPRC5D	Left
PSORS1C2	Right
SPRR1A	Right
LY6G6D	Right
TYRP1	Right
PADI3	Right
CRYM	Right
SCEL	Right
SFN	Right
CALML3	Right
KLK7	Right
PERP	Right
SERPINB5	Right
TRIM29	Right
COL17A1	Right
SI	Right
S100A14	Right
AQP3	Right
DNASE1L2	Right
IVL	Right

Gene	Side
MSX2	Right
CRYBA4	Right
DSP	Right
GPNMB	Right
LYPD3	Right
BNC1	Right
RBM35B	Right
ANXA9	Right
PKP3	Right
EHF	Right
TACSTD2	Right
CTSE	Right
PKP1	Right
PRDM1	Right
GABRP	Right
SLC39A8	Right
IRX4	Right
KLRD1	Right
KERA	Right
GATA3	Right
ST14	Right
CELSR1	Right
BDH1	Right
COL9A3	Right
GRHL2	Right
TGM1	Right
AP1M2	Right
SPINT1	Right
ACPP	Right
MOXD1	Right
STEAP1	Right
FHOD3	Right

Gene	Side
SOX9	Right
MCM5	Right
LY75	Right
COL7A1	Right
TNK1	Right
RAB20	Right
CCL22	Right
KIF20A	Right
SPAG5	Right
TSPAN1	Right
PHLDA2	Right
CCNF	Right
INADL	Right
VDR	Right
SCNN1B	Right
MTM1	Right
PLK1	Right
DHCR24	Right
PTGS2	Right
LRRC16	Right
CCL5	Right
LPXN	Right
TUBB3	Right
UPK3A	Right
IER3	Right
MANSC1	Right
SULT2B1	Right
CCND1	Right
BIRC5	Right
KIT	Right
IL2RG	Right
TUBB2B	Right

B. Pathway analysis of microarray

Right side pathways	**Adjusted *P***
FOXM1 transcription factor network	0.005208
CXCR3-mediated signaling events	0.007896
Direct p53 effectors	0.007896
Syndecan-1-mediated signaling events	0.012216

Table 2. RT-PCR primers

Primer sets used for RT-PCR are listed. For experiments that were confirmed by alternate primer sets, the primers used to generate the results presented in the Figures are indicated (*).

Gene	Forward	Reverse
GPRC5D	ATTCAGCTGCAGAGTGCTGAT	TCTTGCTGTGGGCTTAGTGT
GATA3	TCCTTGCTACTCAGGTGATCG	TGACCACACTGCACACTGAT
FOXM1	CCTGTGAGGGTCAAAGCTTGC	CCGTCTTTTGAGAATCAGTGGC
STMN1	CCAGGTCTGTTGGTGCTCAGA	TACACAATCCACTGGCAAGGAAA
GAPDH	CAGCAAGGACACTGAGCAAGA	TATGGGGGTCTGGGATGGAAA
Nodal	GCGCAAGATGTGGACGTGAC	CTCCGCCCATACCAGATCCT
Pitx2	GAGGTGCATACAATCTCCGATA	TGCCGCTTCTTCTTGGAC
ERα	CTGGCTACGTCAAGTCGGTT	AGGTGCTGGACAGAAACGTG
Notch-1	AATGGAGGGAGGTGCGAAGT	GGTGTGCTGAGGCAAGGATT
CD24	TTCTGGCACTGCTCCTACCC	CTGGTTACCGGGAAACGGT
Numb	CTCGGCCACGTAGAAGTTGA	CCCGTTTTTCCAAAGAAGCCT
ErbB2 (1)*	AACAGCTCGGAGACCTGCTA	GTAGTGGGCACAAGCCTCA
ErbB2 (2)	CTGACTGCCCTGACAGACTG	ATATTCACCTGGGGCCTCCT
Neu (1)*	ATTGGCTCTGATTCACCGCA	CAAGCCCTCGAGACCACAAT
Neu (2)	GCTCAGAGACCTGCTTTGGA	AGGAGGACGAGTCCTTGTAGTG
EGFR	ACCTGTGTGAAGAAGTGCCC	TCGTAGTAGTCAGGCCCACA
PR	CCAGCATGTCGTCTGAGAAA	GCCTGGCTCTCGTTAGGAA
ELF5	TGCCTTTGAGCATCAGACAG	TACTGGTCGCAGCAGAATTG
b-casein	GGTGAATCTCATGGGACAGC	AGATGGTTTGAGCCTGAGCA
Sox9	AACTTCTGTGGGAGCGACAA	CACTTGCACCTCGTCTCTCTT
SMA	ATCATTGCCCCTCCAGAACG	GAAGGTAGACAGCGAAGCCA
p63	AGCCTCCTGGCTACATACCT	CACGAGAAATGAGCTGGGGT
Cd1d	CCAGAGCCTTTGTGTACCAGT	CAGGCAGCGGAAGGTGTAAT
RXRα	CATCTTTGACAGGGTGCTAACA	GGGTTTGAGAGCCCCTTAGAG
FGF8	GCAGAAGACGGAGACCCCTT	GCCTTTGCCGTTGCTCTTGG
Wnt10b	ATCCTGCACCTGAACCGCTG	TGCTTAGAGCCCGACTGAACA
Hes1	CGGACAAACCAAAGACGGC	GAATGCCGGGAGCTATCTTTCT
Cyp26	CAAGCAGCGAAAGAAGGTGAT	CTGCTGACTTCCTCAGCGAT

HER2/*Neu* causes L-R asymmetric ductal growth and alters L-R gene expression in TMGs

To address the possibility that mammary ductal epithelium might be primed for differential growth during neoplasia, we quantified ductal networks in MMTV-cNeu$^{Tg/Tg}$ mice, which are a commonly used model of HER2+ breast cancer (Hutchinson and Muller 2000). Compared to WT, the ductal network area was smaller in 4-week MMTV-cNeu$^{Tg/Tg}$ TMGs and in particular, left-sided MMTV-cNeu$^{Tg/Tg}$ networks were significantly smaller than their right-sided counterparts (Figure 9A, C). Left-sided networks also contained fewer branch points, and had higher fractal dimension, relative density, and number of TEBs (Figure 9A, C). Morphological asymmetry persisted through the end of pubertal development, with left-sided networks maintaining decreased area and higher numbers of branch points and TEBs (Figure 9B, C). Given the L-R differences in MMTV-cNeu$^{Tg/Tg}$ ductal network growth and pattern, we evaluated whether MMTV-cNeu$^{Tg/Tg}$ TMGs have asymmetric *ErbB2*/*Neu* expression or activity. Although RT-PCR showed that *Neu* expression was elevated in right-side TMGs, endogenous *ErbB2* expression was L-R equivalent, as was *Numb*, a notch inhibitor whose expression is regulated by ErbB2 (Lindsay, Jiao et al. 2008) (Figure 9D). Moreover, phospho-ErbB2/Neu immunoprecipitation showed equivalent levels in left and right side TMGs, suggesting similar activation of ErbB2/Neu signaling on both sides (Figure 9D).

Further analysis of MMTV-cNeu$^{Tg/Tg}$ TMGs indicated that molecular laterality was amplified, sustained, or inverted in a gene-specific manner by comparison to WT.

Notch-1 expression was approximately 3-fold higher in right-sided 4-week MMTV-cNeu$^{Tg/Tg}$ TMGs (Figure 9E), which is an amplification of the modest *Notch-1* asymmetry that was present in WT TMGs (Figure 8E and Figure 10). In 10-week MMTV-cNeu$^{Tg/Tg}$ TMGs, asymmetric *Notch-1* expression was inverted, with approximately 2-fold higher expression in left-side glands (Figure 9E). Because *Notch* influences breast cancer cell sensitivity to several therapeutic agents, including trastuzumab, gefitinib, docetaxel, and tamoxifen (Wang, Li et al. 2010), the L-R uncoupled regulation of *Notch-1* expression in MMTV-cNeu$^{Tg/Tg}$ TMGs may be important in the context of differential disease progression. In addition, *FoxM1* and *Gata-3*, which were left-side elevated in 4-week WT TMGs (Figure 8E), were decreased on both sides in MMTV-cNeu$^{Tg/Tg}$ TMGs; however, the fold decrease for *FoxM1* was greater on the left side (Figure 10) resulting in net L-R symmetric expression (Figure 9E). Analysis of 10-week MMTV-cNeu$^{Tg/Tg}$ TMGs showed that *FoxM1* expression was further decreased, albeit the fold decrease was greater for right-side glands (Figure 9E and Figure 10). Given the additional role of *FoxM1* in modulating endocrine and chemotherapeutic resistance in breast cancer cells (Carr, Park et al. 2010, Kwok, Peck et al. 2010, Millour, Constantinidou et al. 2010), the L-R uncoupled regulation of *FoxM1* expression in MMTV-cNeu$^{Tg/Tg}$ TMGs was notable. We also found similar L-R asymmetric regulation of *Gata-3* in MMTV-cNeu$^{Tg/Tg}$ TMGs, which resulted in modestly higher left-sided expression by 10-weeks (Figure 9E and Figure 10).

Genes with symmetric expression in 4-week MMTV-cNeu$^{Tg/Tg}$ TMGs included *ER*α, *CD24*, *nodal*, and *Pitx2* (Figure 9E). However, by 10 weeks their

expression was elevated in left-sided glands, with the exception of *nodal*, which was elevated on both sides (Figure 9E). *GPRC5D*, which was right-side elevated in 4-week WT TMGs (Figure 8E), also was right-side elevated in 4-week MMTV-cNeu$^{Tg/Tg}$ TMGs (Figure 9E), despite an overall marked reduction in expression on both sides (Figure 10). *Stmn-1* was asymmetric in 4-week MMTV-cNeu$^{Tg/Tg}$ TMGs (Figure 9D, Figure 10) but by week-10 was increased only on the left-side, resulting in inverted asymmetric expression (Figure 9E).

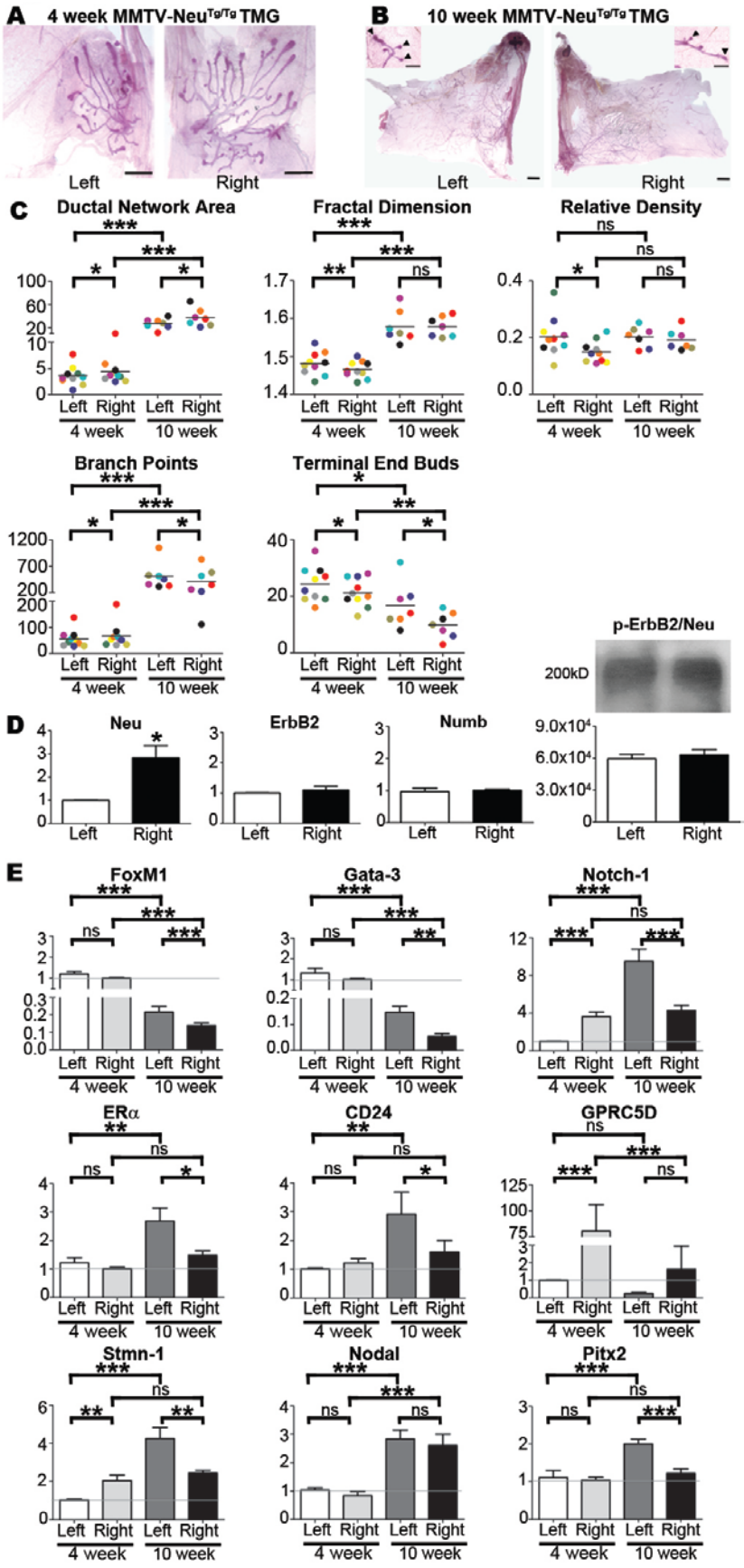
A
4 week MMTV-Neu^Tg/Tg TMG
Left
Right
B
10 week MMTV-Neu^Tg/Tg TMG
Left
Right
C
Ductal Network Area
Fractal Dimension
Relative Density
Branch Points
Terminal End Buds
p-ErbB2/Neu
200kD
Left Right Left Right
4 week
10 week
D
Neu
ErbB2
Numb
Left
Right
E
FoxM1
Gata-3
Notch-1
ERα
CD24
GPRC5D
Stmn-1
Nodal
Pitx2

Figure 9. Morphological and molecular analysis of MMTV-cNeu$^{Tg/Tg}$ TMGs. TMGs from MMTV-cNeu$^{Tg/Tg}$ mice such as the representative L-R matched pairs shown at 4-weeks (A) and 10-weeks (B) were processed for morphometric analysis and data for matched L-R pairs in individual mice were color coded as described in Figure 8 and tested by Grubb's Outlier test, which indicated an absence of outliers. Ductal network area, fractal dimension, relative density, branch points, and TEBs exhibited significant L-R differences at 4 weeks (C) as determined by one-tailed paired student's t-test (*$p<0.05$; **$p<0.01$). Ductal network area, branch points, and TEBs remained significantly L-R different at 10 weeks (C). SYBR Green-based RT-PCR showed asymmetric expression of *Neu*, but symmetric mRNA expression of *ErbB2* and *Numb* (D). Bars represent mean ± SEM. $N \geq 5$, *$p = 0.003$. Results were confirmed with a second primer set listed in Table 1. Total ErbB2/Neu protein was immunoprecipitated from left or right TMGs immunoblotted, and probed with anti-phospho-ErbB2/Neu. Densitometry of triplicate results indicated no significant L-R differences (D). SYBR Green-based RT-PCR analysis of gene expression in left vs. right TMGs of MMTV-cNeu$^{Tg/Tg}$ mice was performed as described in Figure 8 E. Bars represent mean ± SEM of 5 mice, *$p<0.05$; **$p<0.01$; *** $p<0.001$ (two-tailed paired student's t-tests).

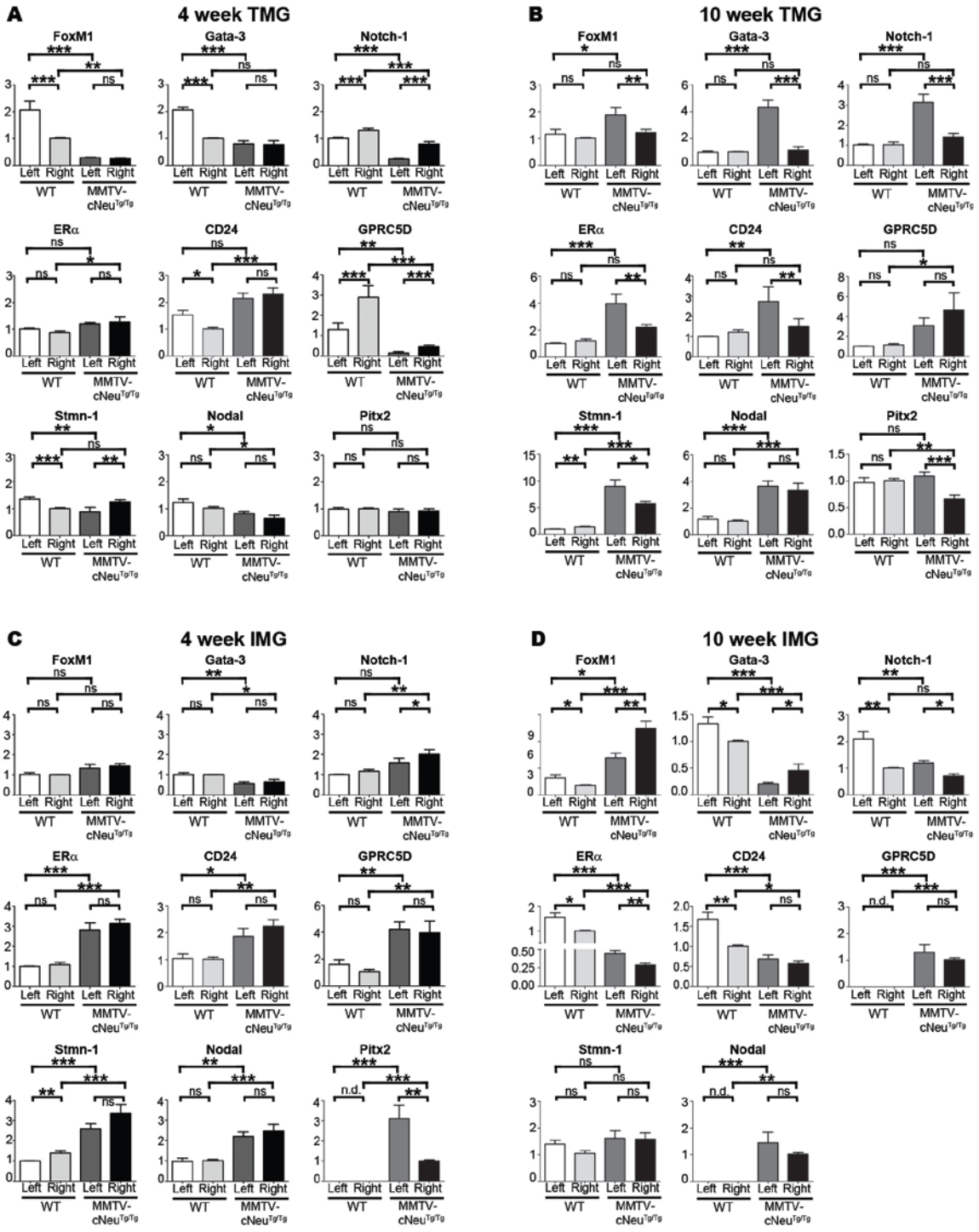
A
4 week TMG
B
10 week TMG
C
4 week IMG
D
10 week IMG
FoxM1
Gata-3
Notch-1
ERα
CD24
GPRC5D
Stmn-1
Nodal
Pitx2
Left Right Left Right
WT
MMTV-cNeuTg/Tg
n.d.

Figure 10. RT-PCR analysis of mammary gene expression in wild type versus MMTV-cNeu$^{Tg/Tg}$ mice. RT-PCR was used to assess gene expression in L-R paired 4-week TMGs (A), 10-week TMGs (B), 4-week IMGs (C), 10-week IMGs (D). For 4-week TMGs, data were normalized relative to WT right-sided glands for all genes except *Notch-1, ERα, and GPRC5D* , which were normalized relative to WT left-sided glands. Comparison of fold differences between WT and MMTV-cNeu$^{Tg/Tg}$ glands indicated that *FoxM1*, *Gata-3*, *Notch-1*, CD24, *GPRC5D*, and *Stmn-1* were independently up or down-regulated in left versus right-sided glands. For 10-week TMGs, data were normalized relative to WT left-sided glands for all genes except *FoxM1, Gata-3, Nodal, and Pitx2*, which were normalized relative to WT right-sided glands. Comparison of fold differences between WT and MMTV-cNeu$^{Tg/Tg}$ glands indicated that *FoxM1*, *Gata-3*, *Notch-1*, CD24, *GPRC5D*, and *Pitx2* were independently up or down-regulated in left versus right-sided glands. For 4-week IMGs, data were normalized relative to WT right-sided glands, except for *Notch-1, ERα, and Stmn-1,* which were normalized to WT left-sided glands. Comparison of fold differences between WT and MMTV-cNeu$^{Tg/Tg}$ glands indicated that all genes examined were similarly up or down-regulated in left versus right-sided glands except *Notch-1*, which was slightly more elevated in MMTV-cNeu$^{Tg/Tg}$ right-sided glands compared to WT. RT-PCR showed gene expression in 10-week left vs. right IMGs (D). For 10-week IMGs, data were normalized relative to WT right-sided glands for all genes. Comparison of fold differences between WT and MMTV-cNeu$^{Tg/Tg}$ glands indicated that *FoxM1*, *Gata-3*, *Notch-1*, ERα, and *CD24* were independently up or down-regulated in left versus right-sided

glands. Bars represent mean ± SEM of ≥ 3 mice, *p<0.05; **p<0.01; *** p<0.001, two-tailed paired student's t-tests.

IMGs are refractory to *HER2*/*Neu*-induced asymmetric growth and show delayed L-R asymmetric gene expression

Although mouse TMGs share more similarity with human mammary glands than inguinal mammary glands (IMGs) (Veltmaat, Ramsdell et al. 2013), IMGs are more commonly used in experimentation because of their larger size and easier accessibility (Cardiff and Wellings 1999, Brill, Boecher et al. 2008). Therefore, we also examined IMGs. Like TMGs, IMGs showed no significant L-R differences in morphology at either 4-weeks or 10-weeks (Figure 11A-C). Unlike TMGs, early pubertal IMGs showed an absence of significant molecular asymmetry except for *Stmn-1*, which was modestly right-side increased (Figure 11D). However, by the end of puberty, 10-week IMGs had developed molecular L-R asymmetry similar to that observed in 4-week WT TMGs, with left-side elevated expression of *FoxM1*, *Gata-3*, *Notch-1*, *ER*α, and *CD24* (Figure 11D).

As previously reported (Mukherjee, Louie et al. 2000), ductal networks in MMTV-cNeu$^{Tg/Tg}$ IMGs were smaller compared to WT, and we found symmetric morphology at both 4 and 10-weeks (Figure 11A-C). Although there were overall changes in gene expression relative to WT (Figure 10), 4-week MMTV-cNeu$^{Tg/Tg}$ IMGs did not exhibit molecular L-R asymmetry, with the exception of modest right-side elevation of *Notch-1* and a more robust 3.5-fold left-side elevation of *Pitx2* (Figure 11H). Although *Pitx2* was not associated with asymmetric ductal growth *per se* in either TMGs or IMGs, given that altered *Pitx2* methylation occurs in breast and other cancer types (Wilting and Hagedorn 2011) the overall changes in *Pitx2* expression nevertheless suggest a potential role in *HER2*/*Neu*-induced neoplasia.

By the end of puberty, MMTV-cNeu$^{Tg/Tg}$ IMGs showed pronounced molecular asymmetry, as exemplified by right-side elevated *FoxM1* and *Gata-3* expression and left-side elevated *ER*α and *Notch-1* (Figure 11H). Thus by comparison to TMGs, both WT and MMTV-cNeu$^{Tg/Tg}$ IMGs were temporally delayed in developing molecular asymmetry, which may account for their remaining refractory to *HER2*/*Neu*-induced asymmetric epithelial growth and morphogenesis.

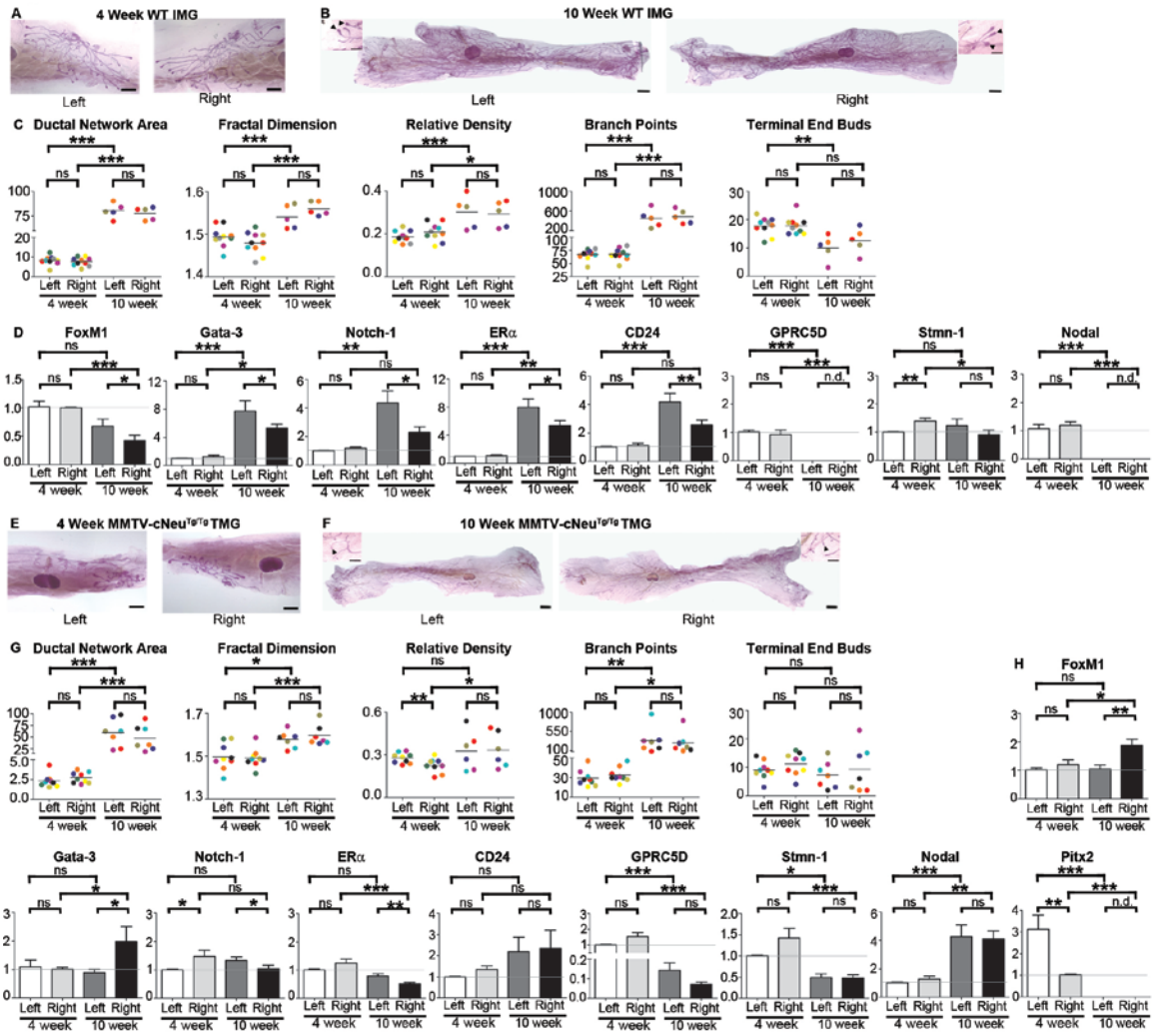

Figure 11. Morphological and molecular analysis of IMGs. L-R pairs of IMGs from 4-week (A) and 10-week (B) wild type and 4-week (E) and 10-week (F) old MMTV-cNeu$^{Tg/Tg}$ mice were processed and analyzed as described in Figure 8 A-C. Ductal network area, fractal dimension, relative density, branch points, and TEBs did not exhibit significant L-R differences (C, G) as determined by one-tailed paired student's t-test. SYBR Green-based qRT-PCR analysis of gene expression of left vs. right IMGs of wild type (D) and MMTV-cNeu$^{Tg/Tg}$ (H) mice was performed as described in Figure 8 E. *Pitx2* was not detectable in wild type IMGs at either

age nor in MMTV-cNeu$^{Tg/Tg}$ IMGs at 4 weeks. Bars represent mean ± SEM of ≥3 mice, *p = 0.01 (two-tailed paired student's t-tests).

TMG molecular laterality is associated with differential breast cancer patient survival

To determine if L-R differences detected in mouse mammary glands are clinically relevant, the genes identified in our microarray experiment (Figure 8D) were evaluated in a large number of breast tumor gene expression data sets for which corresponding patient outcome is also known (n=1334). Of the 161 transcripts identified in the microarray, we were able to map 96 of them by Unigene ID to their human transcript counterpart for each patient.

Because the sidedness of tumor location was not available in the clinical annotation files, patients were assigned to left (n=642) or right-side (n=692) groups based on whether their tumor gene expression profiles more closely matched with the left or right profiles identified in the mouse microarray. Notably, right-side gene expression was linked to poorer patient survival (Figure 12A). We next analyzed subsets of patients with HER2+ and HER2- tumors. Whereas the relationship between L-R gene expression and outcome fell just short of significance in the HER2 over-expressing subset (Figure 12B), the relationship was significant in the HER2- subset (Figure 12C). It should be noted that because HER2 status was not available in the clinical annotation files, we assigned patients to the HER2+ and HER2- subsets based on mean *ERBB2* transcript levels. For this reason, and also because of statistical power limitations due to the HER2+ subset containing far fewer patients (n=276) than the HER2- subset (n=1058), the relationship between HER2+ patient survival and L-R gene expression may be unclear and require additional investigation with a larger HER2+ test cohort.

Since ER status also is tightly linked to breast cancer patient outcome (Sotiriou and Pusztai 2009), we evaluated L-R gene expression patterns in ER+ and ER- patient subsets. In both subsets, right-side gene expression was associated with decreased survival (Figure 12D, E). Lastly, we performed univariate Cox-regression survival analyses with each of the L-R transcripts, which identified a 20-gene subset that likely drove the predictive capacity of the complete 96-gene set (*$p<0.05$, Cox-regression) (Figure 12F). Indeed, the evaluation of these 20 genes among the 1334 patient cohort outperformed the original 96 L-R gene set (Figure 12G). Thus, the L-R gene expression profiles identified in mouse mammary glands are significantly linked to breast cancer patient survival rates, and demonstrate that right-sided gene expression is associated with poorer survival.

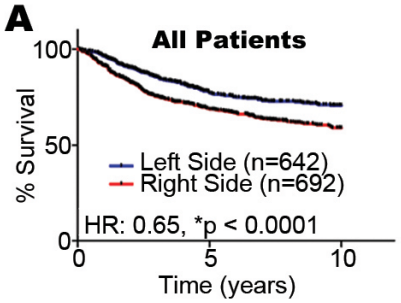

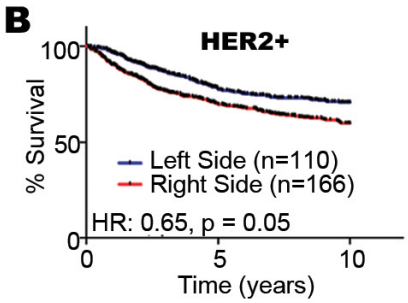

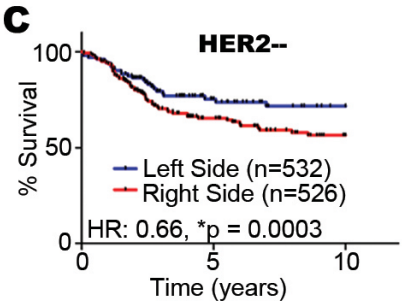

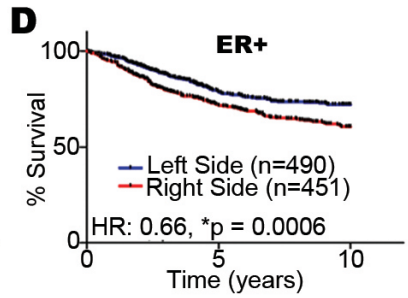

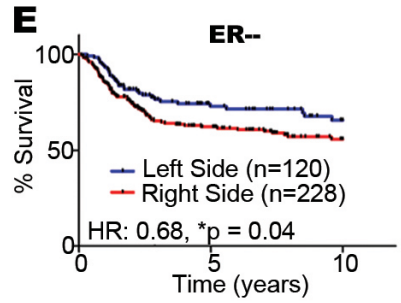

F

Gene	Hazard ratio	p-value	Side	References
TMEM59	0.80	<0.0001	Left	N/A
EHHADH	0.88	0.04	Left	N/A
SCEL	1.11	0.003	Right	N/A
PADI3	1.11	0.007	Right	(52)
TYRP1	1.12	0.0003	Right	(53-55)
AQP3	1.13	0.002	Right	(56-59)
AP1M2	1.13	0.01	Right	(60)
MCM5	1.14	0.003	Right	(61-63)
SCNN1B	1.15	0.0004	Right	(64)
IVL	1.15	0.002	Right	N/A
TUBB3	1.17	0.0008	Right	(65-67)
PKP3	1.18	0.0004	Right	(68-69)
PHLDA2	1.18	<0.0001	Right	N/A
PLK1	1.19	<0.0001	Right	(70-74)
BIRC5	1.20	<0.0001	Right	(75-80)
SFN	1.20	<0.0001	Right	(81-85)
CCNF	1.21	<0.0001	Right	N/A
RBM35B	1.23	<0.0001	Right	N/A
KIF20A	1.24	<0.0001	Right	(86-88)
SPAG5	1.26	<0.0001	Right	N/A

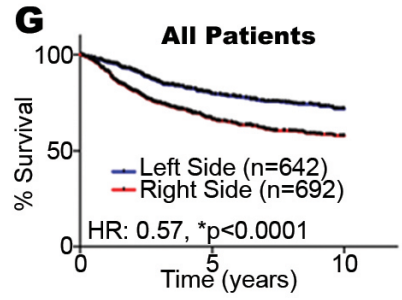

Figure 12. Comparative genomic analysis of mouse L-R mammary gene expression profiles with human breast tumors and the relationship to breast cancer patient survival. Compilation of a large cohort of breast cancer patients from multiple studies available through the Gene Expression Omnibus (http://www.ncbi.nlm.nih.gov/geo/) was compared to the microarray in Figure 8 to

test the association between laterality associated genes and patient survival. Hazard ratios (HR) are indicated for all patients (A), and HER2+ (B), HER2- (C), ER+ (D), ER- (E) subsets. A 20-gene subset of the 96 L-R TMG gene expression set (F) is a robust predictor of outcome among all breast cancer patients (G). References are provided for genes previously implicated in oncogenesis; those with none available (N/A) are indicated. Survival curves were graphed using Graphpad Prism® 5 and statistical tests were completed in R.

DISCUSSION

Our results indicate that despite their morphological symmetry, mammary glands are molecularly lateralized. Although left and right glands express the same genes, the relative levels of gene expression significantly differ and are subject to L-R uncoupled regulation during pubertal development. Our results also demonstrate that many of the genes associated with the left side are down-regulated, yet remain elevated or amplified on the right-side in TMGs of MMTV-cNeu$^{Tg/Tg}$ mice, consistent with more aggressive disease progression reported for right-sided breast tumors (Fatima, Zaman et al. 2013). Moreover, the L-R uncoupled gene expression is accompanied by asymmetric growth and morphogenesis of the ductal epithelium. The molecular laterality of mammary glands at the start of puberty appears to be important in potentiating *HER2*/*Neu* oncogene-mediated asymmetric growth since IMGs, which exhibit L-R differences in gene expression at the end of puberty, but not at the start, fail to undergo L-R asymmetric growth in MMTV-cNeu$^{Tg/Tg}$ mice. From the perspective of modeling human breast development and cancer, these results confirm there are significant differences between thoracic and inguinal glands and provide the first evidence that each mammary pair is independently L-R regulated regardless of its anterior or posterior location. By analogy to anterior-posterior differences that underlie differential development and neoplastic susceptibility of mouse TMGs versus IMGs (Veltmaat, Ramsdell et al. 2013), as well as the processes that establish molecular L-R differences in other bilaterally symmetric tissues (Golding, Partridge et al.

2004, Golding, Tsoni et al. 2004, Chintapalli, Terhzaz et al. 2012), we hypothesize that mammary laterality may be rooted in embryonic patterning. Therefore, future investigation to determine the connections between positional differences in gene expression, axial patterning, and the relationship to mammary development and tumorigenesis will be revealing. Furthermore, given the roles of *ErbB2*/*HER2* in normal and neoplastic mammary development (Eccles 2011), as well as the significant link we found between L-R gene expression and breast cancer patient survival, our findings highlight laterality as a parameter that warrants greater consideration in experimental design in mouse mammary models as well as clinical analysis of breast cancer patients.

CHAPTER THREE

CHAPTER 3.2: MAMMARY STEM CELLS EXHIBIT LEFT-RIGHT DIFFERENCES IN SELF-RENEWAL CAPACITY AND LAPATINIB SENSITIVITY IN WILD TYPE AND MMTV-CNEU MICE

INTRODUCTION

Breast cancer laterality is an understudied aspect of breast cancer tumorigenesis and biology. Epidemiological reports demonstrate that more tumors form in the left breast (Perkins, Hotes et al. 2004, Roychoudhuri, Putcha et al. 2006, Saleh and Abdeen 2007, Arkoob, Al-Nsour et al. 2010, Wilting and Hagedorn 2011, Fatima, Zaman et al. 2013, Veltmaat, Ramsdell et al. 2013, Zeeneldin, Ramadan et al. 2013), and that tumors that develop in the right breast are more aggressive metastasize more frequently than tumors that form in the left breast (Saleh and Abdeen 2007, Fatima, Zaman et al. 2013, Zeeneldin, Ramadan et al. 2013). These L-R differences in tumor incidence and breast cancer progression indicate that there may be L-R differences in mammary gland biology. Previously, our lab has demonstrated that in wild-type (WT) mice the left (L) and right (R) thoracic mammary glands (TMGs) are indeed lateralized in gene expression and in response to oncogene overexpression (Fuseler, Robichaux et al. 2014, Robichaux, Hallett et al. 2014). Pathway analysis of microarray data from L and R TMGs converge on pathways that regulate mammary stem cell (MaSC) differentiation and self-renewal (Smalley and Ashworth 2003, Cicalese, Bonizzi et al. 2009, Carr, Kiefer et al. 2012, Robichaux, Hallett et al. 2014), suggesting L-R differences in MaSCs.

MaSCs are a focus of both breast cancer biology as well as mammary gland biology because not only do MaSCs give rise to the entire ductal network, but these long lived cells are hypothesized to be tumor initiating cells when mutations are acquired over time (Dontu, Al-Hajj et al. 2003, Dontu, El-Ashry et al. 2004, Spike, Engle et al. 2012, Makarem, Kannan et al. 2013). MaSC self-renewal and differentiation regulation vary throughout the life-span of the organism. During embryogenesis, puberty, pregnancy, and lactation MaSCs undergo rapid proliferation, differentiation, and self-renewal to meet the developmental needs of the organism. However, outside of these distinct developmental windows, MaSCs remain quiescent and turn over very slowly (Hens and Wysolmerski 2005, Oakes, Hilton et al. 2006, Anderson, Rudolph et al. 2007, Watson and Khaled 2008, Cicalese, Bonizzi et al. 2009, Asselin-Labat, Vaillant et al. 2010, Diaz-Guerra, Lillo et al. 2012, Howard 2012, Makarem, Kannan et al. 2013, Makarem, Spike et al. 2013, Boras-Granic, Dann et al. 2014, Rios, Fu et al. 2014). These periods of rapid growth and proliferation of MaSCs closely mirrors the proliferation during tumorigenesis (Dontu, Al-Hajj et al. 2003, Hens and Wysolmerski 2005, Prat and Perou 2009). In addition, recent studies show the longest lived MaSCs arise embryonically and persist through adulthood (Boras-Granic, Dann et al. 2014). These long lived MaSCs express higher levels of ErbB2 than adult MaSC (Spike, Engle et al. 2012). HER2/ErbB2/Neu is amplified in 20-30% of breast cancers and is associated with aggressive tumor phenotype and early drug resistance (Korkaya, Paulson et al. 2008, McDermott and Wicha 2010, Reichman, Altekruse et al. 2010, Ithimakin, Day et al. 2013). Additionally, a recent study reports that

HER2 amplification in metastatic tumors occurs more frequently in the right breast (Fatima, Zaman et al. 2013). Furthermore, studies demonstrate that ErbB2/HER2 increases MaSC populations and mammosphere formation *in vitro* (Korkaya, Paulson et al. 2008, McDermott and Wicha 2010, Ithimakin, Day et al. 2013, Korkaya and Wicha 2013), suggesting ErbB2 regulates MaSC self-renewal and proliferation. Our previous findings demonstrate that the L and R mammary glands are differentially susceptible to ErbB2/Neu overexpression and L-R different in asymmetric enrichment in pathways that regulate MaSC differentiation and self-renewal (Robichaux, Hallett et al. 2014). Studies by others demonstrate the importance of ErbB2/Neu signaling in MaSC differentiation and self-renewal. Therefore we hypothesize that MaSCs are lateralized in quantity and function and are regulated by ErbB2 signaling L-R differently.

Here, we demonstrate for the first time that WT MaSCs are indeed L-R different in number, ErbB2 and EGFR expression, *in vitro* growth and self-renewal. In addition WT MaSCs respond L-R different to treatment with Lapatinib, a small molecule inhibitor that binds to both ErbB2 and EGFR. ErbB2/Neu overexpression results in a molecular inversion of upregulation of ErbB2 and EGFR expression as well as an inversion *in vitro* growth and self-renewal, and response to Lapatinib. Suggesting that ErbB2 and EGFR expression regulates response to Lapatinib treatment, and that normal MaSCs are altered L-R differently by Lapatinib.

MATERIALS AND METHODS

Mice

All experiments were performed in accordance with the regulations of the Medical University of South Carolina Institutional Animal Care and Use Committee. FVB/N wild-type and FVB/N-TgN (MMTVNeu) 202Mul mice were obtained from Taconic (Germantown, NY, USA) and JAX® Mice and Services (Bar Harbor, ME, USA). Wild-type and MMTV-cNeu$^{Tg/Tg}$ mice were fed Harlan Teklad rodent diet 2918 and provided water *ad libitum*.

RT-PCR

SYBR Green-based real time RT-PCR was performed with primers listed in Table 2. Real-time PCR miner was used to calculate Ct values and replication efficiency (Zhao and Fernald 2005). Fold changes relative to RPL7 mRNA were determined by delta-delta Ct.

Immunofluorescence

Secondary mammospheres were placed in 1.5ml tubes, briefly trypsinized, washed, then fixed in 4% paraformaldehyde for 15 minutes at room temperature. Cells were washed with PBS 2 times, then re-suspended in 2% FBS L15 media, and spun onto glass slides using a cytospin. Cells were permeabilized in 0.1% Tween-20 in PBS for 10 minutes, then blocked in 10% Normal Goat Serum (NGS) for 1 hour. Primary antibodies Anti-Chicken K8 (Novus Biologicals), and Anti-

mouse K14 (Santa Cruz) diluted at 1:50 in 0.1% Tween-20-5% NGS-PBS were incubated on slides overnight at 4ºC. Primary Antibody was removed and slides were washed with PBS 3 times. Secondary antibodies, Goat anti-chicken Alexafluor 596, and Goat anti-mouse Alexafluor 488 (Jackson Immunoreseach) were incubated on slides for 1 hour in the dark. Secondary antibody was removed and slides were washed 3 times with PBS and 2 drops of SlowFade Gold with DAPI mounting media (Invitrogen) was added to each slide. Slides were coverslipped, sealed, and then stored covered at 4ºC.

Confocal Images

Slides were imaged on a Leica Sp5 confocal imaging microscope. Images were then compiled using a xyz stack within the Leica-AF Lite software, and snapshots were converted to TIFF files and exported.

Dissociation of Thoracic Mammary Glands (TMGs)

TMGs were harvested from 4 week old euthanized virgin females. Glands were manually dissociated using a McIlwain tissue chopper then enzymatically dissociated in Leibovitz's L-15 medium without phenol red (Invitrogen), 1.5mg/ml trypsin (Sigma), and 3mg/ml collagenase I (Invitrogen) for 1 hour at 37ºC. Glands were then processed to single cells as previously described previously (Smalley 2010).

Fluorescence-activated cell sorting (FACS)

Single cell suspension of mammary epithelial cells was blocked with 5% fetal bovine serum (FBS, Invitrogen) in L15 media and incubated with the following antibodies: Anti-Mouse CD24 FITC (eBiosciences), Mouse Hematopoietic Lineage eFluor 450 Cocktail (eBiosciences), PerCP/Cy5.5 anti-human/mouse CD49f (BioLegend), and Live/Dead Stain-APC-Cy7 (Invitrogen). Cells were gated as shown in Figure 13, and the population labeled MaSC was collected.

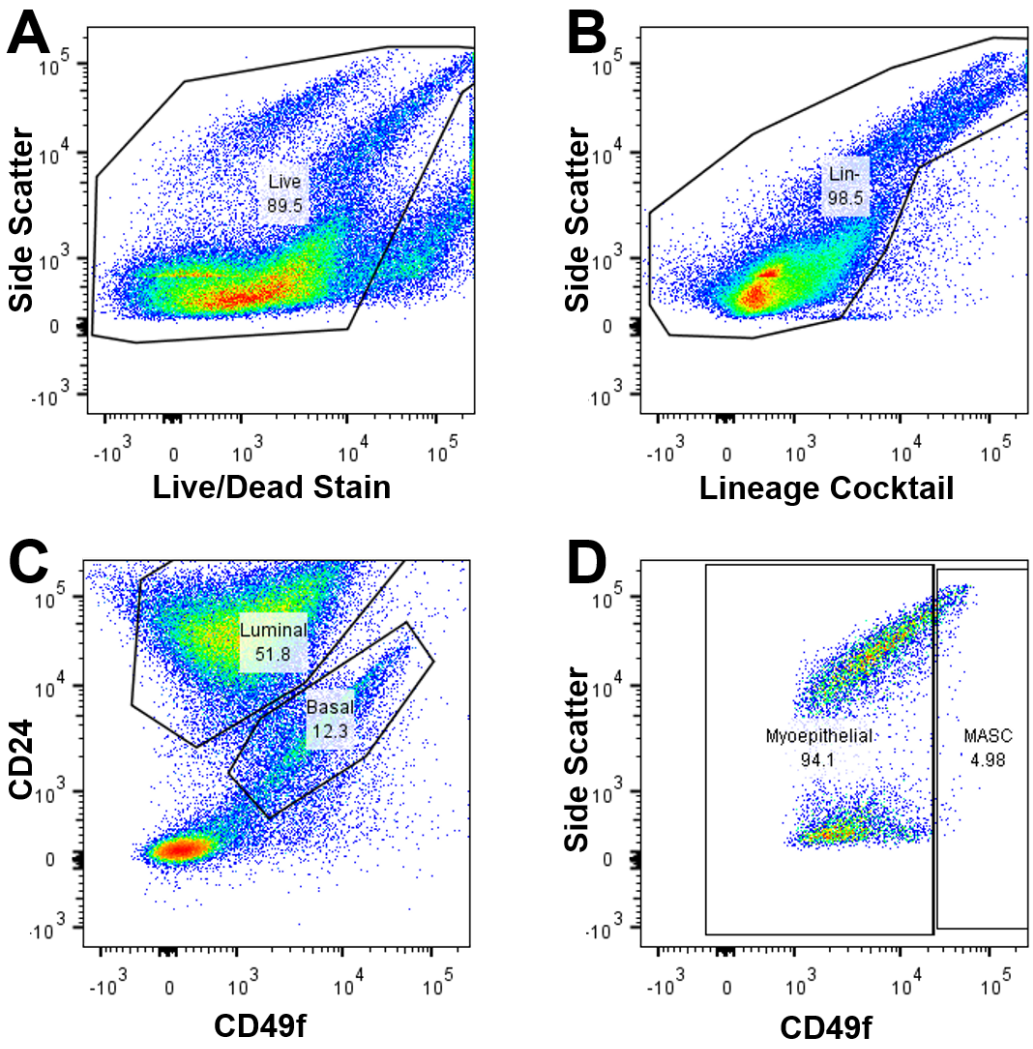

Figure 13: Mammary Stem Cell Isolation Approach. MaSCs are isolated by first removing dead cells using Live/Dead Stain APC-Cy7 conjugated (A), and selecting for cells that are lineage negative (Lin-) using lineage cocktail (B). Next, luminal and basal cells are separated by CD24-FITC conjugated antibodies and CD49f-PercP-Cy5.5 conjugated antibodies (Smalley, Titley et al. 2005, Smalley 2010, Shehata, Teschendorff et al. 2012, Smalley, Kendrick et al. 2012, Nautiyal, Steel et al. 2013) (C). MaSCs are selected by taking the top 5% CD49f staining basal cells of the LTMG (Smalley, Titley et al. 2005, Shackleton, Vaillant et al. 2006, Stingl, Eirew et al. 2006, Smalley 2010, Shehata, Teschendorff et al. 2012,

Smalley, Kendrick et al. 2012, Nautiyal, Steel et al. 2013) (D). CD24- and CD49f-cells located at the bottom left hand corner represent mammary stroma such as fibroblast and adipocytes.

Mammosphere Culture and Lapatinib Treatment

Freshly sorted TMG MaSCs were plated on ultra-low-adherence 96 well plates (Corning) at 400 cells/well for WT MaSCs and 100 cells/well for MMTV-Neu$^{Tg/Tg}$ MaSCs in 100μL of MEBM media (Lonza) supplemented with B-27 (Invitrogen), Pen/Strep (Invitrogen), 20ng/ml basic fibroblast growth factor (bFGF, Invitrogen), 20ng/ml EGF (Invitrogen), and 4μg/ml heparin sodium salt (Sigma). Cells were fed 100μL every 2-3 days. Primary spheres were counted 7 days after plating. Sphere forming efficiency (SFE) was calculated by number of spheres counted divided by number of spheres plated times 100. Secondary spheres were derived by collecting primary spheres in 1.5ml tubes, spinning down at 300 x g, and trypsinizing cells for 2 minutes at 37ºC. Trypsin was inhibited by 5% FBS L15 media then removed. Cells were washed twice in Hanks Balanced Salt Solution (Invitrogen), then re-suspended in mammosphere media and visually checked for complete sphere dissociation. Secondary spheres were collected after 14 days. Mammosphere size was determined using ImageJ by outlining mammospheres using the freehand tool, then measurement tool. Self-renewal was calculated as described by (Shaw, Harrison et al. 2012). For Lapatinib treatment, Lapatinib (Santa Cruz) was diluted in DMSO and added to media at 1:1000 dilutions to make stock Lapatinib containing media. DMSO controls were 0.1% DMSO in mammosphere media. Cells were maintained in Laptainib or DMSO during the entirety of the mammosphere experiments. All experiments were run in technical and biological triplicate.

RESULTS

WT MaSCs are quantitatively and functionally L-R different

Previous studies by our lab show that although WT mammary glands appear identical in morphology, the L and R TMGs are molecularly different, and respond to Neu oncogene overexpression differently (Fuseler, Robichaux et al. 2014, Robichaux, Hallett et al. 2014). Molecular L-R differences of the TMGs converge on several pathways including pathways that regulate MaSC differentiation (Robichaux, Hallett et al. 2014). Therefore, we hypothesized that MaSCs are L-R different in number and function. Using FACS analysis, we isolated L and R MaSCs TMGs of WT mice as described in figure 13, and validated via RT-PCR that cells isolated were bona fide MaSCs (Figure 14) based off of both fetal and adult MaSC markers previously described by others (Spike, Engle et al. 2012). Interestingly, fetal and adult MaSC markers were lateralized in expression demonstrating that MaSCs are heterogenous within a single side as well as L-R different in gene expression (Figure 14). In addition, the expression of both fetal and adult stem cell markers suggest that MaSCs at puberty are at a transition state between the fetal and adult states. Using FACS analysis we found that there are approximately 2.5 times more MaSCs in the LTMG compared to the RTMG (1.6 vs. 0.6) at 4 weeks of age (Figure 15A). Moreover, at 10 weeks, there was no change in the number of MaSCs in the LTMG, but a greater than two-fold increase in MaSCs in the RTMG, suggesting that pubescent MaSCs *in vivo* have L-R differences in growth properties. Because L and R TMGs show a differential

response to Neu overexpression (Fuseler, Robichaux et al. 2014, Robichaux, Hallett et al. 2014), and L-R differences in growth properties which are regulated by EGF family of receptor signaling, RT-PCR was used to determine if L and R MaSCs express ErbB family members L-R differently. ErbB2 was found to be L-side elevated by 40-fold as compared R-sided MaSCs (Figure 15B). In addition, EGFR was found to be upregulated in R-sided MaSCs by a remarkable 70-fold difference as compared to L-sided MaSCs (Figure 15B).

To test the functional capabilities of isolated MaSCs, FACS sorted and counted L and R MaSCs were plated at identical cell numbers and allowed to form secondary mammospheres (Figure 15C). L MaSCs formed more secondary mammospheres than R MaSCs, but R MaSCs formed larger mammospheres (Figure 15D) demonstrating that MaSCs are functionally different depending on the side of origin. To ensure that mammospheres forming were indeed composed of MaSCs, secondary mammospheres were stained using luminal marker, K8, and basal marker, K14, to determine if cells stain positive for both luminal and basal lineages, a trait of MaSCs (Shackleton, Vaillant et al. 2006, Asselin-Labat, Vaillant et al. 2008, Visvader and Smith 2011, Rios, Fu et al. 2014, Visvader and Stingl 2014). Confcoal Z-stacked images of secondary mammospheres from both L and R MaSCs stained positive for both K8 and K14 indicative of MaSCs (Figure 15E). Taken together, these data demonstrate that MaSCs from WT mice are lateralized in total stem cell number, gene expression, as well as function *in vitro*.

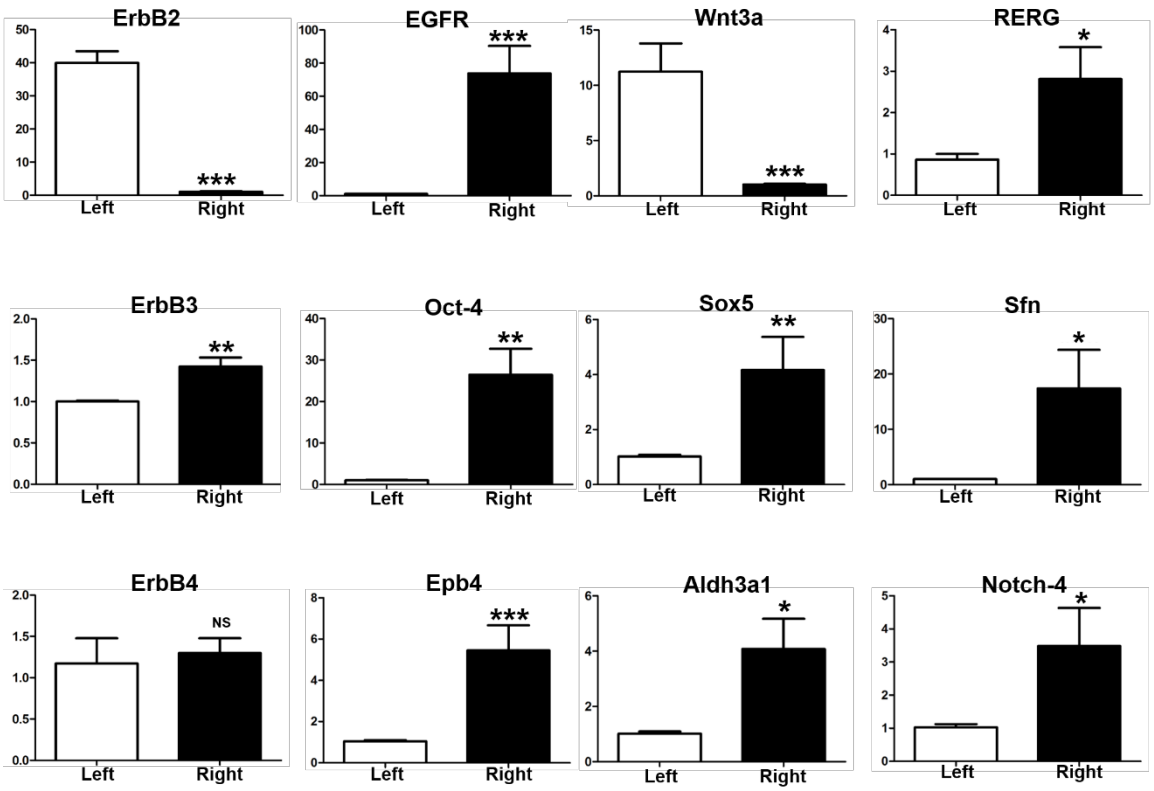

Figure 14: FACS isolated MaSCs express both fetal and adult MaSC markers and are L-R different. RT PCR demonstrates that isolated cells isolated by FACS are MaSCs. MaSCs from WT L and R TMGs express both fetal and adult MaSC markers (N=3).

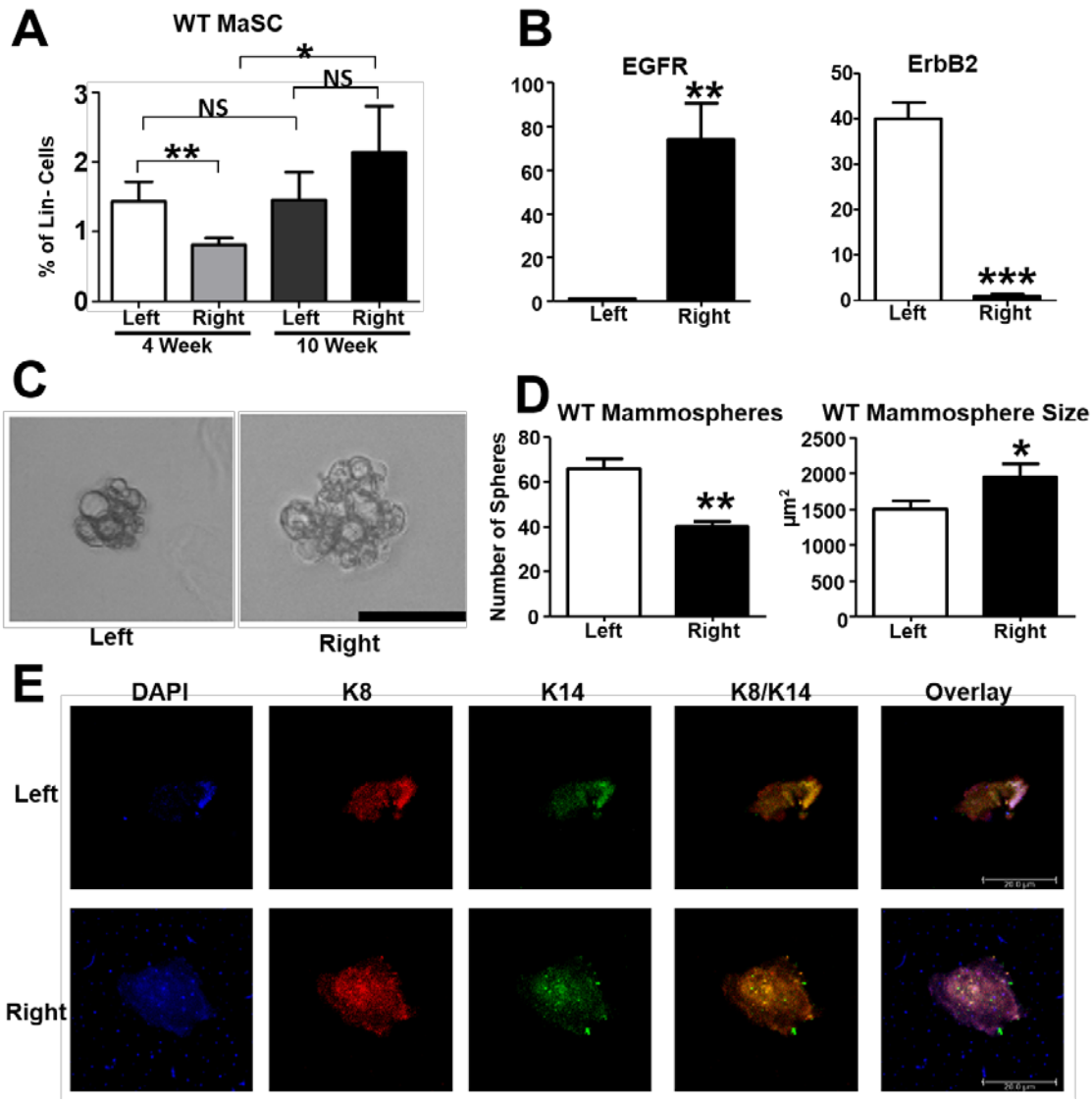

Figure 15: WT MaSCs are quantitatively and functionally L-R different. FACS analysis shows there are more MaSCs in WT LTMGs than RTMGs (N=6 at 4 weeks and N= 3 at 10 weeks; mice per N = 3-6 mice) (A). RT-PCR shows that WT MaSCs have L-R different expression of EGFR and ErbB2 (N=3) (B). Representative images of MaSCs from LTMGs and RTMGs are functionally different as demonstrated by the mammosphere assay (scale 50µm, N=3) (C). MaSCs from LTMGs form more mammospheres, but MaSCs from RTMGs form

larger mammospheres (D). Confocal images of L and R TMG MaSC derived mammospheres show that spheres co-express K14 and K8 indicative of MaSCs (scale 20 μm) (E). Students' t-test was used to determine statistical significance *, $p<0.05$ **, $p<0.01$ ***, $p<0.001$.

Neu overexpression in MMTV-Neu$^{Tg/Tg}$ mice affects MaSCs L-R differently

Since both EGFR and ErbB2 were asymmetrically expressed in WT MaSCs and MMTV-Neu$^{Tg/Tg}$ mice have asymmetric ductal network formation as well as discordant gene regulation (Robichaux, Hallett et al. 2014), we sought to characterize the effect of Neu/ErbB2 overexpression on MaSC laterality. Using FACS analysis, we isolated MaSCs from MMTV-Neu$^{Tg/Tg}$ TMGs and verified that isolated cells were indeed MaSCs (Figure 16). Again in MaSCs isolated from MMTV-Neu$^{Tg/Tg}$ TMGs, MaSCs express L-R different levels of fetal and adult MaSC markers suggesting that the populations in the L and R TMGs are heterogeneous in MaSC populations (Figure 16). Interestingly, Neu transgene expression was L-side elevated (Figure 16). Neu overexpression in MMTV-Neu$^{Tg/Tg}$ mice resulted in approximately doubling the number of L-sided MaSCs but no significant increase in the number of R-sided MaSCs resulting in MMTV-Neu$^{Tg/Tg}$ mice having amplified L-R asymmetry in MaSC numbers (Figure 17A). To determine the effect of Neu overexpression on EGFR and ErbB2 signaling, RT-PCR was used to determine if L-R differences in EGFR and ErbB2 expression were altered in MMTV-Neu$^{Tg/Tg}$ MaSCs. ErbB2 was found to be R-side elevated by approximately 6-fold as compared L-sided MaSCs (Figure 17B), whereas in WT animals ErbB2 was L-side elevated. In addition, EGFR was found to be upregulated in L-sided MaSCs by 15-fold difference as compared to R-sided MaSCs (Figure 17B), whereas in WT animals, EGFR was R-side elevated.

To determine if over-expression of Neu and inverted EGFR/ErbB2 gene expression would affect the growth properties of MaSCs, MaSCs from L and R

TMGs if MMTV-Neu$^{Tg/Tg}$ mice were plated as previously described to form secondary mammospheres (Figure 17C). In contrast to WT, MMTV-Neu$^{Tg/Tg}$ R-sided MaSCs formed more secondary mammospheres; however, MMTV-Neu$^{Tg/Tg}$ L and R-sided MaSC derived mammospheres were similar in size (Figure 17D). These results indicate that Neu over-expression inverts MaSCs growth properties *in vitro*. In addition, the data demonstrates a correlation between ErbB2 and increased mammosphere formation. To determine that MMTV-Neu$^{Tg/Tg}$ MaSC derived mammospheres were indeed composed of MaSCs, secondary mammospheres were again stained using K8 and K14. Confcoal Z-stacked images of secondary mammospheres from MMTV-Neu$^{Tg/Tg}$ L and R MaSCs stained positive for both K8 and K14 indicative of MaSCs (Figure 17E). Taken together, these data demonstrate that Neu overexpression affects MaSCs L-R differently, increasing L-sided MaSCs, and inverting EGFR and ErbB2 expression as well as MaSC in vitro growth properties suggesting a relationship between EGFR, ErbB2, and MaSC growth and self-renewal.

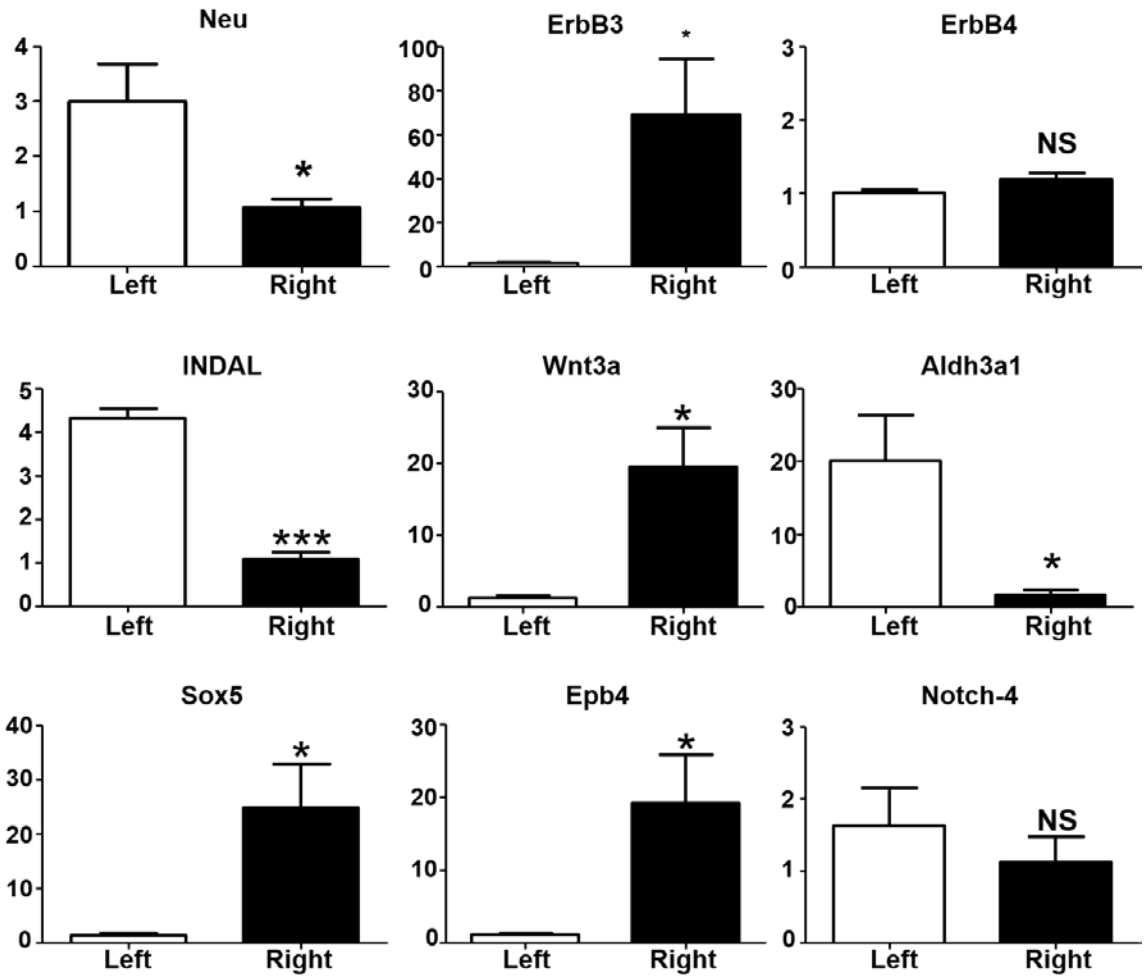

Figure 16: FACS isolated MaSCs from MMTV-Neu$^{Tg/Tg}$ TMGs have L-R differently expressed fetal and adult MaSC markers. RT PCR demonstrates that isolated cells isolated by FACS are MaSCs. MaSCs from MMTV-Neu$^{Tg/Tg}$ L and R TMGs express both fetal and adult MaSC markers albeit L-R differently.

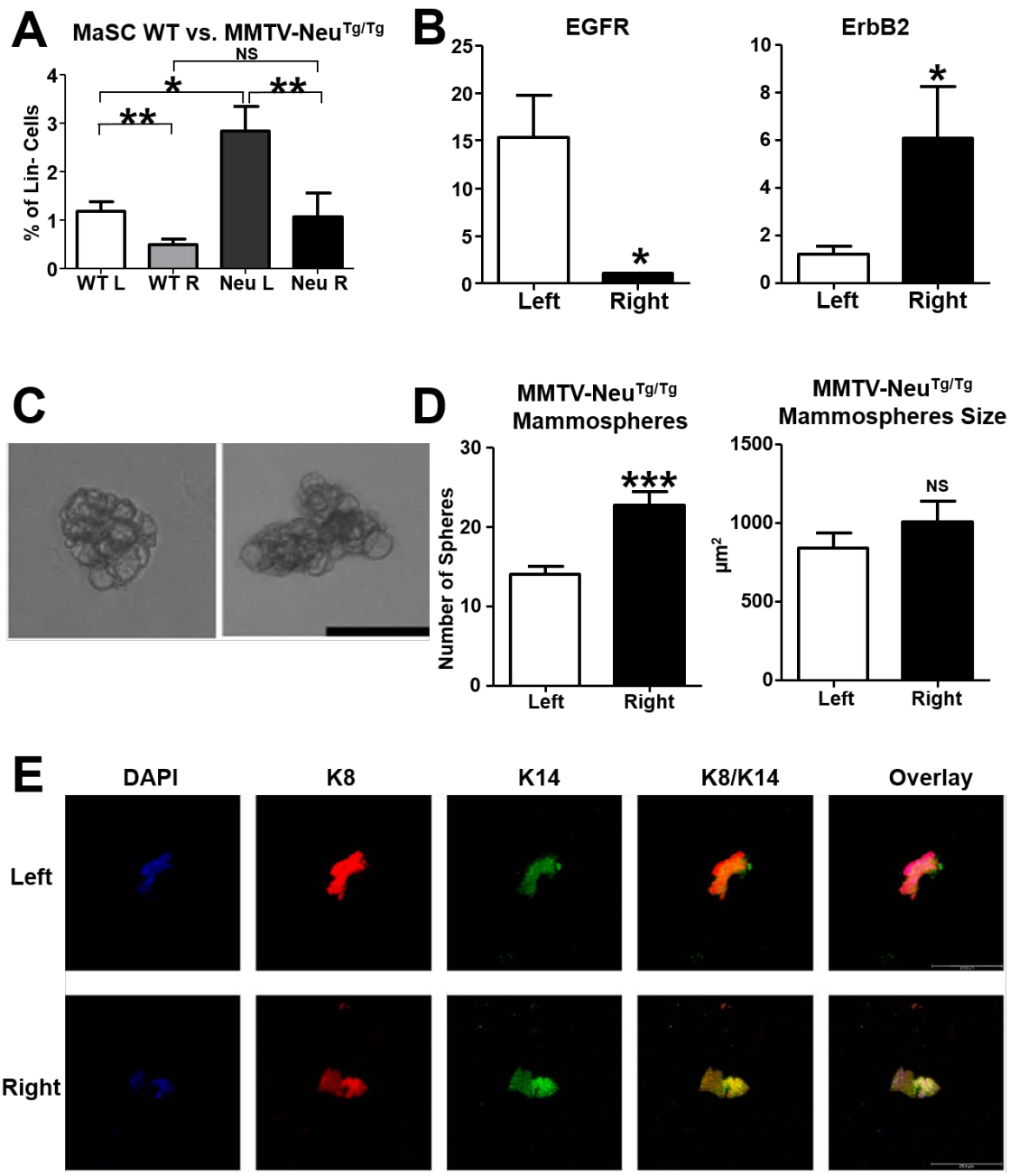

Figure 17. Neu overexpression in MMTV-Neu$^{Tg/Tg}$ mice affects MaSCs L-R differently. FACS analysis shows that MMTV-Neu overexpression causes an increase in L MaSCs but not R MaSCs (N=6) (A). RT-PCR shows that MMTV-Neu$^{Tg/Tg}$ MaSCs have inverted and L-R different expression of EGFR and ErbB2

(N=3) (B). MaSCs from LTMGs and RTMGs of MMTV-Neu$^{Tg/Tg}$ mice are functionally different as shown by the mammosphere assay (scale 50μm, N=3) (C). MaSCs from MMTV-Neu$^{Tg/Tg}$ RTMGs form more mammospheres than LTMGs, while mammosphere size is symmetric in MMTV-Neu$^{Tg/Tg}$ mice (D). Confocal images of L and R MMTV-Neu$^{Tg/Tg}$ TMG MaSC derived mammospheres show that spheres co-express K14 and K8 indicative of MaSCs (scale 20 μm) (E). Students' t-test was used to determine statistical significance *, $p<0.05$ **, $p<0.01$ ***, $p<0.001$.

MaSC L-R differences in EGFR/ErbB2 expression correlate with L-R differential response to Lapatinib treatment

To further understand the relationship between EGFR, ErbB2, and MaSC function, Lapatinib treatment of MaSC derived mammospheres of both WT and MMTV-Neu$^{Tg/Tg}$ mice was utilized. Currently, Lapatinib is FDA approved for patients with metastatic HER2+ (hormone positive or negative) breast tumors after trastuzmab treatment has failed (U.S. Food and Drug Administration 2012). Lapatinib is a small molecule inhibitor targeted to the tyrosine kinase ErbB2 receptor, that inhibits both ErbB2 and EGFR *in vitro* (Baselga, Rischin et al. 2002, Wood, Truesdale et al. 2004, Baselga 2006, Scaltriti, Verma et al. 2009). Lapatinib works by inhibition of receptor phosphorylation, resulting in receptor accumulation and cell toxicity (Scaltriti, Verma et al. 2009). Lapatinib has been shown to have a higher affinity to ErbB2 than EGFR (Scaltriti, Verma et al. 2009); yet, the ability to affect EGFR+ cancer stem cells remains unclear (Zhang, Pal et al. 2008). Since WT MaSCs have L-R different expression of ErbB2 and EGFR, we hypothesized that L and R MaSCs would have a L-R differential response to Lapatinib treatment.

To test this hypothesis, L and R WT MaSC derived mammospheres were treated with 10nM, 100nM, and 1μM Lapatinib throughout primary and secondary mammosphere formation. Left-side derived mammospheres had a dose dependent reduction in sphere formation with a reduction in self-renewal properties at the highest dose of Lapatinib treatment (Figure 18 A, B). Right-side derived mammospheres had no inhibition in sphere formation. Additionally, increasing doses of Lapatinib increase secondary sphere formation and stem-cell self-

renewal (Figure 18 A, B). Only at 1μM did self-renewal decrease for both L and R, however, 1μM Lapatinib is not considered physiologically relevant (Burris, Hurwitz et al. 2005, Chatsiproios 2010). However, this data does show that at a very high dose cell toxicity could be achieved.

To determine the effect of Lapatinib on MaSC differentiation secondary mammospheres treated with Lapatinib were stained with K8 and K14, Confocal Z-stacked images of secondary mammospheres from L-sided MaSCs show differentiated basal cells staining positive for K14, but not K8 (Figure 18C). Confocal imaging of secondary mammospheres from R-sided MaSCs stain positive for both K8, and K14, indicative of a lack of cell differentiation within MaSC pool (Figure 18C). These data suggest that higher levels of ErbB2 increase Lapatinib sensitivity whereas higher levels of EGFR protect MaSCs from Lapatinib.

Since L-R inversion of EGFR and ErbB2 in the MMTV-Neu$^{Tg/Tg}$ model as compared to WT resulted in an inversion of *in vitro* mammosphere growth, we hypothesized that the L-R inversion in EGFR and ErbB2 expression would also result in an inversion of L-R response to Lapatinib treatment as compared to WT. To test this hypothesis mammospheres derived from L and R-sided MMTV-Neu$^{Tg/Tg}$ MaSCs were treated with 10nM, 100nM, and 1μM Lapatinib throughout primary and secondary mammosphere formation (Figure 18D). L-sided MaSCs had a slight increase in mammosphere SFE with low dose Lapatinib, but then a slight decrease with higher doses; however, self-renewal remained unchanged until the highest dose of Lapatinib (Figure 18E). R-sided MaSCs had a dose-dependent reduction in SFE and self-renewal, with 1μM Lapatinib completely

killing all MMTV-Neu$^{Tg/Tg}$ MaSCs (Figure 18E). Overall increased sensitivity to Lapatinib was expected and observed since all MMTV-Neu$^{Tg/Tg}$ mammary epithelial cells overexpress Neu/ErbB2.

To determine the effect of Lapatinib on MMTV-Neu$^{Tg/Tg}$ MaSC differentiation secondary mammospheres treated with Lapatinib were stained with K8 and K14, Confocal Z-stacked images of secondary mammospheres from L-sided MMTV-Neu$^{Tg/Tg}$ MaSCs stain positive for both K8 and K14 suggesting Lapatinib does not induce cell differentiation of L-sided MMTV-Neu$^{Tg/Tg}$ MaSCs (Figure 18F). Confocal imaging of secondary mammospheres from R-sided MMTV-Neu$^{Tg/Tg}$ MaSCs stain positive for both K8, but not K14, indicating cell differentiation into mammary basal cells (Figure 18E). These data support the hypothesis that higher levels of ErbB2 increase Lapatinib sensitivity whereas higher levels of EGFR protect MaSCs from Lapatinib treatment.

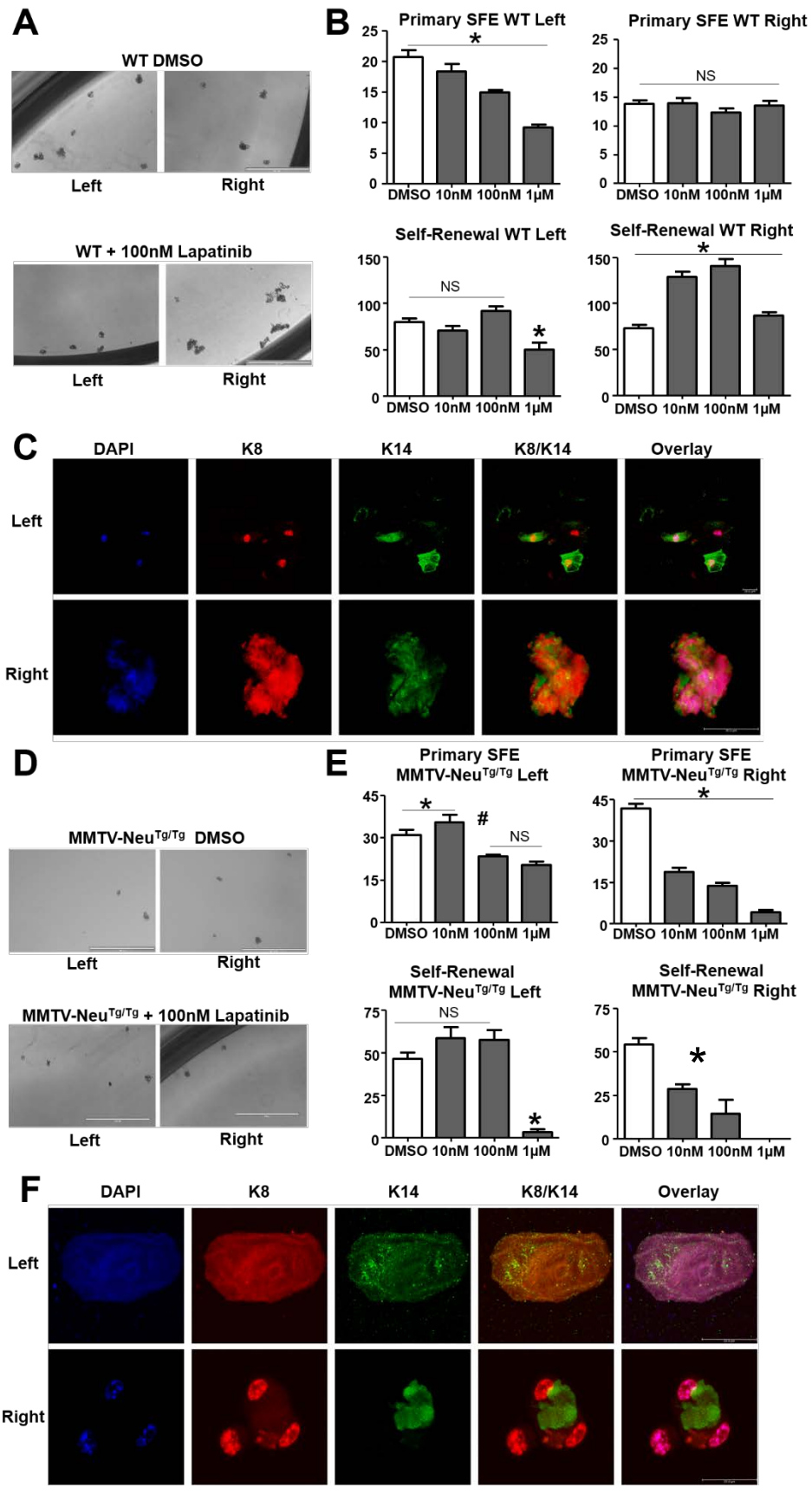
A
WT DMSO
Left
Right
WT + 100nM Lapatinib
Left
Right
B
Primary SFE WT Left
Primary SFE WT Right
NS
Self-Renewal WT Left
Self-Renewal WT Right
NS
DMSO 10nM 100nM 1μM
C
DAPI
K8
K14
K8/K14
Overlay
Left
Right
D
MMTV-Neu^Tg/Tg DMSO
Left
Right
MMTV-Neu^Tg/Tg + 100nM Lapatinib
Left
Right
E
Primary SFE MMTV-Neu^Tg/Tg Left
Primary SFE MMTV-Neu^Tg/Tg Right
NS
Self-Renewal MMTV-Neu^Tg/Tg Left
Self-Renewal MMTV-Neu^Tg/Tg Right
NS
DMSO 10nM 100nM 1μM
F
DAPI
K8
K14
K8/K14
Overlay
Left
Right

Figure 18. MaSC Left-Right differences in EGFR/ErbB2 expression correlate with L-R differential response to Lapatinib treatment. L and R WT MaSC derived mammospheres have a differential response to Lapatinib treatment (A). WT LTMG MaSC derived mammospheres show a steady decrease in primary SFE with increasing concentrations of Lapatinib and no changes in self-renewal until the highest dose of Lapatinib (B, left). However, WT RTMG MaSC derived mammospheres show no change in SFE, and an increase in self-renewal with physiologically relevant doses of Lapatinib (B, right). ANOVA analysis followed by post-test analyses were used to determine statistical significance between indicated bars *, $p < 0.001$. Confocal images of WT LTMG MaSC derived mammospheres show differentiated cells in response to 100nM Lapatinib treatment, whereas confocal images of WT RTMG MaSC derived mammospheres show dual staining for K8 and K14 indicative of MaSCs (scale 20 μm) (C). L and R MMTV-Neu$^{Tg/Tg}$ TMG MaSC derived mammospheres have a differential response to Lapatinib (D). MMTV-Neu$^{Tg/Tg}$ LTMG MaSC derived mammospheres show a slight increase in primary SFE with low dose Lapatinib treatment, and only a slight decrease in SFE with high dose Lapatinib treatment. In addition, no changes in self-renewal are seen until the highest dose of Lapatinib (E). However, MMTV-Neu$^{Tg/Tg}$ RTMG MaSC derived mammospheres show a steady decrease in primary SFE and self-renewal with increasing concentrations of Lapatinib ANOVA analysis was used to determine statistical significance *, $p < 0.001$; #, both DMSO and 10nM doses are statistically significant ($p<0.01$) than 100nM and 1um which are not statistically different (E). Confocal images of MMTV-Neu$^{Tg/Tg}$ LTMG MaSC

derived mammospheres show dual staining for K8 and K14 indicative of MaSCs even in the presence of 100nM Lapatinib, whereas confocal images of WT RTMG MaSC derived mammospheres show differentiated cells in response to 100nM Lapatinib treatment (scale 20 μm) (F).

DISCUSSION

Although our previous worked established that L and R mammary glands are molecularly distinct and could respond to elevated oncogene L-R discordantly, little functional data in L-R differences existed. The data presented here are the first to show quantitative and functional L-R differences in MaSCs. In addition, the data shown are the first to show a L-R differential response to a drug being used clinically.

Our data demonstrates an over 2-fold increase in MaSCs in the LTMG as compared to the RTMG which correlates with increase tumor formation in the left breast in humans (Perkins, Hotes et al. 2004, Roychoudhuri, Putcha et al. 2006, Saleh and Abdeen 2007, Arkoob, Al-Nsour et al. 2010, Wilting and Hagedorn 2011, Fatima, Zaman et al. 2013, Veltmaat, Ramsdell et al. 2013, Zeeneldin, Ramadan et al. 2013). Preliminary experiments show that there is a possible R-sided increase in MaSCs in WT mice suggesting that L and R MaSCs have differences in growth *in vivo.* In addition, this data demonstrates that R-sided MaSCs form larger mammospheres with a slightly higher self-renewal capacity which indicates a more “stem-like” or aggressive phenotype which correlates with more aggressive tumors forming in the right breast in humans (Saleh and Abdeen 2007, Fatima, Zaman et al. 2013, Zeeneldin, Ramadan et al. 2013). Interestingly, our data also shows that over-expression of the Neu oncogene only increases MaSCs unilaterally enhancing the L-R difference in MaSC number.

In addition to L-R differences in WT MaSCs numbers, this data suggests a role of EGFR and ErbB2 expression patterns controlling MaSC growth properties and response to Lapatinib treatment. When ErbB2 was upregulated, more mammospheres formed and mammospheres were sensitive to Lapatinib treatment; however, when EGFR was upregulated fewer mammospheres formed, but mammospheres were refractory to Lapatinib treatment.

In addition to detecting a L-R differential response to therapy in both WT and MMTV-Neu$^{Tg/Tg}$ MaSCs, a peculiar response to Lapatinib was seen in the R-side WT MaSC derived mammosphere: an increase in self-renewal. This increase in self-renewal is significant because women undergoing Lapatinib treatment also have normal tissue, and this data suggests Lapatinib treatment increases the "stem-like" potential of MaSCs in the "normal" tissue. This increased self-renewal could heighten that patient's chances of a secondary reoccurrence of a more aggressive tumor type. However, few studies exist examining the long term effects of common clinical therapies on long term cancer risks. Although the benefits of ErbB family inhibitors often out-weigh the potential risks, further studies of how ErbB family members and their inhibitors regulate stem cell properties are needed.

CHAPTER FOUR

CHAPTER 4: WILD TYPE MICE EXHIBIT A LEFT-RIGHT DIFFERENTIAL RESPONSE TO NEONATAL ESTROGEN EXPOSURE RESULTING IN ASYMMETRIC DUCTAL MORPHOGENESIS

INTRODUCTION

Since the early 1940s the role of estrogens and mammary gland development has been the focus of many studies (Greene RR 1940). In the 1970s, several reports established that neonatal exposure to 17β-estradiol (E2) increased carcinogenesis in mice exposed to the carcinogen 7,12-Dimethylbenz-[a]anthracene (DMBA) at later time demonstrating that early E2 exposure has long term and lasting effects on the mammary gland (Warner and Warner 1975, Mori, Bern et al. 1976). Additionally, studies showed that neonatal E2 exposure effected late but not early pubescent development of each mammary pair in a dose dependent manner increasing ductal network area at the highest doses (Jean 1971, Jean 1971, Mori, Bern et al. 1976, Warner 1976, Bern, Mills et al. 1983). Later studies designed to understand the mechanism of E2 long term effects, showed down regulation of the estrogen receptor alpha (ERα) (DiPaolo and Jones 2000), but an increase in endogenous E2 sensitivity at puberty (Warner, Yau et al. 1980, Wadia, Vandenberg et al. 2007). Although these studies gave insight as to why there was increased ductal network area with E2 exposure in late but not early pubescent development; these studies failed to demonstrate how glands with decreased estrogen receptor had an increased response to E2. Later studies demonstrated that estrogen mimetics such as diethylstilbestrol (DES) or Bisphenol A (BPA) result in increased tumor formation in mice (Walker 1984, Lopez, Ogren

et al. 1988, Walker 1990, Hilakivi-Clarke, Onojafe et al. 1996, Markey, Luque et al. 2001) similar to neonatal E2 exposure, and these changes to normal ductal morphogenesis induced by early estrogen exposures were observed as early as 4 weeks, the beginning of puberty (Hilakivi-Clarke, Cho et al. 1997, Markey, Luque et al. 2001). However, no studies exist to explain how early E2 exposure and down-regulated ERα receptor results in increased mammary gland estrogen sensitivity at puberty.

E2 is an essential regulator of pubescent mammary ductal morphogenesis; ovariectomy or genetic knockout of ERα results in ablation of pubescent ductal elongation (Feng, Manka et al. 2007). In addition, E2 rescued development of the mammary glands in ovariectomized mice (Daniel, Silberstein et al. 1987). However, ERα is not expressed in all mammary epithelial cell types. Some luminal progenitors and differentiated luminal cells express ERα, but MaSCs and basal cells do not express ERα (Clarke, Anderson et al. 2003, Kouros-Mehr, Slorach et al. 2006, Asselin-Labat, Vaillant et al. 2008, Visvader and Smith 2011, Carr, Kiefer et al. 2012, Shehata, Teschendorff et al. 2012, Rios, Fu et al. 2014). More recently, through lineage tracing experiments *in vivo,* MaSCs were shown to be the major contributor to ductal morphogenesis at puberty through both self-renewal and differentiation (Rios, Fu et al. 2014). Previously, E2 has been shown to play a role in regulation of MaSC proliferation and differentiation (Asselin-Labat, Vaillant et al. 2010, Joshi, Jackson et al. 2010, Simoes, Piva et al. 2011); however, the mechanism of how E2 signals to ERα- MaSCs is unclear. A pro-proliferative effect of E2 on ERα- breast cancer stem-like cells has been shown to involve the

FGF/Tbx3 pathway (Fillmore, Gupta et al. 2010), a pathway activated during embryonic mammary gland development (Davenport, Jerome-Majewska et al. 2003, Eblaghie, Song et al. 2004).

In addition to the role of MaSCs during pubescent development, long-lived MaSCs are hypothesized to be tumor-initiating cells due to opportunity of mutations to accumulate over time (Dontu, Al-Hajj et al. 2003, Dontu, El-Ashry et al. 2004, Spike, Engle et al. 2012, Makarem, Kannan et al. 2013). Approximately 60 – 75% of all diagnosed breast cancers are ERα+ (Carey, Perou et al. 2006, Bao, Yu et al. 2014), and estrogen inhibiting drugs such as tamoxifen and other aromatase inhibitors are often use to treat ERα+ breast cancers (Fisher, Costantino et al. 1998). However, breast cancer does not occur at equal rates in both breasts; more tumors form in the left breast, but right-sided tumors are more aggressive (Perkins, Hotes et al. 2004, Roychoudhuri, Putcha et al. 2006, Saleh and Abdeen 2007, Arkoob, Al-Nsour et al. 2010, Wilting and Hagedorn 2011, Fatima, Zaman et al. 2013, Veltmaat, Ramsdell et al. 2013, Zeeneldin, Ramadan et al. 2013). Previous work in our lab has demonstrated that in wild-type (WT) mice the left (L) and right (R) thoracic mammary glands (TMGs) are lateralized in gene expression pathways that regulate MaSC differentiation and self-renewal (Smalley and Ashworth 2003, Cicalese, Bonizzi et al. 2009, Carr, Kiefer et al. 2012, Robichaux, Hallett et al. 2014). In addition our data indicate that MaSCs are L-R asymmetric in number, and L and R MaSCs are molecularly and functionally different (Chapter 3). Therefore we hypothesize that early E2 exposure will also

have L-R different effects on pubescent development due to asymmetric changes in MaSC numbers and/or MaSC differentiation.

Here we show that early E2 exposure results in asymmetric ductal morphogenesis at puberty in TMGs but not inguinal mammary glands (IMGs). In addition TMGs demonstrate a L-R asymmetric down-regulation of ERα and other markers of MaSC differentiation, as well as an increase in basal cell markers and markers of MaSCs. Lastly, we show that neonatal E2 exposure results in an overall and asymmetric decrease in the luminal cell lineage and cell differentiation, as well as an overall and asymmetric increase in MaSCs and basal cell lineage. Although MaSCs are ERα-, paracrine signaling to an increased number of MaSCs may explain the increased sensitivity to endogenous E2 later in puberty as well as increased tumorigenesis when exposed to carcinogen.

MATERIALS AND METHODS

Mice

All experiments were performed in accordance with the regulations of the Medical University of South Carolina Institutional Animal Care and Use Committee. FVB/N wild-type mice were obtained from Taconic (Germantown, NY, USA). To generate E2 treated mice, WT mice were injected interscapularly along the midline with 1µl of 20µg/µl 17-β estradiol (Sigma) in ultra-pure DMSO (Fisher Scientific) for five days beginning one day after birth. Cages were covered and otherwise undisturbed for 7 days; in addition, as soon as sex was reliability determined, males were removed from cages to increase female pup viability. 1µl DMSO injected mice were used as vehicle control. Mice were fed Harlan Teklad rodent diet 2918 and provided water *ad libitum*. Mice were euthanized at 28 days of age and thoracic and inguinal mammary glands were harvested.

Histology and image collection

Carmine red stained whole mounts were prepared as previously described (de Assis, Warri et al. 2010) from #3 and #8 thoracic mammary glands (TMGs) and #4 and #9 inguinal mammary glands (IMGs) of day-28 mice and were imaged on an Olympus SZX12 stereomicroscope equipped with a Spot camera. Overlapping images of each whole mount were processed into a single composite image with Adobe Photoshop®.

Image analysis.

The color images of the mammary glands were converted to 8-bit monochrome images for image and fractal analysis. The mammary gland within an image was outlined and isolated from the background tissue and defined as a Region of Interest (ROI) (Figure 5). The isolated image of the mammary gland was thresholded using the set threshold subroutine of MetaMorph Image analysis software (ver. 6.1). The area (A) and integrated optical density (IOD) of the ductal epithelial networks were measured using the integrated morphometry analysis sub-routine of MetaMorph. The fractal dimension (**D**), was determined by the box counting method using HarFA software (Nezadal, Zemeskal et al. 2001) [http://www.fch.vutbr.cz/lectures/imagesci]) applied to the isolated image of the mammary gland using the same threshold values.

Integrated optical density (IOD).

The IOD of the mammary gland ROI delineated by the thresholded boundaries is considered to be the "mass" of the ROI and a measurement of the total amount of labeled material in the region (Walter and Berns 1986, Fuseler, Merrill et al. 2006, Fuseler, Millette et al. 2007, Rogers and Fuseler 2007, Fuseler and Valarmathi 2012). The IOD of a selected region can be expressed as the weighted sum of the image histogram in which each term in the histogram is multiplied by the gray value it represents. When applied to thresholded boundaries the IOD is defined by the following expression:

$$IOD(T1, T2) = \sum_{GV=T1}^{T2} H(GV) \times GV$$

Where the upper and lower thresholds defining the ROI in the histogram are given by T1 and T2. GV is the gray value of each pixel and H (GV) is the gray level histogram.

Application of the fractal dimension (D)

The thoracic mammary glands in the wild type and E2 treated mice mice appear as irregular and complex objects composed of parts at different levels of resolution (ducts of different bore sizes) which are functionally and physiologically similar (self-similar) to the whole object. Under the conditions of these properties, the thoracic mammary glands can be considered fractal objects and their topological dimension, the fractal dimension (**D**), be expressed by a non-integer number lying between two Euclidian integer topological dimensions (Grizzi, Russo et al. 2005). The values of **D** characterizing the thoracic mammary glands are therefore fractional. Since the thoracic mammary gland is essentially a 2-dimensional object, the **D** values will lie between 1 and 2. As the mammary gland becomes more complex and irregular, its **D** value becomes greater approaching 2. In applying fractal analysis, the **D** value of the mammary gland is determined by applying the box-counting method (Fernandez and Jelinek 2001, Grizzi, Russo et al. 2005). The box-counting method has been the most widely used and general model for applying fractal analysis to biological and non-biological systems. The box-

counting method consists of a grid of boxes of size e superimposed over the image of the structure, and the number of boxes containing any part of the structure recorded as ***N(e)***. A fractal object expresses a straight line when Log[***N(e)***] is plotted against Log(***1/e***). The box fractal dimension **D** can be determined from the slope of the regression line. That is: **D=** Log[***N(e)***] / Log(***1/e***). The **D** values of the thoracic mammary glands were determined using HarFA software (Nezadal, Zemeskal et al. 2001) [http://www.fch.vutbr.cz/lectures/imagesci]. The HarFA software assigned mesh sizes of boxes with **e** values ranging from 2 to 207 pixels and 30 steps within this range were calculated to generate the Log[***N(e)***] versus Log(***1/e*)** lines to determined .

Branch points and terminal end buds (TEBs)

Branch points and TEBs were quantified by manual counting from the images.

RT-PCR

mRNA was isolated using Qiagen lipid RNA mini kits, and converted to cDNA using BioRad iScript kit. SYBR Green-based (BioRad) RT-PCR was performed with primers listed in Table 2. Real-time PCR miner was used to calculate Ct values and replication efficiency (Zhao and Fernald 2005) and fold changes relative to GAPDH mRNA were determined by delta-delta Ct.

Dissociation of Thoracic Mammary Glands (TMGs)

TMGs were harvested from 4 week old euthanized virgin females. Glands were manually dissociated using a McIlwain tissue chopper then enzymatically

dissociated in Leibovitz's L-15 medium without phenol red (Invitrogen), 1.5mg/ml trypsin (Sigma), and 3mg/ml collagenase I (Invitrogen) for 1 hour at 37ºC. Glands were then processed to single cells as previously described by Smalley et al (Smalley 2010).

Fluorescence-activated cell sorting (FACS)

Single cell suspension of mammary epithelial cells was blocked with 5% fetal bovine serum (FBS, Invitrogen) in L15 media and incubated with the following antibodies: Anti-Mouse CD24 FITC (eBiosciences), Mouse Hematopoietic Lineage eFluor 450 Cocktail (eBiosciences), PerCP/Cy5.5 anti-human/mouse CD49f (BioLegend), and Live/Dead Stain-APC-Cy7 (Invitrogen). Cells were gated as shown in Figure 13, and the population labeled MaSC was collected. Briefly, MaSCs are isolated by first removing dead cells using Live/Dead Stain APC-Cy7 conjugated, Lin- cells were selected by selecting cells that did not stain positive for the lineage cocktail antibodies that e450 conjugated. Luminal and basal cells are separated by CD24-FITC conjugated antibodies and CD49f-PercP-Cy5.5 conjugated antibodies, respectively (Smalley, Titley et al. 2005, Smalley 2010, Shehata, Teschendorff et al. 2012, Smalley, Kendrick et al. 2012, Nautiyal, Steel et al. 2013). MaSCs are selected by taking the top 5% CD49f staining basal cells of the WT LTMG (Smalley, Titley et al. 2005, Shackleton, Vaillant et al. 2006, Stingl, Eirew et al. 2006, Smalley 2010, Shehata, Teschendorff et al. 2012, Smalley, Kendrick et al. 2012, Nautiyal, Steel et al. 2013).

RESULTS

Estrogen treated TMGs undergo L-R asymmetric ductal morphogenesis at puberty

To determine if neonatal E2 exposure effects the L and R glands equally, TMGs were harvested at 28 days before first estrous from E2 treated mice. L and R TMGs stained with carmine red from E2 treated mice show L-R asymmetric ductal morphogenesis at puberty (Figure 19A) as compared to symmetric ductal morphogenesis of WT mice (Figure 19B). Ductal network area, branch points, terminal end buds, and fractal dimension were plotted L vs R (Figure 19C). Linear regression modeling demonstrates that L and R TMGs from E2 treated mice are L-R asymmetric in ductal network area, branch points, and terminal end buds (TEBs); however, E2 does not affect fractal dimension L-R differently (Figure 19C). Overall, L-sided networks were dramatically smaller, had fewer branches, and fewer TEBs. L-R differences in fractal dimension were not expected because increases in fractal dimension can indicate early signs of neoplasia (Rangayyan, Banik et al. 2010, Daye, Keller et al. 2013, Rangayyan, Banik et al. 2013, Fuseler, Robichaux et al. 2014) and ER+ breast cancer occurs at a similar rate in each breast (Weiss, Devesa et al. 1996, Fatima, Zaman et al. 2013, Zeeneldin, Ramadan et al. 2013). DMSO treated mice show no L-R differences in morphology as compared to WT (data not shown).

Hormone receptors ERα and progesterone receptor (PR) were examined by RT-PCR (Figure 19D). ERα was down-regulated in the LTMG consistent with

previous reports (DiPaolo and Jones 2000); however, ERα was unchanged in the RTMG demonstrating an L-R asymmetric response to early exposure to systemic E2. By contrast, PR was down-regulated equally on both sides. Classical laterality genes Nodal and Pitx2 were also examined by RT-PCR (Figure 19D). Nodal remained unchanged with early E2 exposure; however, Pitx2 was similarly down-regulated on the L-side as was ERα, and upregulated on the R-side possibly maintaining ERα expression on the right as previously reported in chick ovarian development (Ishimaru, Komatsu et al. 2008).

To determine if mammary epithelial cell differentiation was effected by early E2 exposure, markers of luminal cell lineage determination (Figure 19D, middle row) and markers of basal cell lineage including MaSCs (Figure 19D, bottom row) were examined via RT-PCR. Markers of luminal cell differentiation, FoxM1 (Carr, Kiefer et al. 2012), Gata3 (Kouros-Mehr, Slorach et al. 2006, Asselin-Labat, Sutherland et al. 2007), Elf-5 (Oakes, Naylor et al. 2008, Chakrabarti, Wei et al. 2012), and β-casein (Liu, Robinson et al. 1997, Anderson, Rudolph et al. 2007) were significantly reduced in both the L and R TMGs in response to E2 treatment, but more so in the LTMG, suggesting a lack of cell differentiation especially in the LTMG. Additionally, markers of basal cell lineage determination and differentiation Sox9 and SMA (Guo, Keckesova et al. 2012, Zhao, Malhotra et al. 2012) , were also down-regulated in both LTMGs and RTMGs of E2 treated mice, further suggesting a lack of MaSC differentiation. In addition, markers of MaSCs, p63 and Cd1d (Zhao, Malhotra et al. 2012, dos Santos, Rebbeck et al. 2013) were both upregulated suggesting an increase in MaSCs. Taken together this data suggests

that early E2 exposure increases MaSCs and prevents MaSC differentiation, especially in the LTMG. DMSO treated mice show no differences (L or R) from WT mice in gene expression (data not shown).

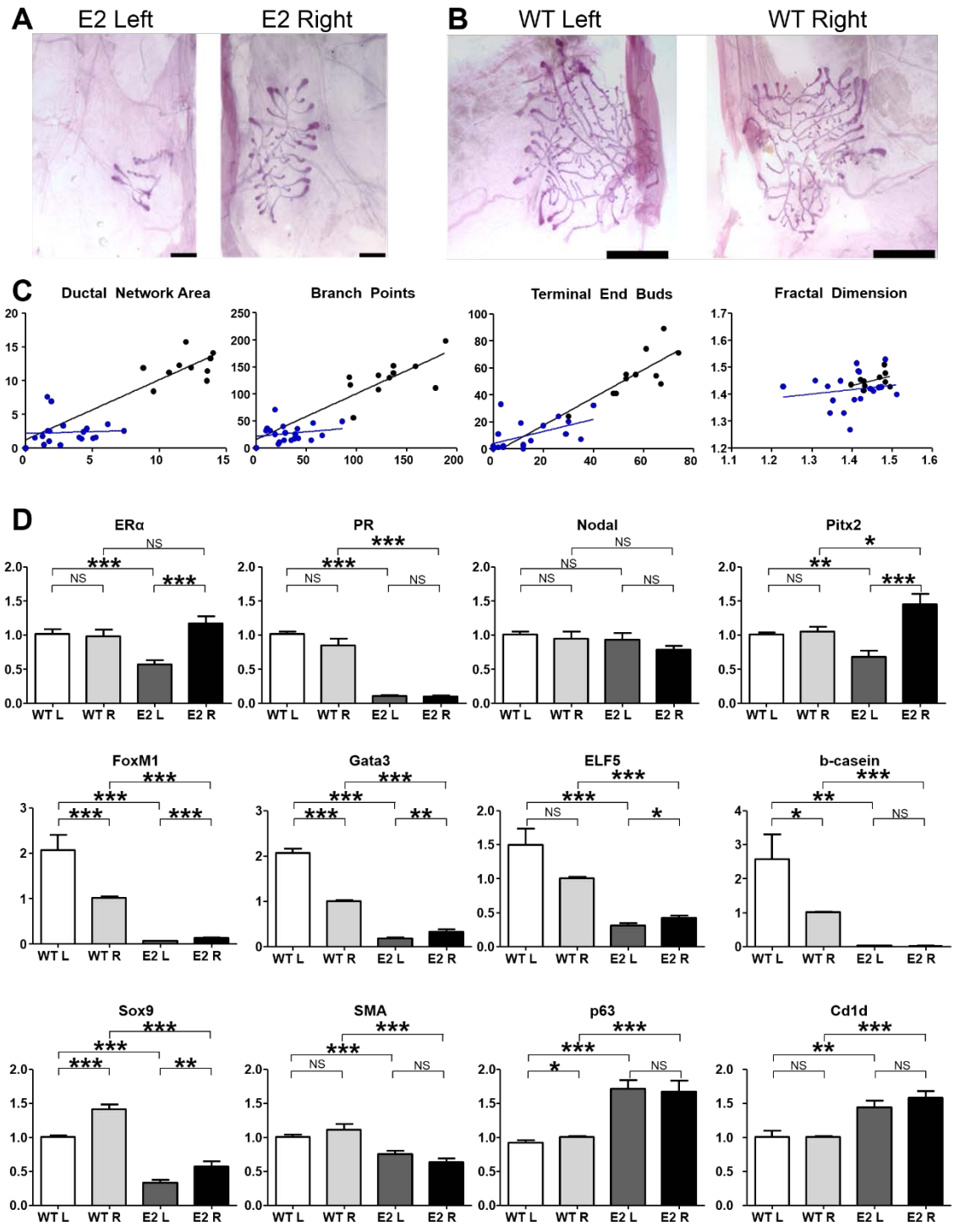

Figure 19. Estrogen treated TMGs undergo L-R asymmetric ductal morphogenesis at puberty. L and R E2 treated TMGs (A) show L-R asymmetric

ductal morphogenesis, whereas L and R WT TMGs (B) are morphometrically symmetric. Linear regression modeling of E2 treated TMGs (blue, N=19) demonstrate that E2 treated TMGs are asymmetric in most morphological parameters compared to WT TMGs (black, N=10) (C). Slopes were tested using an ANCOVA. RT-PCR of WT vs. E2 treated TMGs show an asymmetric response to E2 treatment and L-R different gene expression for genes known to regulate ductal morphogenesis and MaSC differentiation (D). Bars are representative of means ± SEM of N= 5. Paired Student's t-test was used to determine statistical differences, *$p<0.05$; **$p<0.01$; *** $p<0.001$; NS= not statistically different.

Estrogen treated IMGs are resistant to E2 induced asymmetric ductal morphogenesis at puberty

Although mouse TMGs more similarity to human mammary glands in anatomical position and early embryonic signaling than IMGs (Veltmaat, Ramsdell et al. 2013), IMGs are more commonly used in studies of mammary gland development because of their larger size and easier accessibility (Cardiff and Wellings 1999, Brill, Boecher et al. 2008). Therefore, we also examined IMGs. IMGs of E2 treated mice are not L-R asymmetric in ductal morphogenesis as compared to WT IMGs (Figure 20A, B) or DMSO treated IMGs (data not shown). Linear regression modeling of L vs. R ductal network areas, branch points, TEBs, and fractal dimension analyses show that IMGs of E2 treated mice are L-R symmetric and do not significantly differ from WT IMGs (Figure 20C). RT-PCR of ERα shows L-R symmetric expression. In addition, markers of luminal cell differentiation FoxM1 and Gata3 (Kouros-Mehr, Slorach et al. 2006, Asselin-Labat, Sutherland et al. 2007, Carr, Kiefer et al. 2012) were also L-R symmetric (Figure 20D). Interestingly, traditional laterality genes Nodal and Pitx2 were L-R different and asymmetrically altered by early E2 exposure (Figure 20D) but did not result in asymmetric ductal morphogenesis therefore are unlikely to contribute to the asymmetric ductal morphogenesis observed in TMGs.

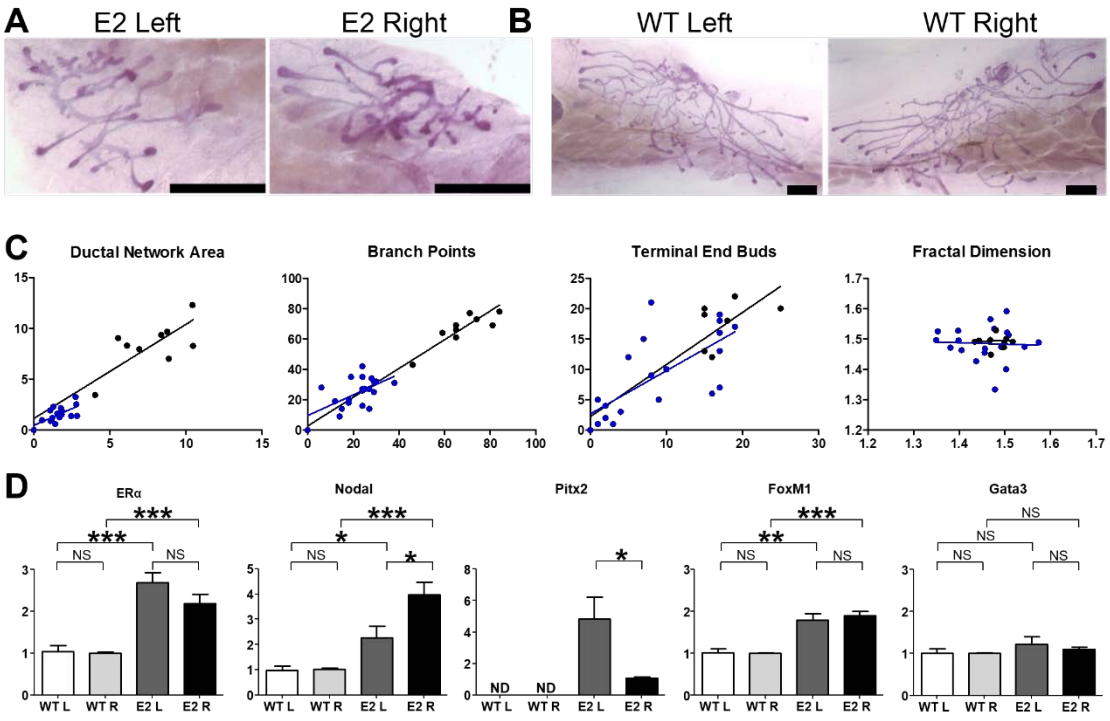

Figure 20. Estrogen treated IMGs are resistant to E2 induced asymmetric ductal morphogenesis at puberty. Both L and R E2 treated IMGs (A) as well as L and R WT IMGs (B) are morphometrically symmetric. Linear regression modeling of E2 treated IMGs (blue, N=19) demonstrate that E2 IMGs and WT IMGs (black, N=10) are symmetric in morphological parameters (C). Slopes were tested using an ANCOVA. RT-PCR of WT vs. E2 treated IMGs show symmetric gene expression in genes known to regulate ductal morphogenesis and MaSC differentiation (D). Bars are representative of means ± SEM of N= 5. Paired Student's t-test was used to determine statistical differences, *p<0.05; **p<0.01; *** p<0.001; NS= not statistically different; ND= not detected.

Estrogen treated TMGs have increased MaSCs and decreased cell differentiation at puberty

Although studies over several decades have demonstrated that neonatal E2 exposure has long term effects on mammary gland development resulting in an increased risk for mammary gland tumorigenesis (Warner and Warner 1975, Mori, Bern et al. 1976, Warner 1976, Warner, Yau et al. 1980, Bern, Mills et al. 1983), no studies have examined the effects of neonatal E2 exposure on pubescent MaSCs and cell differentiation. L-R differences in markers of MaSCs and MaSC differentiation (Figure 1D) suggests that early E2 exposure may increase MaSCs and/or prevent MaSC differentiation. To test this hypothesis, label retaining experiments, using 5-ethyl-2'-deoxyuridine (EdU) pulse-chase labeling were performed (outlined in Figure 21A) were used to determine if E2 treated mice have increased or L-R different numbers of stem and progenitor cells. Label retaining experiments show that WT mice have more label retaining cells (LRCs) in the LTMG than RTMG, and that E2 treated mice have no change in L-side LRCs, but a decrease in R-side LRCs exaggerating the L-R in MaSCs as compared to WT (Figure 21B).

Previous studies have shown that LRCs are a heterogeneous population of stem and progenitor cells (Booth, Boulanger et al. 2008, Park, Raafat et al. 2013); therefore FACS is necessary to determine if decreases in LRCs in the RTMG are due to decreases in MaSCs or progenitor cell populations. FACS analysis of WT TMGs vs. E2 treated TMGs (Figure 21C) show decreases in the luminal cell compartment and increases in the basal cell compartment containing the MaSCs.

Quantification of FACS analysis (Figure 21D) shows a significant decrease in luminal cell commitment, particularly on the left side consistent with the RT-PCR data in Figure 1. Conversely, FACS data show an asymmetric increase in the basal cell compartment resulting in more basal cells in the LTMG. Lastly, FACS data exhibit an increase in both L and R MaSCs compared to WT (Figure 21D). While the L-side prevalence of MaSCs was maintained, RTMGs showed a significant 8-fold increase in MaSCs (0.5 vs. 4.1%) compared to LTMGs which increase 5-fold (1.2 vs. 5.9) over WT. These data show the ability of individual mammary epithelial cell populations to respond L-R differently to estrogen exposure.

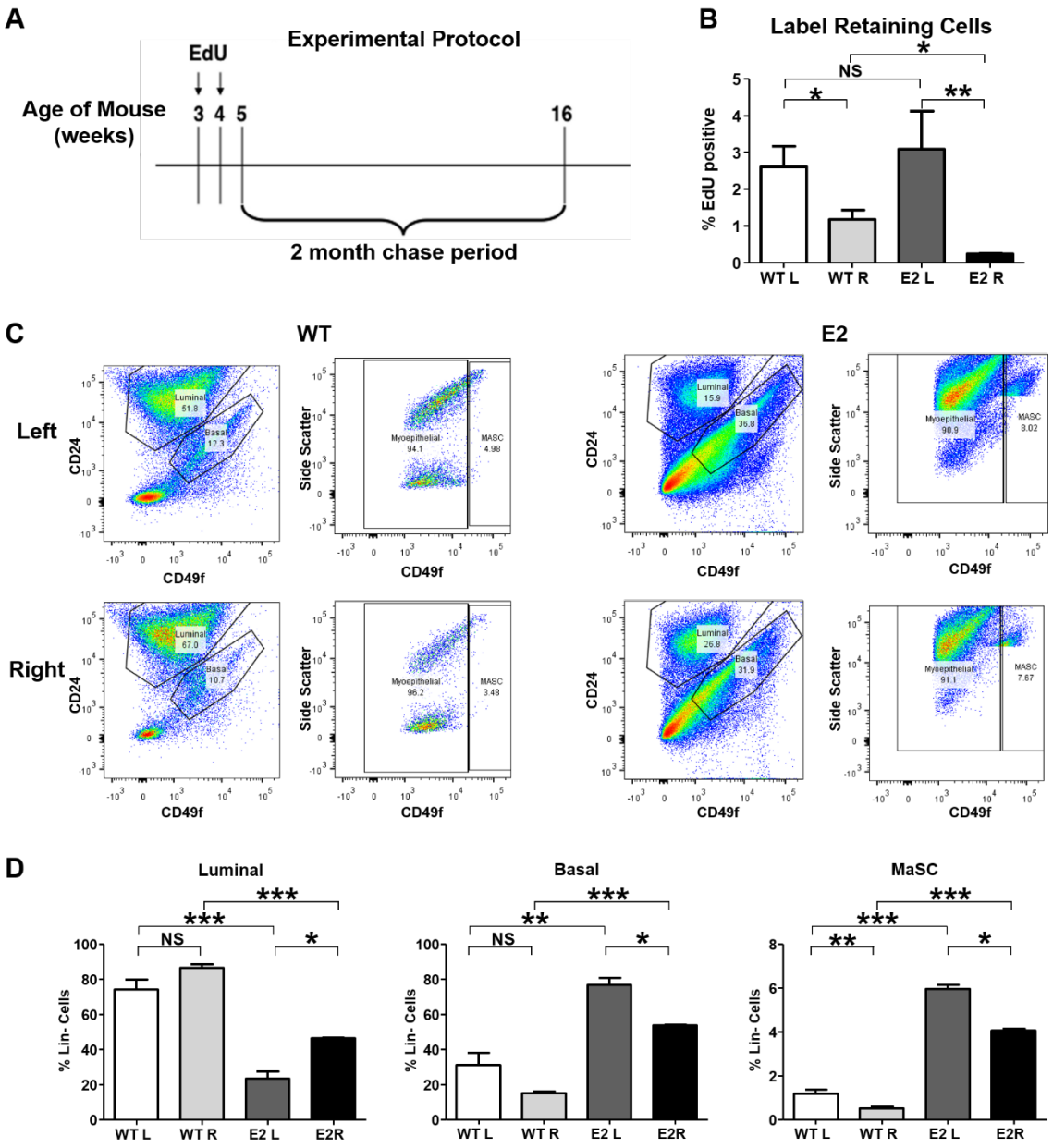

Figure 21. Estrogen treated TMGs have increased MaSCs and decreased cell differentiation at puberty. Long label retaining experiments (A) demonstrate that both WT and E2 treated TMGs have asymmetric stem/progenitor populations (B). Bars are representative of average ± SEM, N= 8 WT and N=5 E2. FACS analysis (C) of WT (left) and E2 treated (right) show L-R differences in luminal lineages, Basal lineages, and MaSCs (N=6 for WT with 3-6 glands/N, N=2 for E2 with 15-20

glands/N). Quantification of FACS analysis demonstrates discordant L-R regulation of MaSCs (right), and mammary epithelial cell lineage determination (left, D). Bars are representative of mean ± SEM, N= 6 WT and N=2 E2. Student's t-test was used to determine statistical differences, *p<0.05; **p<0.01; *** p<0.001; NS= not statistically different.

DISCUSSION

Previous work examining the effects of neonatal estrogen exposure consistently show that E2 induces long-term effects on mammary gland development and increases risk for later tumor formation when exposed to carcinogen (Warner and Warner 1975, Mori, Bern et al. 1976, Warner 1976, Warner, Yau et al. 1980, Bern, Mills et al. 1983). In addition, early E2 exposure has also been designated a risk factor for breast cancer by the National Cancer Institute (NCI) (Feigelson and Henderson 1996, Persson 2000, Lippman, Krueger et al. 2001). However, no studies existed to examine if early E2 exposure resulted in changes in mammary epithelial cell populations during puberty; moreover, no previous studies have examined L-R differences in response to early E2 exposure. Here we show for the first time that early E2 exposure results in asymmetric ductal morphogenesis during puberty, asymmetrically down-regulates transcription factors that induce MaSC differentiation, and asymmetrically increases MaSC populations.

Previous reports indicating that early E2 exposure increased mammary gland sensitivity to endogenous E2 (Warner, Yau et al. 1980, Wadia, Vandenberg et al. 2007), but decreased ERα expression (DiPaolo and Jones 2000) at first seem counter intuitive. However the data presented here give a possible explanation. Although ERα+ luminal progenitor cells are decreased at puberty, MaSCs, the cells shown to contribute the most to pubescent development (Rios, Fu et al. 2014) are increased. In addition, ERα+ luminal progenitor cells signal to MaSCs through

paracrine signaling, and with more MaSCs available, the response to that paracrine signaling may be intensified resulting in a larger ductal networks later in puberty (Jean 1971, Jean 1971, Mori, Bern et al. 1976, Warner 1976, Bern, Mills et al. 1983). In addition to reconciling previous reports of ERα regulation and long term effects of early E2 exposure on development, the data presented here may also give insight into why early E2 exposure increases risk for mammary tumorigenesis. Increases in MaSCs are thought to increase risk for later tumorigenesis, because MaSCs are long-lived allowing these cells to accumulate mutations over time (Dontu, Al-Hajj et al. 2003, Dontu, El-Ashry et al. 2004, Spike, Engle et al. 2012, Makarem, Kannan et al. 2013).

Lastly, this report is the first to show that the L and R TMGs are differentially susceptible to changes induced by E2. Clinically, this may be relevant to endocrine therapies used to treat ER+ breast cancers as well as hormone replacement therapy. It is conceivable that if TMGs are differentially susceptible to early estrogen exposure, the L and R breasts may also respond L-R differently to estrogen exposures post-menopause increasing breast cancer risks for one breast more than the other, or estrogen inhibition through the use of aromatase inhibitors in breast cancer patients.

CHAPTER FIVE

CHAPTER 5: ALTERED RXRα SIGNALING RESULTS IN ASYMMETRIC DUCTAL MORPHOGENESIS

INTRODUCTION

Left-right (L-R) asymmetry exists within many paired organs, such as lungs, kidneys, heart, and brain. L-R asymmetry is established during early embryogenesis and is essential to organ development and proper positioning of the visceral organs. Recently our lab has found that the mammary glands are also L-R asymmetric although bilaterally paired (Fuseler, Robichaux et al. 2014, Robichaux, Hallett et al. 2014). However, the origin of mammary gland laterality is unknown. For other bilaterally paired asymmetric organs, the origin of laterality is embryonic. In mice, L-R asymmetry is established at the node where unilateral expression of genes such as Nodal, Lefty and Pitx2 establish a feedback loop of L-side expression that elicits L-R differences in developing organs (Nakamura and Hamada 2012).

Although L-R asymmetry is essential in organogenesis, bilateral symmetry is also necessary during somite development (Kawakami, Raya et al. 2005, Vermot, Gallego Llamas et al. 2005, Brend and Holley 2009). Somites are segmented mesodermal structures that later give rise to important structures such as vertebrae, skeletal muscle, and ribs, but also signal to surrounding tissues to initiate growth and development (Gilbert 2000, Cho, Kwon et al. 2012). Despite the bilateral symmetry of somites, somites are lateralized structures with L-R differences in gene expression (Golding, Partridge et al. 2004, Golding, Tsoni et

al. 2004). Bilateral symmetry of somites is conditional on proper spatiotemporal expression of retinoic acid (RA) to block the effects of L-R patterning during embryogenesis (Kawakami, Raya et al. 2005, Vermot, Gallego Llamas et al. 2005, Brend and Holley 2009, Vilhais-Neto, Maruhashi et al. 2010). Chemical inhibition of RA signaling *ex vivo* results in obliteration of Lef1, a Wnt responsive gene and an essential regulator of mammary gland induction demonstrating the necessity of RA signaling during mammary gland initiation (Chu, Hens et al. 2004, Veltmaat, Van Veelen et al. 2004, Cho, Kwon et al. 2012). Reduced RA signaling results in asymmetric somite formation for somites 9-16 at embryonic day 8-9.5 (E8.5-9) (Kawakami, Raya et al. 2005, Vermot, Gallego Llamas et al. 2005, Vilhais-Neto, Maruhashi et al. 2010). In addition, thoracic mammary gland (TMG) pairs 2 and 3 require somitic FGF for initiation and reside over somites 11-16 (Veltmaat, Relaix et al. 2006). However, reduced RA signaling does not affect somite symmetry after somite 16 development. Inguinal mammary gland (IMG) pair 4 develops overlaying somites 22-24 and does not require somitic FGF for initiation (Veltmaat, Relaix et al. 2006), therefore should not be affected by altered somite formation due to reduced RA signaling. Therefore, if lateralized somitic signals regulate L-R patterning of the TMGs, altered RA signaling will result in L-R different alterations of the TMGs, but not IMGs.

To test this hypothesis, the Retinoic X Receptor alpha (RXRα) knockout mouse were used. Complete homozygous RXRα knockout ($RXR\alpha^{-/-}$) is embryonic lethal, therefore partial RXRα knockout, mice heterozygous for RXRα knockout ($RXR\alpha^{-/+}$) mice were used. RXR is one of two types of nuclear receptors for which

RA signals with the second being Retinoic Acid Receptor (RAR) family of receptors (di Masi, Leboffe et al. 2014). These receptors often act as heterodimers that act on retinoic acid response elements (RAREs) of target genes (di Masi, Leboffe et al. 2014). Previous studies examining the role of RARα1 on mammary gland development found that knockout of RARα1 resulted in hyperplastic ductal morphogenesis and increased luminal progenitors, but decreased mammary stem cells and protected against Wnt-1 driven tumorigenesis in IMGs (Cohn, Ossowski et al. 2010). Interestingly, although authors did not quantify changes in TMGs, representative images of RARα1 KO TMGs appear to have smaller ductal networks than representative images of WT TMGs suggesting that altered RA signaling effects TMGs and IMGs differently. The role of RXRα has been shown to be essential for normal heart development, and the primary isotype of RXR receptors embryonically expressed (Mark, Ghyselinck et al. 2009); however, no previous studies have examined the role of RXRα on mammary gland development. In this study, we demonstrate that knockdown of RXRα via the $RXR\alpha^{+/-}$ mouse results in two distinct phenotypes of TMG development as compared to WT. In addition, we show that LTMGs are more sensitive to perturbations in RXRα signaling compared to RTMGs, and lastly, that IMGs are not sensitive to $RXR\alpha^{+/-}$ knockout.

MATERIALS AND METHODS

Mice

All experiments were performed in accordance with the regulations of the Medical University of South Carolina Institutional Animal Care and Use Committee. C57BL/6 wild-type mice were obtained from Harlan. RXRα$^{+/-}$ mice were bred at MUSC and generously provided by Dr. Steven Kubalak. Mice were fed Harlan Teklad rodent diet 2918 and provided water *ad libitum*. Mice were euthanized at 28 days of age and thoracic and inguinal mammary glands were harvested.

Histology and image collection

Carmine red stained whole mounts were prepared as previously described (de Assis, Warri et al. 2010) from #3 and #8 thoracic mammary glands (TMGs) and #4 and #9 inguinal mammary glands (IMGs) of day-28 mice and were imaged on an Olympus SZX12 stereomicroscope equipped with a Spot camera. Overlapping images of each whole mount were processed into a single composite image with Adobe Photoshop®.

Image analysis

The color images of the mammary glands were converted to 8-bit monochrome images for image and fractal analysis. The mammary gland within an image was outlined and isolated from the background tissue and defined as a Region of Interest (ROI) (Figure 5). The isolated image of the mammary gland was

thresholded using the set threshold subroutine of MetaMorph Image analysis software (ver. 6.1). The area (A) and integrated optical density (IOD) of the ductal epithelial networks were measured using the integrated morphometry analysis sub-routine of MetaMorph. The fractal dimension (**D**), was determined by the box counting method using HarFA software (Nezadal, Zemeskal et al. 2001) [http://www.fch.vutbr.cz/lectures/imagesci]) applied to the isolated image of the mammary gland using the same threshold values.

Integrated optical density (IOD).

The IOD of the mammary gland ROI delineated by the thresholded boundaries is considered to be the "mass" of the ROI and a measurement of the total amount of labeled material in the region (Walter and Berns 1986, Fuseler, Merrill et al. 2006, Fuseler, Millette et al. 2007, Rogers and Fuseler 2007, Fuseler and Valarmathi 2012). The IOD of a selected region can be expressed as the weighted sum of the image histogram in which each term in the histogram is multiplied by the gray value it represents. When applied to thresholded boundaries the IOD is defined by the following expression:

$$IOD(T1, T2) = \sum_{GV=T1}^{T2} H(GV) \times GV$$

Where the upper and lower thresholds defining the ROI in the histogram are given by T1 and T2. GV is the gray value of each pixel and H (GV) is the gray level histogram.

Application of the fractal dimension (D)

The thoracic mammary glands appear as irregular and complex objects composed of parts at different levels of resolution (ducts of different bore sizes) which are functionally and physiologically similar (self-similar) to the whole object. Under the conditions of these properties, the thoracic mammary glands can be considered fractal objects and their topological dimension, the fractal dimension (**D**), expressed by a non-integer number lying between two Euclidian integer topological dimensions (Grizzi, Russo et al. 2005). The values of **D** characterizing the thoracic mammary glands are therefore fractional. Since the thoracic mammary gland is essentially a 2-dimensional object, the **D** values will lie between 1 and 2. As the mammary gland becomes more complex and irregular, its **D** value becomes greater, approaching 2. In applying fractal analysis, the **D** value of the mammary gland is determined by applying the box-counting method (Fernandez and Jelinek 2001, Grizzi, Russo et al. 2005). The box-counting method has been the most widely used and general model for applying fractal analysis to biological and non-biological systems. The box-counting method consists of a grid of boxes of size e superimposed over the image of the structure, and the number of boxes containing any part of the structure recorded as ***N(e)***. A fractal object expresses a straight line when Log[***N(e)***] is plotted against Log(***1/e***). The box fractal dimension **D** can be determined from the slope of the regression line. That is: **D=** Log[***N(e)***] / Log(***1/e***). The **D** values of the thoracic mammary glands were determined using HarFA software (Nezadal, Zemeskal et al. 2001) [http://www.fch.vutbr.cz/lectures/imagesci]. The HarFA software assigned mesh

sizes of boxes with **e** values ranging from 2 to 207 pixels and 30 steps within this range were calculated to generate the Log[***N(e)***] versus Log(***1/e***) lines to determined.

Branch points and terminal end buds (TEBs)

Branch points and TEBs were quantified by manual counting from the images.

Results

RXRα$^{+/-}$ TMGs have two distinct phenotypes during pubescent ductal morphogenesis

To test the hypothesis that mammary gland laterality originates embryonically, RXRα knockout mice were used. RXRα$^{-/-}$ mice are embryonic lethal and could not be used for this study (Sucov, Dyson et al. 1994); therefore RXRα$^{+/-}$ mice were used. Approximately half of the RXRα$^{+/-}$ mice had TMGs with pronounced hypoplastic development as compared to WT (Figure 22A, E). In addition to decreased ductal network development, these mice had observable L-R differences in morphology (Figure 22A). In hypoplastic RXRα$^{+/-}$ mice, RTMGs had larger ductal network areas, more terminal end buds (TEBs), more branch points, and higher IOD (mass) as compared to LTMGs (Figure 22B). However, hypoplastic RXRα$^{+/-}$ mice had no L-R differences in fractal dimension (complexity) or relative density (Figure 22B). The other half of RXRα$^{+/-}$ mice were hyperplastic in development as compared to WT (Figure 22C, E) and had no L-R differences in morphology similar to WT (Figure 22D, F). Interestingly, C57/Bl6 WT TMGs are L-R different in fractal dimension, a measure of ductal complexity (Figure 22F) a L-R difference not observed in FVB/N WT TMGs (Robichaux, Hallett et al. 2014). Overall this data demonstrates that RXRα$^{+/-}$ TMGs have two distinct phenotypes as compared to WT during pubescent development, and that reduction of RA signaling results in aberrations in mammary gland development leading to L-R differences in ductal morphogenesis.

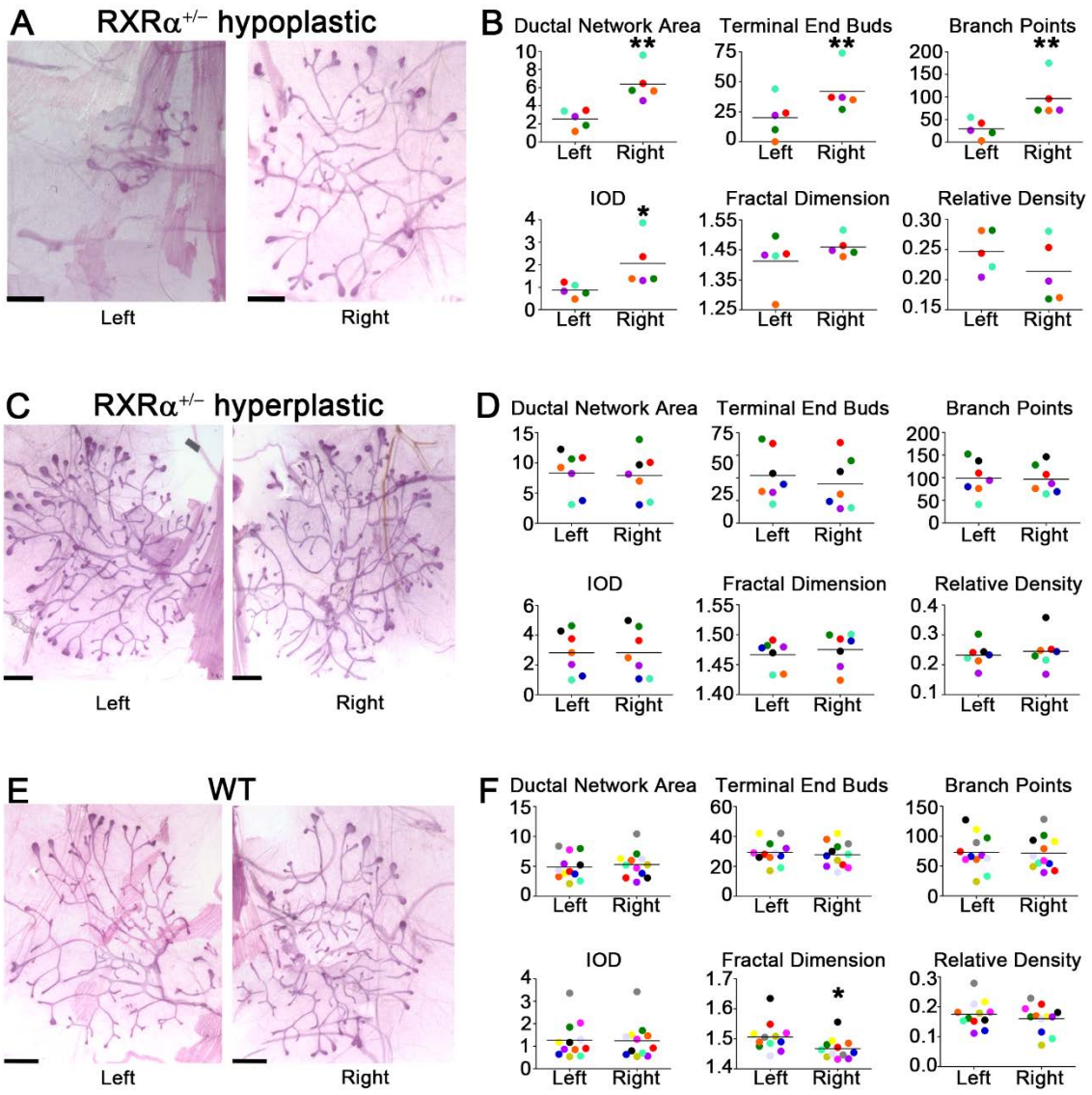

Figure 22. RXRα$^{+/-}$ TMGs have two distinct phenotypes during pubescent ductal morphogenesis. Hypoplastic TMGs from RXRα$^{+/-}$ mice (A) are L-R asymmetric in ductal network area, TEBs, Branch Points, and IOD, but not fractal dimension or relative density (N=7, B). Hyperplastic TMGs from RXRα$^{+/-}$ mice (C) are distinct from hyperplastic RXRα$^{+/-}$ TMGs, and are L-R symmetric in all morphometric parameters (N=5, D). TMGs from WT mice (E) are symmetric in all morphometric parameters except fractal dimension (N=12, F). Statistical differences were determined by students' t-tests, *, $p<0.05$; **, $p<0.01$.

LTMGs are more vulnerable to RXRα$^{+/-}$ knockout than RTMGs

To determine if L and R TMGs are equally sensitive to RXRα$^{+/-}$ knockdown, L and R TMGs of both RXRα$^{+/-}$ hyperplastic TMGs and hypoplastic TMGs were compared to WT TMGs independently. LTMGs of hyperplastic RXRα$^{+/-}$ mice have increased ductal network areas, terminal end buds, IOD, and density compared to WT (Figure 23A). In addition, hyperplastic RXRα$^{+/-}$ LTMGs have increased ductal network areas, terminal end buds, branch points, and IOD compared to RXRα$^{+/-}$ hypoplastic LTMGs (Figure 23A). When RXRα$^{+/-}$ hypoplastic LTMGs were compared to WT LTMGs, RXRα$^{+/-}$, hypoplastic LTMGs were found to have reduced ductal network areas, branch points, IOD, fractal dimension, but had elevated density compared to WT LTMGs (Figure 23A). However, RTMGs of hyperplastic RXRα$^{+/-}$ mice and hypoplastic RXRα$^{+/-}$ mice only vary slightly from WT mice (Figure 23B). RTMGs of hyperplastic RXRα$^{+/-}$ mice and hypoplastic RXRα$^{+/-}$ mice have no differences from WT in ductal network area, terminal end buds, branch points, or fractal dimension (Figure 23B). Minor increases in IOD were detected for hyperplastic RXRα$^{+/-}$ mice, and WT mice have decreased density compared to both RTMGs of hyperplastic RXRα$^{+/-}$ mice and hypoplastic RXRα$^{+/-}$ mice. This data demonstrates that LTMGs are more sensitive to perturbations in RA signaling and RXRα$^{+/-}$ knockdown compared to RTMGs.

Figure 23. LTMGs are more vulnerable to RXRα$^{+/-}$ knockout than RTMGs. Hyperplastic LTMGs RXRα$^{+/-}$ TMGs are have larger ductal network areas, more

TEBs, increased IOD and increased relative density compared to WT LTMGs; whereas hypoplastic RXRα$^{+/-}$ LTMGs have smaller ductal networks, fewer branch points, and decreased IOD and fractal dimension compared to WT LTMGs (A). Hyperplastic and hypoplastic RXRα$^{+/-}$ RTMGs have no differences ductal network area, TEBs, branch points, or fractal dimension compared to WT RTMGs (B). IOD and relative density are the only morphometric parameters increased with RXRα knockdown. Statistical differences were determined by ANOVA and Bonferroni's post-tests, *, $p<0.05$; **, $p<0.01$.

IMGs are unaffected by RXRα$^{+/-}$ knockout

Asynchrony in somite formation with reduced RA signaling is limited to early, thoracic somites 9-14; whereas more posterior somites that develop past approximately 16 somites develop symmetrically (Vermot, Gallego Llamas et al. 2005). The somites underlying the inguinal mammary glands (approximately somites 22-24) (Veltmaat, Relaix et al. 2006), are unaffected by reduced RA signaling; therefore IMGs of RXRα$^{+/-}$ mice should develop normally. RXRα$^{+/-}$ IMGs (Figure 24A) appear L-R symmetric and similar to WT IMGs (Figure 24B). Neither RXRα$^{+/-}$ IMGs nor WT IMGs have L-R differences in any morphometric parameter (Figure 24C, D). Independent L and R analysis of RXRα$^{+/-}$ IMGs vs. WT IMGs show slight symmetric increases in ductal network area and branch points for both LIMG and RIMGs of RXRα$^{+/-}$ mice compared to WT mice, but no other changes (Figure 24E, F). This data is consistent with a previous study showing increases in ductal network area and branch points in IMGs of RARα1 knockout mice (Cohn, Ossowski et al. 2010). This data demonstrates that IMGs are not sensitive to RXRα$^{+/-}$ knockout. The lack of response to RXRα$^{+/-}$ knockout in IMGs and presence of pronounced L-R differences in TMG response to RXRα$^{+/-}$ knockout demonstrate the importance of somitic signals to the TMGs and suggests that L-R differences in mammary gland development are indeed rooted in embryonic patterning.

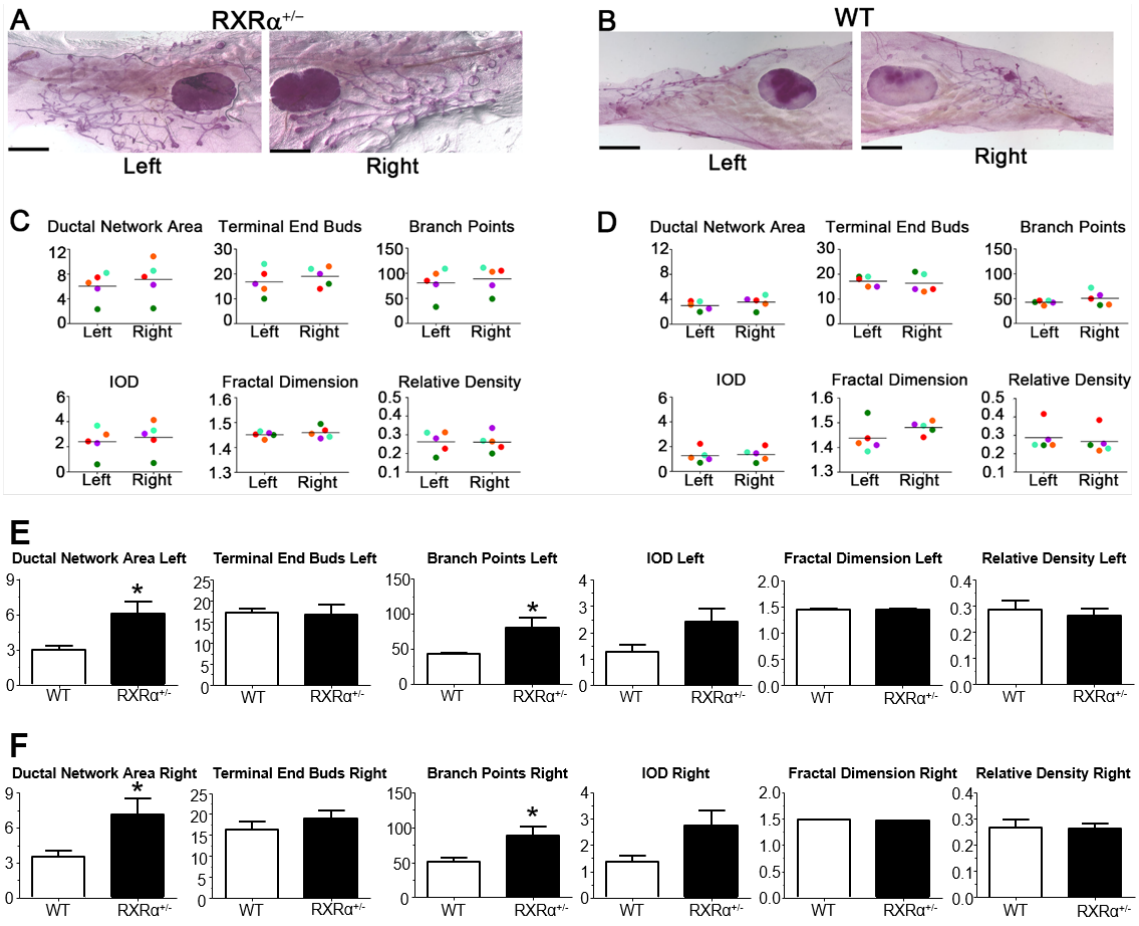

Figure 24. IMGs are unaffected by RXRα$^{+/-}$ knockout. RXRα$^{+/-}$ IMGs (A) nor WT IMGs (B) have L-R differences in any morphometric parameter (C, D). LIMGs (E) and RIMGs (F) of RXRα$^{+/-}$ mice have increased ductal network areas and branch points as compared to WT IMGs, but no other morphometric parameter is different in the RXRα$^{+/-}$ model compared to WT. Statistical differences were determined by students' t-tests, *, $p<0.05$ (N=5).

Discussion

Due to the differences in phenotypes of the TMGs in RXRα$^{+/-}$ mice, RT-PCR was not a viable approach to determine consistent molecular differences in RXRα$^{+/-}$ vs. WT mice. Gene expression patterns were not consistent, therefore reliably segregating the RT-PCR results into two groups that may correlate with each of the phenotypes was not possible with the above sample size; therefore, an experimental design allowing visualization of the morphology of the ductal networks before RNA isolation is necessary. Crossing RXRα$^{+/-}$ mice with MMTV-GFP mice, which have a fluorescent ductal epithelium, would allow for segregation into the two phenotypic groups before RNA isolation allowing us to probe for a molecular reason in the two different phenotypes of TMGs in RXRα$^{+/-}$ mice. However, the reason for the two different phenotypes of TMGs in RXRα$^{+/-}$ mice was not attributable to parents' genetics (i.e. mother vs. father being RXRα$^{+/-}$ or WT) or the mother's milk as both phenotypes came from the same liter in some instances.

In the L-R different TMG phenotype, L-R differences may be attributable to L-R differences in FGF and Notch signaling. When asynchronous somite development takes place in Raldh2 knockout model, the embryos have an increase in FGF8 on the right side and an increase of Hes7, a Notch target gene, on the left side. Half of the RXRα$^{+/-}$ TMGs have larger networks on the right side and over-expression of FGF in TMGs is associated with hyperplastic growth and tumorigenesis (Ngan, Ma et al. 2002). In addition, RXRα$^{+/-}$ TMGs with hypoplastic

growth had severely stunted LTMGs. Studies have shown that Notch signaling in mammary glands induces MaSC differentiation and luminal cell lineage determination (Bouras, Pal et al. 2008, Chakrabarti, Wei et al. 2012, Park, Raafat et al. 2013, Sale, Lafkas et al. 2013). As MaSCs proliferate symmetrically, up-regulation of Notch signaling on the left side of the embryo could induce early differentiation of MaSCs resulting in decreased growth potential at puberty due to a limited number of remaining MaSCs. Further studies are needed to determine the effects of RXRα knockout on early placode initiation and later pubescent development. Tissue specific knockout would allow for later studies of complete RXRα knockout reducing variability due to heterozygous genetics.

Here we show that RXRα$^{+/-}$ knockout results in two distinct phenotypes of TMG development: 1.) L-R asymmetric hypoplastic development, and 2.) L-R symmetric hyperplastic development. In addition, LTMGs were much more sensitive to RXRα$^{+/-}$ knockout than RTMGs. LTMGs of both phenotype were altered as compared to WT, but RTMGs of both phenotypes only had changes from WT in ductal density. Lastly, we show that IMGs of RXRα$^{+/-}$ do not develop differently from WT IMGs. These data taken together demonstrate that TMGs are more sensitive to changes in RA signaling than IMGs, and that alterations in L-R embryonic patterning effect the L and R TMGs differently. This data is the first to suggest that L-R patterning of mammary glands is embryonic in origin and that perturbations in embryonic L-R patterning have long term effects on mammary gland development.

CHAPTER SIX

CHAPTER 6: SUMMARY AND FUTURE DIRECTIONS

SUMMARY

When beginning this project, a standardized objective method of quantifying mammary gland ductal networks did not exist. The current methods, were subjective and ambiguous. Chapter 2 details a sensitive, quantitative, and objective method of analyzing mammary ductal networks: fractal dimension analysis. Using fractal dimension analysis in conjunction with conventional morphometrics we detected differences in wild-type (WT) and MMTV-Neu$^{Tg/+}$ murine thoracic ductal network morphogenesis during pubescent development. Furthermore, fractal dimension analysis allowed us to observe left (L) side MMTV-Neu$^{Tg/+}$ thoracic mammary glands (TMGs) show increased signs of neoplasia as compared to right (R) side MMTV-Neu$^{Tg/+}$ TMGs. This L-R difference in fractal dimension analysis of MMTV-Neu$^{Tg/+}$ TMGs was the first documentation of L-R differences in pubescent mammary gland development. Not only does fractal dimension analysis serve as a quantitative and sensitive approach in mice, but this technique if followed up on in human patients, could develop a more sensitive method of early neoplasia detection before overt breast tumor formation. Previous retrospective studies have shown that fractal dimension analysis of mammograms detected changes in mammary architecture over a year before clinical diagnosis (Rangayyan, Banik et al. 2010, Daye, Keller et al. 2013, Rangayyan, Banik et al.

2013). This suggests a window of preventative medicine for women with early neoplastic changes.

In chapter 3 WT mice are characterized for L-R differences during normal development and L-R differences are then challenged by ErbB2/Neu overexpression by using the MMTV-Neu$^{Tg/Tg}$ mouse model. In chapter 3.1, despite the morphological symmetry of WT TMGs, L and R TMGs are demonstrated to be molecularly different by microarray analysis which was validated by RT-PCR. In addition, L-R different gene expression pathway analysis converged on mammary epithelial cell differentiation (Smalley and Ashworth 2003, Cicalese, Bonizzi et al. 2009, Carr, Kiefer et al. 2012, Robichaux, Hallett et al. 2014).

When the ErbB2/Neu transgene is overexpressed by the Murine Mammary Tumor Virus (MMTV) promoter as in the MMTV-Neu$^{Tg/Tg}$ mouse model, TMGs develop asymmetrically with right side TMGs forming larger ducts, but left side TMGs forming more complex ducts. In addition, overexpression MMTV-Neu$^{Tg/Tg}$ resulted in discordant gene regulation of novel laterality genes, and down-regulation of transcription factors regulating mammary stem cell (MaSC) differentiation.

In addition, inguinal mammary glands (IMGs) were shown to be less sensitive to MMTV-Neu$^{Tg/Tg}$ overexpression and delayed in L-R asymmetric gene expression, not showing molecular laterality until after pubescent development for both WT and MMTV-Neu$^{Tg/Tg}$ IMGs. Lastly, comparative genomic analysis of novel laterality genes to patient tumor situs displayed decreased patient survival when tumors had “right-side” laterality gene expression. This decreases in survival with

“right-side” gene expression exists across various breast cancer subtypes exhibiting the clinical relevance of molecular L-R differences. Chapter 3.1 was the first report demonstrating molecular L-R differences in WT mammary glands and the ability of genes to be un-coupled in regulation by transgenic overexpression of an oncogene in mammary glands. In addition, discordant gene regulation between TMGs and IMGs L vs. R show that each mammary gland is regulated independently along the anterior and posterior axis as well as the L-R axis.

In chapter 3.2 MaSCs of WT mice were studied for L-R differences in the presence or absence Lapatinib, a small molecule inhibitor targeting both ErbB2 and EGFR. In addition, to determine the effect of ErbB2 over-expression on L and R MaSCs, L-R differences of MaSCs in the MMTV-Neu$^{Tg/Tg}$ mouse model were also examined in the presence or absence of Lapatinib. WT mice have 2.5 fold more MaSCs in LTMGs as compared to RTMGs. Moreover, WT MaSCs from LTMGs have drastically upregulated ErbB2 expression, whereas WT MaSCs from RTMGs have dramatically upregulated EGFR expression. In addition to molecular differences, L-sided MaSCs form more mammospheres that are sensitive to treatment with Lapatinib. Conversely, R-sided MaSCs form larger mammospheres, and increase in self-renewal with increasing concentrations of Lapatinib treatment.

In addition to L-R differences of WT TMG derived MaSCs, MMTV-Neu$^{Tg/Tg}$ TMG derived MaSCs also display L-R differences in MaSC number. Neu overexpression in the MMTV-Neu$^{Tg/Tg}$ model resulted in a statically significant increase in L-sided MaSCs, but not R-sided MaSCs enhancing the already existing

MaSC laterality. MMTV-Neu$^{Tg/Tg}$ TMG derived MaSCs also displayed a L-R difference in ErbB2 and EGFR expression however, the L-R pattern was inverted in MMTV-Neu$^{Tg/Tg}$ TMG derived MaSCs. L-side MMTV-Neu$^{Tg/Tg}$ TMG derived MaSCs had elevated EGFR and R-sided MMTV-Neu$^{Tg/Tg}$ TMG derived MaSCs had elevated ErbB2. Accompanying inversion of EGFR and ErbB2 expression, mammosphere growth and response to Lapatinib was inverted in MMTV-Neu$^{Tg/Tg}$ TMG derived MaSCs. R-sided MMTV-Neu$^{Tg/Tg}$ TMG derived MaSCs formed more mammospheres and responded in a dose dependent manner to Lapatinib treatment; whereas L-sided MMTV-Neu$^{Tg/Tg}$ TMG derived MaSCs showed little response to Lapatinib treatment and had no change in self-renewal. However, all MMTV-Neu$^{Tg/Tg}$ TMG derived MaSCs had elevated sensitivity to Lapatinib treatment as compared to WT, which was expected. Previous studies show that in MMTV- Neu$^{Tg/Tg}$ mice, in general mammary epithelial cells overexpress Neu/ErbB2 (Guy, Webster et al. 1992), although in our study, R-sided MMTV-Neu$^{Tg/Tg}$ TMG derived MaSCs were shown to express more ErbB2 as compared to L sided MMTV-Neu$^{Tg/Tg}$ TMG derived MaSCs. This study not only demonstrates a correlation between ErbB2 expression and Lapatinib sensitivity, but also a novel correlation between EGFR and Lapatinib sensitivity. Moreover, EGFR expression correlated to either protection from Lapatinib treatment as well as a slight stimulation of MaSC self-renewal in WT and MMTV-Neu$^{Tg/Tg}$ MaSCs. Furthermore, this study is the first to show not only a L-R differential response to a clinically used breast cancer therapy, but a possible unilateral adverse effect that may promote future secondary reoccurrence of a more aggressive breast cancer subtype.

Future studies are needed to determine the long term effects of Lapatinib treatment on normal tissue and future breast cancer risks.

Together, chapter 3 is the first to demonstrate that L and R TMGs are lateralized organs with differential response to molecular perturbations. Moreover, L and R MaSCs are non-identical and have L-R differential potential in response to inhibition of growth factors. Overall these studies demonstrate that increases in number of MaSCs, as well as a lack of inhibition to Lapatinib correlate with elevated EGFR expression and poor patient survival. In addition, responsiveness to Lapatinib, as well as patient survival correlate with elevated ErbB2/ErbB3 expression. Moreover, increases in number of MaSCs correlates with smaller (less differentiated) ductal networks (Table 3). From a basic science point of view, these studies enforce the idea that L and R should not be combined for studies of mammary gland biology or breast cancer. From a clinical perspective, these studies demonstrate that tumor situs is an additional parameter of diagnosis that should be taken into account in deciding a method of therapy or prognosis.

In chapter 4, the effect of neonatal exposure to 17β-estradiol (E2) on normal mammary glands is examined. Early E2 exposure is shown to asymmetrically effect pubescent development of TMGs, but not IMGs. TMGs undergo asymmetrical ductal morphogenesis with RTMGs being larger than LTMGs. In addition, early E2 exposure resulted in down-regulation of transcription factors that regulate ductal morphogenesis including transcription factors that regulate both luminal cell and basal cell lineage differentiation. FACS analysis revealed an overall decrease in luminal progenitors, but more so in LTMGs, correlating with

RT-PCR data. RT-PCR demonstrated a larger decrease in luminal progenitor markers as well as ERα in the LTMG. Additionally, FACS revealed an asymmetric increase in MaSCs, corresponding with an increase in MaSC markers by RT-PCR. Chapter 4 was the first report of TMGs capacity to respond L-R different to systemic hormone exposure and reconciled previous reports of down-regulation of ERα, but increased sensitivity to endogenous estrogens later in puberty via demonstration of up-regulation of MaSCs (Warner, Yau et al. 1980, DiPaolo and Jones 2000, Wadia, Vandenberg et al. 2007). Also increases in MaSC populations also may explain why neonatal estrogen exposure increases tumorigenesis with carcinogen exposure later in life (Warner and Warner 1975, Mori, Bern et al. 1976). Summary of the WT, MMTV-Neu$^{Tg/Tg}$, and E2 laterality data is located in table 3.

	WT	MMTV-Neu$^{Tg/Tg}$	E2
Morphology	L=R	L<R	L<R
Number of MaSC	L>R	L>R	L<R
Increase in MaSC	Right (10 weeks)	Left only (compared to WT)	L > R (compared to WT)
Number of Mammospheres	L>R	L<R	Unknown
Size of Mammospheres	L<R	L=R	Unknown
Expression of EGFR	Right	Left	Unknown
Expression of ErbB2	Left	Right	Unknown
Inhibition to Lapatinib	Left	Right	Unknown
Better Patient Survival	Left	Unknown	Unknown

Table 3: Summary of laterality findings in dissertation. Increases in number of MaSCs, as well as a lack of inhibition to Lapatinib correlate with elevated EGFR expression and poor patient survival. In addition, responsiveness to Lapatinib, as well as patient survival correlate with elevated ErbB2/ErbB3 expression. In addition, increases in number of MaSCs correlates with smaller (less differentiated) ductal networks.

Lastly in chapter 5, using the RXRα$^{+/-}$ knockout mouse we find TMGs are more susceptible to changes in RA signaling than IMGs. RXRα$^{+/-}$ knockout TMGs have two distinct phenotypes: 1.) L-R asymmetric hypoplastic development, and 2.) L-R symmetric hyperplastic development. LTMGs were much more sensitive to RXRα$^{+/-}$ knockout than RTMGs. LTMGs of both phenotype were altered as compared to WT, but RTMGs of both phenotypes only had changes from WT in ductal density. In L-R asymmetric hypoplastic TMGs, decreased LTMG development in response to RXRα$^{+/-}$ knockout may be due to decreased MaSCs in LTMGs due to an aberrant increases in Notch signaling as seen in the Raldh2 knockout model (Vilhais-Neto, Maruhashi et al. 2010). Up-regulated Notch signaling is known to increase MaSC differentiation and luminal cell lineage determination reducing MaSC populations (Bouras, Pal et al. 2008, Chakrabarti, Wei et al. 2012, Park, Raafat et al. 2013). To determine if this truly is the mechanism of action, RXRα$^{-/-}$ knockout placodes could be harvested and analyzed by RT-PCR. In addition, increases in RTMG growth could be due to increased FGF signaling as seen in the Raldh2 knockout model (Vilhais-Neto, Maruhashi et al. 2010), because increased FGF results in mammary hyperplasia (Ngan, Ma et al. 2002). Lastly, we show that IMGs of RXRα$^{+/-}$ do not develop differently from WT IMGs. IMG unreceptiveness was expected because IMGs have been shown to develop independently of somitic FGF and the somites underlying the IMGs are not altered by RA reduction (Vermot, Gallego Llamas et al. 2005, Veltmaat, Relaix et al. 2006, Vilhais-Neto, Maruhashi et al. 2010). These data taken together demonstrate that TMGs are more sensitive to changes in RA signaling than IMGs,

and that alterations in L-R embryonic patterning effect the L and R TMGs differently. This data suggests that L-R patterning of mammary glands is embryonic in origin, originates from somitic signals, and that perturbations in embryonic L-R patterning have long term effects on mammary gland development.

The results of the studies within this dissertation form 3 major conclusions: 1.) mammary glands and the cell populations within the mammary glands are lateralized with the potential to response L-R differently to both neoplastic insults as well as drugs used to treat breast cancers; 2.) L-R differences in TMGs originate embryonically like other bilaterally paired organs; and lastly, 3.) TMGs and IMGs are not identical and because TMGs have more similarities to human development, and are more sensitive to outside perturbations, TMGs are more appropriate for studies relating to human health.

FUTURE DIRECTIONS

The data presented here has opened up an entirely new area of mammary gland biology: L vs. R response to experimentation. These type of experiments can be dually informative. Underlying L-R differences under normal conditions have yet to be fully understood and can give insight into disease progression and perhaps disease prevention, but also L-R differences can be exploited to understand relationships between molecular differences and response to experimentation yielding better understanding of mechanism of action. The future directions for this project vary from early embryonic development and additional studies in pubescent development, to branching into later time-points of development not yet studied such as pregnancy, lactation, and involution. In addition to developmental questions, the data here can also continue into studies of cancer biology in attempts to understand how L-R differences in normal mammary gland biology result in L-R differences in tumor biology including response to clinical therapies and long term risks.

Embryonically, a mechanism of how somites deliver a lateralized signal of placode initiation is unknown. Potential studies include mechanistic studies of hb-EGF, a transient left-side dominate somitic ligand that binds to ErbB family members known to effect mammary gland development (Golding, Tsoni et al. 2004). Increases in ErbB family signaling have been shown to increase MaSC populations (Olayioye, Neve et al. 2000, Troyer and Lee 2001, Korkaya, Paulson et al. 2008, Spike, Engle et al. 2012, Ithimakin, Day et al. 2013, Korkaya and Wicha

2013), and could be origin of L-side dominate MaSC numbers. Mouse models with inverted L-R asymmetry such as the *situs inversus* mouse could also give definitive proof if L-R differences in mammary gland biology originate embryonically (Yokoyama, Copeland et al. 1993). Although the FVB/N-Invs^{inv} mouse model of *situs inversus* dies by 7 days of age (Yokoyama, Copeland et al. 1993), embryonic studies of placode formation and L-R differences of primary ducts would determine if mammary gland laterality is a product of embryonic L-R patterning.

To continue the current studies during pubescent development, more studies are needed to tease out the mechanism of ErbB2 and EGFR expression and MaSC response to Lapatinib. The L-R pattern of ErbB2 and EGFR expression correlating with Lapatinib treatment of both WT and MMTV-Neu$^{Tg/Tg}$ MaSCs suggests that ErbB2 and EGFR expression regulates MaSC response to Lapatinib and self-renewal. However, Lapatinib can bind both receptors (Wood, Truesdale et al. 2004, Burris, Hurwitz et al. 2005, Zhang, Pal et al. 2008, Scaltriti, Verma et al. 2009), and studies using a drug that can only bind one receptor or the other are necessary to further tease out the relationship between ErbB2 and EGFR gene expression and self-renewal. Additional studies are also needed to examine other cell populations within the mammary glands. E2 studies demonstrate that E2 can effect luminal populations L-R differently therefore MaSCs are not the only lateralized mammary epithelial population within the mammary glands. Characterizing L-R differences in other cell populations may determine how E2 is capable of asymmetric increases in MaSC populations and if asymmetric response to ErbB2/Neu overexpression effects other cell populations.

In addition to epithelial cell studies, characterization of microenvironmental differences are necessary. Ductal morphogenesis at puberty is not only driven by epithelial cell cross-talk but paracrine signaling from the surrounding stroma. L-R differences could not be supported long-term unless the microenvironment were L-R different. ECM components such as collagen and MMPs have been shown to regulate MaSC proliferation and self-renewal (Barcus, Keely et al. 2013, Chen, Bhat-Nakshatri et al. 2013, Kessenbrock, Dijkgraaf et al. 2013). However, no studies have examined if these ECM components are L-R different. Mammary gland transplantation experiments could determine if L-R different microenvironments play a role in maintaining L-R differences in mammary glands. Because MaSCs and possibly other cell populations have L-R differences in number as well as gene expression, the number and cell type will have to be controlled in these experiments. Therefore, injecting the same number of a single population of mammary epithelial cells from the L and R TMGs into ipsilateral (same) and contralateral (opposite) sides of cleared TMGs would determine if the microenvironment propagates molecular L-R differences in mammary epithelial cells (Figure 25). In addition, this experiment completed in limiting dilutions of MaSCs from the L and R TMGs would give functional *in vivo* data for L-R differences in MaSC self-renewal observed in pervious *in vitro* mammosphere experiments. If the L and R fat pads have different reconstitution potentials with cells from the same side of origin, then the L and R microenvironments are different. If the L (or R) fat pad has a different reconstitution potential depending on the side of origin the cells came from, then the L and R MaSCs are functionally

different *in vivo.* If the L and R fat pads have the same reconstitution potential regardless of the side of origin of the donor cells, the MaSCs and the microenvironment is functionally L-R equivalent *in vivo*.

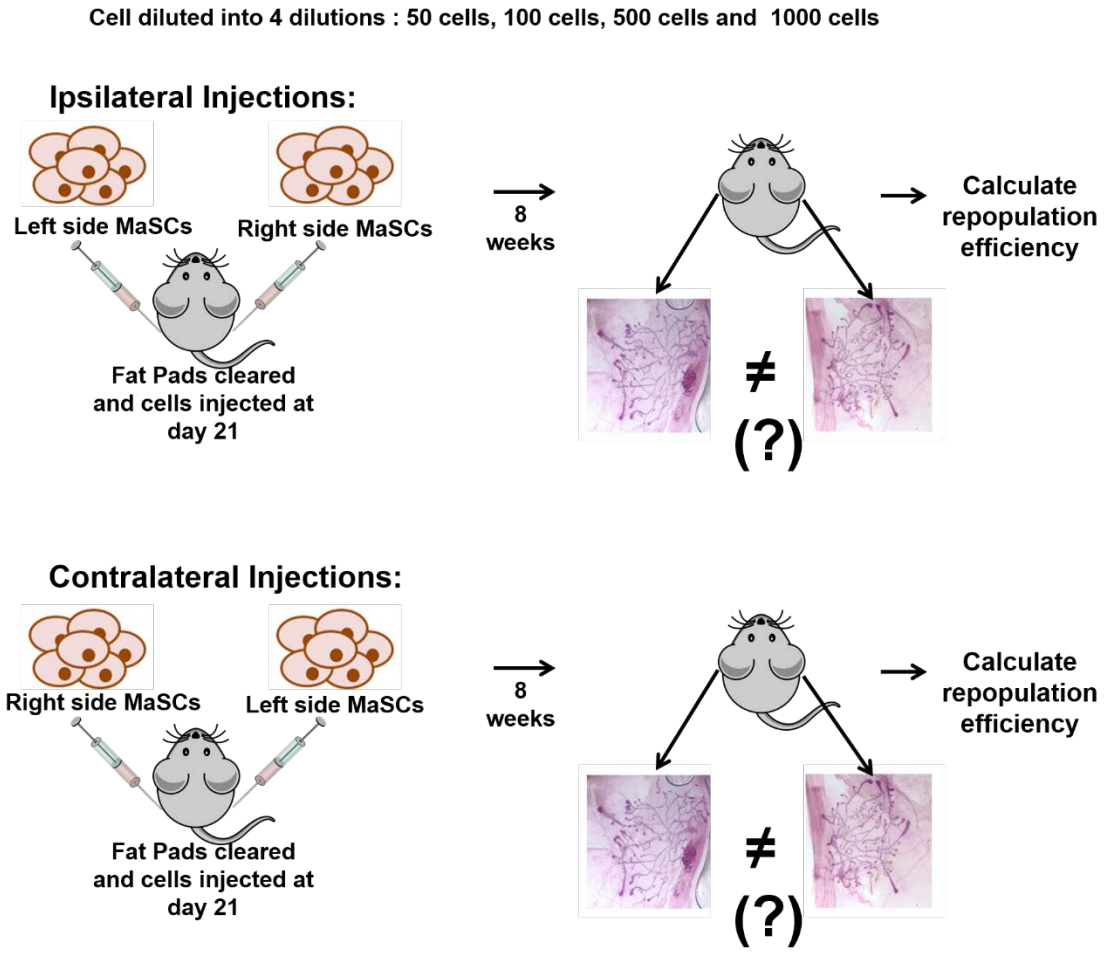

Figure 25. Mammary gland limited dilution repopulation experimental design. Ipsilateral (same side) and contralateral (opposite side) injections of limiting dilutions of MaSCs would determine if WT MaSCs and or microenvironments are functionally different *in vivo*. If the L and R fat pads have different reconstitution potentials with cells from the same side of origin, then the L and R microenvironments are different. If the L (or R) fat pad has a different reconstitution potential depending on the side of origin the cells came from, then the L and R MaSCs are functionally different *in vivo.* If the L and R fat pads have the same reconstitution potential regardless of the side of origin of the donor cells, the MaSCs and the microenvironment is functionally L-R equivalent *in vivo*.

Studies of L-R differences in other developmental time points have yet to be completed by our lab. L-R differences in pathways regulating luminal cell determination would suggest that lactation may also be L-R different. Baseline L-R differences in β-casein (Figure 19D), a milk protein, of WT mice would suggest that milk production may in fact be lateralized; in addition, human studies show that the L and R breast produce milk at different rates (Engstrom, Meier et al. 2007). Marsupials are capable of producing two different types of milk for developing offspring of different ages in contralateral glands (Sebastian, De Matteo et al. 1998), therefore it is conceivable that humans are also capable of producing milk with L-R differences. Studies of mouse milk composition over multiple pregnancies, both pre- and post-partum, would determine if the nutritional composition of milk is lateralized and/or changes over subsequent pregnancies. L-R differences in involution also need examination. Studies show that pregnancy and subsequent involution change the morphology and cell biology of the mammary glands, resulting in decrease risks for breast cancer (D'Cruz, Moody et al. 2002, Albrektsen, Heuch et al. 2005, Meier-Abt, Milani et al. 2013). The effect of pregnancy and involution has not been examined L vs. R. Studies examining MaSC number and function post-partum and after involution would determine if protective changes have symmetrically.

In addition to studies furthering knowledge of normal development, studies examining the role of L-R differences in tumor initiation, progression, and response to therapy are necessary. Results of the Lapatinib study in WT and MMTV-Neu$^{Tg/Tg}$ mice suggest that MaSCs expressing higher levels of EGFR increase in self-

renewal with Lapatinib treatment. This data suggest that Lapatinib treatment may increase MaSC potential and heighten risk for future aggressive breast cancer subtypes. To test this hypothesis, WT mice could be given Lapatinib (or DMSO control) treatment for several weeks then exposed to a carcinogen known to induce mammary tumors such as 7,12-Dimethylbenz[a]anthracene (DMBA). Tumor initiation and tumor histology L vs. R would determine if Lapatinib increases risks for breast cancer long term and if the change in breast cancer risk is lateralized.

The L-R differential response to both Lapatinib and E2 exposure suggest that the mammary glands and MaSCs will respond L-R differently to multiple chemical compounds. Importantly, commonly used clinical therapies such as aromatase inhibitors, the taxol family of drugs, platinum based therapies, as well as radiation should be tested for efficacy and long term risks L vs R. Current studies have never taken L vs. R differences into account in determining effectiveness. Complementary to future studies with Lapatinib, drug screening common clinical therapies L vs. R for both normal MaSCs and tumor derived MaSCs may allow clinicians to also use L vs. R side of tumor origin as an additional parameter in determining the proper and most effective form of treatment while minimizing long-term risks.

The role of tumor situs in metastasis should also be examined. Epidemiological studies show that although more tumors form on the left side, right side tumors appear to be more metastatic and aggressive (Fatima, Zaman et al. 2013). L-R differences in tumor incidence via multiple mouse models such as the MMTV-Neu$^{Tg/Tg}$ model, or the polyoma virus middle T antigen expressing mouse

(MMTV-PyMT), which develops more heterogeneous tumors, would determine L-R differences in tumor laterality. Injecting mice with labeled tumor cells (different colors for different sides) and allowing tumors to grow and metastasize would determine if the microenvironment of the tumor dictates tumor aggressiveness. In addition, injecting tumor derived cells from L and R tumors would determine if L and R tumors differ in metastatic properties such as location of metastasis (tail vain for lung, cardiac injection for brain), number of metastatic sites, or size of metastases. Lastly, tail vain or cardiac injections of L and R fluorescently labeled (different colors for different sides) tumor derived cells simultaneously would determine if L and R tumor cells differ in the aggressiveness of metastases competitively.

Experiments to determine if distinct molecular L-R differences in MaSC populations contribute to differences in tumor biology (ie tumor incidence, progression), response to therapy, and overall survival are still needed. First a duel reporter mouse expressing green fluorescence protein (GFP) when Wnt3a is expressed and expressing red fluorescence protein (RFP) when Epb4 is expressed under the MMTV promoter (to make GFP and RFP expression mammary specific) would need to be created. Because left side MaSCs express higher levels of stem cell marker Wnt3a and low levels of stem cell marker Epb4, left side MaSCs should be predominately GFP expressing; whereas right-side MaSCs express high levels of Epb4 and low levels of Wnt3a, right side MaSCs should be predominately RFP expressing. Then, these duel reporter mice would be treated with the carcinogen 7,12-Dimethylbenz-[a]anthracene (DMBA) at

puberty to induce mammary tumors. Mammary tumors would be examined for GFP and RFP expression to determine if Wnt3a-MaSCs (left side predominate) or Epb4-MaSCs (right side predominate) contribute more often to tumorigenesis. In addition, tumor size, histology, and metastases would be quantified and compared L vs. R as well as GFP-predominate or RFP-predominate to determine if tumor biology differs depending side of tumor origin and/or on the type of MaSC contributing to tumorigenesis, thereby answering the question does MaSC subtype correlate with tumor biology and heterogeneity. In addition overall survival would be compared L vs. R as well as by tumor subtype (GFP-predominate vs. RFP-predominate) to determine if sidedness and/or MaSC gene expression (Wnt3a vs. Epb4) plays a role in overall survival of mice. Also metastatic sites of involvement will be analyzed to determine if Wnt3a-MaSCs or Epb4-MaSCs expressing tumors have larger or more frequent metastases.

Previous reports, as well as our studies in Chapter 3, demonstrate that Epb4 expressing MaSCs are less sensitive to chemotherapeutic agents (Pfefferle, Spike et al. 2015). To determine if L-R differences in MaSCs also relate to therapeutic sensitivity, duel reporter mice with DMBA derived tumors will also be given Lapatinib, taxol, or a combination of both drugs at clinically relevant doses. L-R differences in response to therapy would be quantified by changes in tumor size, changes in metastatic frequency and size, as well as overall survival. In addition, remaining tumors would be dissected to determine if there decreases in GFP and RFP expressing cells occurred and if so if are GFP-Wnt3a and RFP-Epb4 cancer stem cells equally responsive to therapeutic agents. In addition, EGF family of

receptor expression will be analyzed by RT-PCR to determine if receptor expression correlates with MaSC gene expression (Wnt3a vs Epb4), overall survival, and/or response to Lapatinib or taxol. Our studies suggest that MaSCs with higher EGFR expression will correlate with poor survival as well as decreased therapeutic sensitivity. EGFR/ErbB2 expression could not be used as the stem cell specific (L-R different) markers in the reporter mouse, because EGFR and ErbB2 are not specific to MaSCs whereas Wnt3a and Epb4 are MaSC specific. Lastly, reporter mice could be crossed with MMTV-Neu$^{Tg/Tg}$ mice and the experiments repeated to determine if, like MaSC growth properties, will L-R differences in tumor biology, survival, and response to therapy invert in laterality. These experiments would demonstrate that not only are there two distinct subtypes of MaSCs, but these subsets of MaSCs are L-R different, and are the basis of L-R differences in breast cancer epidemiology. In addition, these studies could find novel bio-markers in predicting breast cancer responsiveness.

The field of mammary and tumor laterality is wide open. Mammary gland laterality is another tool to understanding normal mammary gland biology as well as progression into disease and tumor biology. Thorough understanding of normal biology and disease progression leads to increased breast cancer prevention and treatment. Early intervention for breast cancer patients is lacking; current early intervention is often limited to double mastectomy, with little un-invasive pharmaceutical treatment. Using normal mammary gland laterality and tumor laterality as a tool to understand normal and neoplastic development, earlier windows of prevention may be found and exploited to prevent breast cancer in high

risk patients. Moreover, if L-R differences in gene expression regulate therapeutic sensitivity, previously described drug screens to identify drugs that preferentially target specific MaSC populations could be matched to patient tumor gene expression resulting in increased therapeutic response and overall increase patient survival.

REFERENCES

Albrektsen, G., I. Heuch, S. Hansen and G. Kvale (2005). "Breast cancer risk by age at birth, time since birth and time intervals between births: exploring interaction effects." Br J Cancer **92**(1): 167-175.

Alvi, A. J., H. Clayton, C. Joshi, T. Enver, A. Ashworth, M. Vivanco, T. C. Dale and M. J. Smalley (2003). "Functional and molecular characterisation of mammary side population cells." Breast Cancer Res **5**(1): R1-8.

Anderson, S. M., M. C. Rudolph, J. L. McManaman and M. C. Neville (2007). "Key stages in mammary gland development. Secretory activation in the mammary gland: it's not just about milk protein synthesis!" Breast Cancer Res **9**(1): 204.

Arkoob, K., M. Al-Nsour, O. Al-Nemry and B. Al-Hajawi (2010). "Epidemiology of breast cancer in women in Jordan: patient characteristics and survival analysis." East Mediterr Health J **16**(10): 1032-1038.

Asselin-Labat, M. L., K. D. Sutherland, H. Barker, R. Thomas, M. Shackleton, N. C. Forrest, L. Hartley, L. Robb, F. G. Grosveld, J. van der Wees, G. J. Lindeman and J. E. Visvader (2007). "Gata-3 is an essential regulator of mammary-gland morphogenesis and luminal-cell differentiation." Nat Cell Biol **9**(2): 201-209.

Asselin-Labat, M. L., F. Vaillant, M. Shackleton, T. Bouras, G. J. Lindeman and J. E. Visvader (2008). "Delineating the epithelial hierarchy in the mouse mammary gland." Cold Spring Harb Symp Quant Biol **73**: 469-478.

Asselin-Labat, M. L., F. Vaillant, J. M. Sheridan, B. Pal, D. Wu, E. R. Simpson, H. Yasuda, G. K. Smyth, T. J. Martin, G. J. Lindeman and J. E. Visvader (2010). "Control of mammary stem cell function by steroid hormone signalling." Nature **465**(7299): 798-802.

Aupperlee, M. D., J. R. Leipprandt, J. M. Bennett, R. C. Schwartz and S. Z. Haslam (2013). "Amphiregulin mediates progesterone-induced mammary ductal development during puberty." Breast Cancer Res **15**(3): R44.

Balinsky, B. I. (1950). "On the prenatal growth of the mammary gland rudiment in the mouse." J Anat **84**(3): 227-235.

Bao, J., K. D. Yu, Y. Z. Jiang, Z. M. Shao and G. H. Di (2014). "The effect of laterality and primary tumor site on cancer-specific mortality in breast cancer: a SEER population-based study." PLoS One **9**(4): e94815.

Baquero, M. T., J. A. Hanna, V. Neumeister, H. Cheng, A. M. Molinaro, L. N. Harris and D. L. Rimm (2012). "Stathmin expression and its relationship to microtubule-associated protein tau and outcome in breast cancer." Cancer **118**(19): 4660-4669.

Barcus, C. E., P. J. Keely, K. W. Eliceiri and L. A. Schuler (2013). "Stiff collagen matrices increase tumorigenic prolactin signaling in breast cancer cells." J Biol Chem **288**(18): 12722-12732.

Baselga, J. (2006). "Targeting tyrosine kinases in cancer: the second wave." Science **312**(5777): 1175-1178.

Baselga, J., D. Rischin, M. Ranson, H. Calvert, E. Raymond, D. G. Kieback, S. B. Kaye, L. Gianni, A. Harris, T. Bjork, S. D. Averbuch, A. Feyereislova, H. Swaisland, F. Rojo and J. Albanell (2002). "Phase I safety, pharmacokinetic, and pharmacodynamic trial of ZD1839, a selective oral epidermal growth factor receptor tyrosine kinase inhibitor, in patients with five selected solid tumor types." J Clin Oncol **20**(21): 4292-4302.

Bern, H. A., K. T. Mills and L. A. Jones (1983). "Critical period for neonatal estrogen exposure in occurrence of mammary gland abnormalities in adult mice." Proc Soc Exp Biol Med **172**(2): 239-242.

Biro, F. M. and J. Deardorff (2013). "Identifying opportunities for cancer prevention during preadolescence and adolescence: puberty as a window of susceptibility." J Adolesc Health **52**(5 Suppl): S15-20.

Bizzarri, M., A. Giuliani, A. Cucina, F. D'Anselmi, A. M. Soto and C. Sonnenschein (2011). "Fractal analysis in a systems biology approach to cancer." Semin Cancer Biol **21**(3): 175-182.

Bodicoat, D. H., M. J. Schoemaker, M. E. Jones, E. McFadden, J. Griffin, A. Ashworth and A. J. Swerdlow (2014). "Timing of pubertal stages and breast cancer risk: the Breakthrough Generations Study." Breast Cancer Res **16**(1): R18.

Bonnette, S. G. and D. L. Hadsell (2001). "Targeted disruption of the IGF-I receptor gene decreases cellular proliferation in mammary terminal end buds." Endocrinology **142**(11): 4937-4945.

Booth, B. W., C. A. Boulanger and G. H. Smith (2008). "Selective segregation of DNA strands persists in long-label-retaining mammary cells during pregnancy." Breast Cancer Res **10**(5): R90.

Boras-Granic, K., P. Dann and J. J. Wysolmerski (2014). "Embryonic cells contribute directly to the quiescent stem cell population in the adult mouse mammary gland." Breast Cancer Res **16**(6): 487.

Borisenkov, M. F., Bazhenov, S. M. (2001). "Survival in Human Breast Cancer: Effects of Tumor Laterality and the Time of the Year of Surgery." Human Physiology **27**(5): 631-634.

Bouras, T., B. Pal, F. Vaillant, G. Harburg, M. L. Asselin-Labat, S. R. Oakes, G. J. Lindeman and J. E. Visvader (2008). "Notch signaling regulates mammary stem cell function and luminal cell-fate commitment." Cell Stem Cell **3**(4): 429-441.

Braverman, B. and M. Tambasco (2013). "Scale-specific multifractal medical image analysis." Comput Math Methods Med **2013**: 262931.

Brend, T. and S. A. Holley (2009). "Balancing segmentation and laterality during vertebrate development." Semin Cell Dev Biol **20**(4): 472-478.

Brill, B., N. Boecher, B. Groner and C. S. Shemanko (2008). "A sparing procedure to clear the mouse mammary fat pad of epithelial components for transplantation analysis." Lab Anim **42**(1): 104-110.

Brisken, C. (2002). "Hormonal control of alveolar development and its implications for breast carcinogenesis." J Mammary Gland Biol Neoplasia **7**(1): 39-48.

Brisken, C., S. Park, T. Vass, J. P. Lydon, B. W. O'Malley and R. A. Weinberg (1998). "A paracrine role for the epithelial progesterone receptor in mammary gland development." Proc Natl Acad Sci U S A **95**(9): 5076-5081.

Burris, H. A., 3rd, H. I. Hurwitz, E. C. Dees, A. Dowlati, K. L. Blackwell, B. O'Neil, P. K. Marcom, M. J. Ellis, B. Overmoyer, S. F. Jones, J. L. Harris, D. A. Smith, K. M. Koch, A. Stead, S. Mangum and N. L. Spector (2005). "Phase I safety, pharmacokinetics, and clinical activity study of lapatinib (GW572016), a reversible dual inhibitor of epidermal growth factor receptor tyrosine kinases, in heavily pretreated patients with metastatic carcinomas." J Clin Oncol **23**(23): 5305-5313.

Cardiff, R. D. and S. R. Wellings (1999). "The comparative pathology of human and mouse mammary glands." J Mammary Gland Biol Neoplasia **4**(1): 105-122.

Carey, L. A., C. M. Perou, C. A. Livasy, L. G. Dressler, D. Cowan, K. Conway, G. Karaca, M. A. Troester, C. K. Tse, S. Edmiston, S. L. Deming, J. Geradts, M. C. Cheang, T. O. Nielsen, P. G. Moorman, H. S. Earp and R. C. Millikan (2006). "Race, breast cancer subtypes, and survival in the Carolina Breast Cancer Study." JAMA **295**(21): 2492-2502.

Carr, J. R., M. M. Kiefer, H. J. Park, J. Li, Z. Wang, J. Fontanarosa, D. DeWaal, D. Kopanja, E. V. Benevolenskaya, G. Guzman and P. Raychaudhuri (2012). "FoxM1 regulates mammary luminal cell fate." Cell Rep **1**(6): 715-729.

Carr, J. R., H. J. Park, Z. Wang, M. M. Kiefer and P. Raychaudhuri (2010). "FoxM1 mediates resistance to herceptin and paclitaxel." Cancer Res **70**(12): 5054-5063.

Chakrabarti, R., Y. Wei, R. A. Romano, C. DeCoste, Y. Kang and S. Sinha (2012). "Elf5 regulates mammary gland stem/progenitor cell fate by influencing notch signaling." Stem Cells **30**(7): 1496-1508.

Chatsiproios, D. (2010). "Safety Profile and Clinical Recommendations for the Use of Lapatinib." Breast Care (Basel) **5**(s1): 16-21.

Chen, D., P. Bhat-Nakshatri, C. Goswami, S. Badve and H. Nakshatri (2013). "ANTXR1, a stem cell-enriched functional biomarker, connects collagen signaling to cancer stem-like cells and metastasis in breast cancer." Cancer Res **73**(18): 5821-5833.

Chintapalli, V. R., S. Terhzaz, J. Wang, M. Al Bratty, D. G. Watson, P. Herzyk, S. A. Davies and J. A. Dow (2012). "Functional correlates of positional and gender-specific renal asymmetry in Drosophila." PLoS One **7**(4): e32577.

Chiquet-Ehrismann, R., E. J. Mackie, C. A. Pearson and T. Sakakura (1986). "Tenascin: an extracellular matrix protein involved in tissue interactions during fetal development and oncogenesis." Cell **47**(1): 131-139.

Cho, K. W., H. J. Kwon, J. O. Shin, J. M. Lee, S. W. Cho, C. Tickle and H. S. Jung (2012). "Retinoic acid signaling and the initiation of mammary gland development." Dev Biol **365**(1): 259-266.

Chou, J., S. Provot and Z. Werb (2010). "GATA3 in development and cancer differentiation: cells GATA have it!" J Cell Physiol **222**(1): 42-49.

Chu, E. Y., J. Hens, T. Andl, A. Kairo, T. P. Yamaguchi, C. Brisken, A. Glick, J. J. Wysolmerski and S. E. Millar (2004). "Canonical WNT signaling promotes mammary placode development and is essential for initiation of mammary gland morphogenesis." Development **131**(19): 4819-4829.

Cicalese, A., G. Bonizzi, C. E. Pasi, M. Faretta, S. Ronzoni, B. Giulini, C. Brisken, S. Minucci, P. P. Di Fiore and P. G. Pelicci (2009). "The tumor suppressor p53 regulates polarity of self-renewing divisions in mammary stem cells." Cell **138**(6): 1083-1095.

Clarke, R. B., E. Anderson, A. Howell and C. S. Potten (2003). "Regulation of human breast epithelial stem cells." Cell Prolif **36 Suppl 1**: 45-58.

Cohn, E., L. Ossowski, S. Bertran, C. Marzan and E. F. Farias (2010). "RARalpha1 control of mammary gland ductal morphogenesis and wnt1-tumorigenesis." Breast Cancer Res **12**(5): R79.

Colby, D. R. and J. G. Vandenberg (1974). "Regulatory effects of urinary pheromones on puberty in the mouse." Biol Reprod **11**(3): 268-279.

Cross, S. S. (1997). "Fractals in pathology." J Pathol **182**(1): 1-8.

Cross, S. S., J. P. Bury, T. J. Stephenson and R. F. Harrison (1997). "Image analysis of low magnification images of fine needle aspirates of the breast produces useful discrimination between benign and malignant cases." Cytopathology **8**(4): 265-273.

D'Cruz, C. M., S. E. Moody, S. R. Master, J. L. Hartman, E. A. Keiper, M. B. Imielinski, J. D. Cox, J. Y. Wang, S. I. Ha, B. A. Keister and L. A. Chodosh (2002). "Persistent parity-induced changes in growth factors, TGF-beta3,

and differentiation in the rodent mammary gland." Mol Endocrinol **16**(9): 2034-2051.

Daniel, C. W., G. B. Silberstein and P. Strickland (1987). "Direct action of 17 beta-estradiol on mouse mammary ducts analyzed by sustained release implants and steroid autoradiography." Cancer Res **47**(22): 6052-6057.

DasGupta, R. and E. Fuchs (1999). "Multiple roles for activated LEF/TCF transcription complexes during hair follicle development and differentiation." Development **126**(20): 4557-4568.

Davenport, T. G., L. A. Jerome-Majewska and V. E. Papaioannou (2003). "Mammary gland, limb and yolk sac defects in mice lacking Tbx3, the gene mutated in human ulnar mammary syndrome." Development **130**(10): 2263-2273.

Daye, D., B. Keller, E. F. Conant, J. Chen, M. D. Schnall, A. D. Maidment and D. Kontos (2013). "Mammographic parenchymal patterns as an imaging marker of endogenous hormonal exposure: a preliminary study in a high-risk population." Acad Radiol **20**(5): 635-646.

de Assis, S., A. Warri, M. I. Cruz and L. Hilakivi-Clarke (2010). "Changes in mammary gland morphology and breast cancer risk in rats." J Vis Exp(44).

Delahunt, B., P. Bethwaite and J. N. Nacey (1994). "Renal cell carcinoma in New Zealand: a national survival study." Urology **43**(3): 300-309.

Desmedt, C., F. Piette, S. Loi, Y. Wang, F. Lallemand, B. Haibe-Kains, G. Viale, M. Delorenzi, Y. Zhang, M. S. d'Assignies, J. Bergh, R. Lidereau, P. Ellis, A. L. Harris, J. G. Klijn, J. A. Foekens, F. Cardoso, M. J. Piccart, M. Buyse

and C. Sotiriou (2007). "Strong time dependence of the 76-gene prognostic signature for node-negative breast cancer patients in the TRANSBIG multicenter independent validation series." Clin Cancer Res **13**(11): 3207-3214.

Dey, P. and S. K. Mohanty (2003). "Fractal dimensions of breast lesions on cytology smears." Diagn Cytopathol **29**(2): 85-86.

Di Giovanni, P., T. S. Ahearn, S. I. Semple, L. M. Lovell, I. Miller, F. J. Gilbert, T. W. Redpath, S. D. Heys and R. T. Staff (2012). "The biological correlates of macroscopic breast tumour structure measured using fractal analysis in patients undergoing neoadjuvant chemotherapy." Breast Cancer Res Treat **133**(3): 1199-1206.

di Masi, A., L. Leboffe, E. De Marinis, F. Pagano, L. Cicconi, C. Rochette-Egly, F. Lo Coco, P. Ascenzi and C. Nervi (2014). "Retinoic acid receptors and cancer: From molecular mechanisms to therapy." Mol Aspects Med.

Diaz-Guerra, E., M. A. Lillo, S. Santamaria and J. A. Garcia-Sanz (2012). "Intrinsic cues and hormones control mouse mammary epithelial tree size." FASEB J **26**(9): 3844-3853.

DiPaolo, D. and L. A. Jones (2000). "Neonatal estradiol exposure alters mouse mammary estrogen receptor alpha expression." Int J Oncol **16**(5): 935-941.

Dontu, G., M. Al-Hajj, W. M. Abdallah, M. F. Clarke and M. S. Wicha (2003). "Stem cells in normal breast development and breast cancer." Cell Prolif **36 Suppl 1**: 59-72.

Dontu, G., D. El-Ashry and M. S. Wicha (2004). "Breast cancer, stem/progenitor cells and the estrogen receptor." Trends Endocrinol Metab **15**(5): 193-197.

dos Santos, C. O., C. Rebbeck, E. Rozhkova, A. Valentine, A. Samuels, L. R. Kadiri, P. Osten, E. Y. Harris, P. J. Uren, A. D. Smith and G. J. Hannon (2013). "Molecular hierarchy of mammary differentiation yields refined markers of mammary stem cells." Proc Natl Acad Sci U S A **110**(18): 7123-7130.

Durnberger, H. and K. Kratochwil (1980). "Specificity of tissue interaction and origin of mesenchymal cells in the androgen response of the embryonic mammary gland." Cell **19**(2): 465-471.

Eblaghie, M. C., S. J. Song, J. Y. Kim, K. Akita, C. Tickle and H. S. Jung (2004). "Interactions between FGF and Wnt signals and Tbx3 gene expression in mammary gland initiation in mouse embryos." J Anat **205**(1): 1-13.

Eccles, S. A. (2011). "The epidermal growth factor receptor/Erb-B/HER family in normal and malignant breast biology." Int J Dev Biol **55**(7-9): 685-696.

Engstrom, J. L., P. P. Meier, B. Jegier, J. E. Motykowski and J. L. Zuleger (2007). "Comparison of milk output from the right and left breasts during simultaneous pumping in mothers of very low birthweight infants." Breastfeed Med **2**(2): 83-91.

Eroles, P., A. Bosch, J. A. Perez-Fidalgo and A. Lluch (2012). "Molecular biology in breast cancer: intrinsic subtypes and signaling pathways." Cancer Treat Rev **38**(6): 698-707.

Farnie, G. and R. B. Clarke (2007). "Mammary stem cells and breast cancer--role of Notch signalling." Stem Cell Rev **3**(2): 169-175.

Fata, J. E., Z. Werb and M. J. Bissell (2004). "Regulation of mammary gland branching morphogenesis by the extracellular matrix and its remodeling enzymes." Breast Cancer Res **6**(1): 1-11.

Fatima, N., M. U. Zaman, A. Maqbool, S. H. Khan and N. Riaz (2013). "Lower incidence but more aggressive behavior of right sided breast cancer in Pakistani women: does right deserve more respect?" Asian Pac J Cancer Prev **14**(1): 43-45.

Feigelson, H. S. and B. E. Henderson (1996). "Estrogens and breast cancer." Carcinogenesis **17**(11): 2279-2284.

Feng, Y., D. Manka, K. U. Wagner and S. A. Khan (2007). "Estrogen receptor-alpha expression in the mammary epithelium is required for ductal and alveolar morphogenesis in mice." Proc Natl Acad Sci U S A **104**(37): 14718-14723.

Fenton, S. E. (2006). "Endocrine-disrupting compounds and mammary gland development: early exposure and later life consequences." Endocrinology **147**(6 Suppl): S18-24.

Fenton, S. E. (2006). "Endocrine-Disrupting Compounds and Mammary Gland Development: Early Exposure and Later Life Consequences." Endocrinology **147**(6): s18-24.

Fenton, S. E., C. Reed and R. R. Newbold (2012). "Perinatal environmental exposures affect mammary development, function, and cancer risk in adulthood." Annu Rev Pharmacol Toxicol **52**: 455-479.

Fernandez, E. and H. F. Jelinek (2001). "Use of fractal theory in neuroscience: methods, advantages, and potential problems." Methods **24**(4): 309-321.

Fillmore, C. M., P. B. Gupta, J. A. Rudnick, S. Caballero, P. J. Keller, E. S. Lander and C. Kuperwasser (2010). "Estrogen expands breast cancer stem-like cells through paracrine FGF/Tbx3 signaling." Proc Natl Acad Sci U S A **107**(50): 21737-21742.

Fisher, B., J. P. Costantino, D. L. Wickerham, C. K. Redmond, M. Kavanah, W. M. Cronin, V. Vogel, A. Robidoux, N. Dimitrov, J. Atkins, M. Daly, S. Wieand, E. Tan-Chiu, L. Ford and N. Wolmark (1998). "Tamoxifen for prevention of breast cancer: report of the National Surgical Adjuvant Breast and Bowel Project P-1 Study." J Natl Cancer Inst **90**(18): 1371-1388.

Fuseler, J. W., D. M. Merrill, J. A. Rogers, M. B. Grisham and R. E. Wolf (2006). "Analysis and quantitation of NF-kappaB nuclear translocation in tumor necrosis factor alpha (TNF-alpha) activated vascular endothelial cells." Microsc Microanal **12**(3): 269-276.

Fuseler, J. W., C. F. Millette, J. M. Davis and W. Carver (2007). "Fractal and image analysis of morphological changes in the actin cytoskeleton of neonatal cardiac fibroblasts in response to mechanical stretch." Microsc Microanal **13**(2): 133-143.

Fuseler, J. W., J. P. Robichaux, H. I. Atiyah and A. F. Ramsdell (2014). "Morphometric and fractal dimension analysis identifies early neoplastic changes in mammary epithelium of MMTV-cNeu mice." Anticancer Res **34**(3): 1171-1177.

Fuseler, J. W., J. P. Robichaux, H. I. Atiyah and A. F. Ramsdell (2014). "Morphometric and fractal dimension analysis identifies early neoplastic changes in mammary epithelium of MMTV-cNeu mice." Anticancer Res. **34**(3): 1171-1177.

Fuseler, J. W. and M. T. Valarmathi (2012). "Modulation of the migration and differentiation potential of adult bone marrow stromal stem cells by nitric oxide." Biomaterials **33**(4): 1032-1043.

Gilbert, S. (2000). Paraxial Mesoderm: The somites and their derivatives. Sunderland, MA, Sinauer Associates.

Golding, J. P., T. A. Partridge, J. R. Beauchamp, T. King, N. A. Brown, M. Gassmann and P. S. Zammit (2004). "Mouse myotomes pairs exhibit left-right asymmetric expression of MLC3F and alpha-skeletal actin." Dev Dyn **231**(4): 795-800.

Golding, J. P., S. Tsoni, M. Dixon, K. T. Yee, T. A. Partridge, J. R. Beauchamp, M. Gassmann and P. S. Zammit (2004). "Heparin-binding EGF-like growth factor shows transient left-right asymmetrical expression in mouse myotome pairs." Gene Expr Patterns **5**(1): 3-9.

Greene RR, B. M., Ivy AC (1940). "The effects of estrogens on the antenatal development of the rat." American Journal of Anatomy **67**: 305-345.

Grizzi, F., C. Russo, P. Colombo, B. Franceschini, E. E. Frezza, E. Cobos and M. Chiriva-Internati (2005). "Quantitative evaluation and modeling of two-dimensional neovascular network complexity: the surface fractal dimension." BMC Cancer **5**: 14.

Group, U. S. C. S. W. (2013). "United States Cancer Statistics: 199-2009 Incidence and Mortality Web-based Report." from Available at: www.cdc.gov/uscs.

Guo, W., Z. Keckesova, J. L. Donaher, T. Shibue, V. Tischler, F. Reinhardt, S. Itzkovitz, A. Noske, U. Zurrer-Hardi, G. Bell, W. L. Tam, S. A. Mani, A. van Oudenaarden and R. A. Weinberg (2012). "Slug and Sox9 cooperatively determine the mammary stem cell state." Cell **148**(5): 1015-1028.

Guy, C. T., M. A. Webster, M. Schaller, T. J. Parsons, R. D. Cardiff and W. J. Muller (1992). "Expression of the neu protooncogene in the mammary epithelium of transgenic mice induces metastatic disease." Proc Natl Acad Sci U S A **89**(22): 10578-10582.

Hallett, R. M., A. Dvorkin-Gheva, A. Bane and J. A. Hassell (2012). "A gene signature for predicting outcome in patients with basal-like breast cancer." Sci Rep **2**: 227.

Hallett, R. M., G. Pond and J. A. Hassell (2012). "A target based approach identifies genomic predictors of breast cancer patient response to chemotherapy." BMC Med Genomics **5**: 16.

Han, Z. X., H. M. Wang, G. Jiang, X. P. Du, X. Y. Gao and D. S. Pei (2013). "Overcoming Paclitaxel Resistance in Lung Cancer Cells Via Dual Inhibition of Stathmin and Bcl-2." Cancer Biother Radiopharm.

Hartveit, F., M. Tangen and E. Hartveit (1984). "Side and survival in breast cancer." Oncology **41**(3): 149-154.

Hatzis, C., L. Pusztai, V. Valero, D. J. Booser, L. Esserman, A. Lluch, T. Vidaurre, F. Holmes, E. Souchon, H. Wang, M. Martin, J. Cotrina, H. Gomez, R. Hubbard, J. I. Chacon, J. Ferrer-Lozano, R. Dyer, M. Buxton, Y. Gong, Y. Wu, N. Ibrahim, E. Andreopoulou, N. T. Ueno, K. Hunt, W. Yang, A. Nazario, A. DeMichele, J. O'Shaughnessy, G. N. Hortobagyi and W. F. Symmans "A genomic predictor of response and survival following taxane-anthracycline chemotherapy for invasive breast cancer." JAMA **305**(18): 1873-1881.

Hens, J. R. and J. J. Wysolmerski (2005). "Key stages of mammary gland development: molecular mechanisms involved in the formation of the embryonic mammary gland." Breast Cancer Res **7**(5): 220-224.

Heuberger, B., I. Fitzka, G. Wasner and K. Kratochwil (1982). "Induction of androgen receptor formation by epithelium-mesenchyme interaction in embryonic mouse mammary gland." Proc Natl Acad Sci U S A **79**(9): 2957-2961.

Hilakivi-Clarke, L., E. Cho, M. Raygada and N. Kenney (1997). "Alterations in mammary gland development following neonatal exposure to estradiol, transforming growth factor alpha, and estrogen receptor antagonist ICI 182,780." J Cell Physiol **170**(3): 279-289.

Hilakivi-Clarke, L., I. Onojafe, M. Raygada, E. Cho, R. Clarke and M. E. Lippman (1996). "Breast cancer risk in rats fed a diet high in n-6 polyunsaturated fatty acids during pregnancy." J Natl Cancer Inst **88**(24): 1821-1827.

Howard, B. A. (2012). "In the beginning: the establishment of the mammary lineage during embryogenesis." Semin Cell Dev Biol **23**(5): 574-582.

Howard, B. A. and B. A. Gusterson (2000). "Human breast development." J Mammary Gland Biol Neoplasia **5**(2): 119-137.

Hutchinson, J. N. and W. J. Muller (2000). "Transgenic mouse models of human breast cancer." Oncogene **19**(53): 6130-6137.

Inaguma, Y., M. Kusakabe, E. J. Mackie, C. A. Pearson, R. Chiquet-Ehrismann and T. Sakakura (1988). "Epithelial induction of stromal tenascin in the mouse mammary gland: from embryogenesis to carcinogenesis." Dev Biol **128**(2): 245-255.

Incassati, A., A. Chandramouli, R. Eelkema and P. Cowin (2010). "Key signaling nodes in mammary gland development and cancer: beta-catenin." Breast Cancer Res **12**(6): 213.

Irizarry, R. A., B. Hobbs, F. Collin, Y. D. Beazer-Barclay, K. J. Antonellis, U. Scherf and T. P. Speed (2003). "Exploration, normalization, and summaries of high density oligonucleotide array probe level data." Biostatistics **4**(2): 249-264.

Ishimaru, Y., T. Komatsu, M. Kasahara, Y. Katoh-Fukui, H. Ogawa, Y. Toyama, M. Maekawa, K. Toshimori, R. A. Chandraratna, K. Morohashi and H. Yoshioka (2008). "Mechanism of asymmetric ovarian development in chick embryos." Development **135**(4): 677-685.

Ithimakin, S., K. C. Day, F. Malik, Q. Zen, S. J. Dawsey, T. F. Bersano-Begey, A. A. Quraishi, K. W. Ignatoski, S. Daignault, A. Davis, C. L. Hall, N. Palanisamy, A. N. Heath, N. Tawakkol, T. K. Luther, S. G. Clouthier, W. A.

Chadwick, M. L. Day, C. G. Kleer, D. G. Thomas, D. F. Hayes, H. Korkaya and M. S. Wicha (2013). "HER2 drives luminal breast cancer stem cells in the absence of HER2 amplification: implications for efficacy of adjuvant trastuzumab." Cancer Res **73**(5): 1635-1646.

Ivshina, A. V., J. George, O. Senko, B. Mow, T. C. Putti, J. Smeds, T. Lindahl, Y. Pawitan, P. Hall, H. Nordgren, J. E. Wong, E. T. Liu, J. Bergh, V. A. Kuznetsov and L. D. Miller (2006). "Genetic reclassification of histologic grade delineates new clinical subtypes of breast cancer." Cancer Res **66**(21): 10292-10301.

Jean, C. (1971). "[Analysis of mammary deformities in the newborn induced by the injection of estrogens into the pregnant mother, in the rat and mouse]." Arch Anat Microsc Morphol Exp **60**(2): 147-168.

Jean, C. (1971). "[Postnatal mammary development of mice born of mothers treated with estradiol during pregnancy. Study at puberty and adult age under various experimental and physiological conditions]." Arch Sci Physiol (Paris) **25**(2): 145-185.

Joshi, P. A., H. W. Jackson, A. G. Beristain, M. A. Di Grappa, P. A. Mote, C. L. Clarke, J. Stingl, P. D. Waterhouse and R. Khokha (2010). "Progesterone induces adult mammary stem cell expansion." Nature **465**(7299): 803-807.

Kawakami, Y., A. Raya, R. M. Raya, C. Rodriguez-Esteban and J. C. Izpisua Belmonte (2005). "Retinoic acid signalling links left-right asymmetric patterning and bilaterally symmetric somitogenesis in the zebrafish embryo." Nature **435**(7039): 165-171.

Kenney, N. J., G. H. Smith, E. Lawrence, J. C. Barrett and D. S. Salomon (2001). "Identification of Stem Cell Units in the Terminal End Bud and Duct of the Mouse Mammary Gland." J Biomed Biotechnol **1**(3): 133-143.

Kessenbrock, K., G. J. Dijkgraaf, D. A. Lawson, L. E. Littlepage, P. Shahi, U. Pieper and Z. Werb (2013). "A role for matrix metalloproteinases in regulating mammary stem cell function via the Wnt signaling pathway." Cell Stem Cell **13**(3): 300-313.

Kontos, D., L. C. Ikejimba, P. R. Bakic, A. B. Troxel, E. F. Conant and A. D. Maidment (2011). "Analysis of parenchymal texture with digital breast tomosynthesis: comparison with digital mammography and implications for cancer risk assessment." Radiology **261**(1): 80-91.

Korkaya, H., A. Paulson, F. Iovino and M. S. Wicha (2008). "HER2 regulates the mammary stem/progenitor cell population driving tumorigenesis and invasion." Oncogene **27**(47): 6120-6130.

Korkaya, H. and M. S. Wicha (2013). "HER2 and breast cancer stem cells: more than meets the eye." Cancer Res **73**(12): 3489-3493.

Kouros-Mehr, H., E. M. Slorach, M. D. Sternlicht and Z. Werb (2006). "GATA-3 maintains the differentiation of the luminal cell fate in the mammary gland." Cell **127**(5): 1041-1055.

Kratochwil, K. (1969). "Organ specificity in mesenchymal induction demonstrated in the embryonic development of the mammary gland of the mouse." Dev Biol **20**(1): 46-71.

Kratochwil, K. (1977). "Development and loss of androgen responsiveness in the embryonic rudiment of the mouse mammary gland." Dev Biol **61**(2): 358-365.

Kwok, J. M., B. Peck, L. J. Monteiro, H. D. Schwenen, J. Millour, R. C. Coombes, S. S. Myatt and E. W. Lam (2010). "FOXM1 confers acquired cisplatin resistance in breast cancer cells." Mol Cancer Res **8**(1): 24-34.

Laughney, A. M., V. Krishnaswamy, E. J. Rizzo, M. C. Schwab, R. J. Barth, B. W. Pogue, K. D. Paulsen and W. A. Wells (2012). "Scatter spectroscopic imaging distinguishes between breast pathologies in tissues relevant to surgical margin assessment." Clin Cancer Res **18**(22): 6315-6325.

Lee, A. V., P. Zhang, M. Ivanova, S. Bonnette, S. Oesterreich, J. M. Rosen, S. Grimm, R. C. Hovey, B. K. Vonderhaar, C. R. Kahn, D. Torres, J. George, S. Mohsin, D. C. Allred and D. L. Hadsell (2003). "Developmental and hormonal signals dramatically alter the localization and abundance of insulin receptor substrate proteins in the mammary gland." Endocrinology **144**(6): 2683-2694.

Lee, H. J., D. Gallego-Ortega, A. Ledger, D. Schramek, P. Joshi, M. M. Szwarc, C. Cho, J. P. Lydon, R. Khokha, J. M. Penninger and C. J. Ormandy (2013). "Progesterone drives mammary secretory differentiation via RankL-mediated induction of Elf5 in luminal progenitor cells." Development **140**(7): 1397-1401.

Levin, M. (2005). "Left-right asymmetry in embryonic development: a comprehensive review." Mech Dev **122**(1): 3-25.

Li, M., X. Liu, G. Robinson, U. Bar-Peled, K. U. Wagner, W. S. Young, L. Hennighausen and P. A. Furth (1997). "Mammary-derived signals activate programmed cell death during the first stage of mammary gland involution." Proc Natl Acad Sci U S A **94**(7): 3425-3430.

Lim, E., F. Vaillant, D. Wu, N. C. Forrest, B. Pal, A. H. Hart, M. L. Asselin-Labat, D. E. Gyorki, T. Ward, A. Partanen, F. Feleppa, L. I. Huschtscha, H. J. Thorne, kConFab, S. B. Fox, M. Yan, J. D. French, M. A. Brown, G. K. Smyth, J. E. Visvader and G. J. Lindeman (2009). "Aberrant luminal progenitors as the candidate target population for basal tumor development in BRCA1 mutation carriers." Nat Med **15**(8): 907-913.

Lindsay, J., X. Jiao, T. Sakamaki, M. C. Casimiro, L. A. Shirley, T. H. Tran, X. Ju, M. Liu, Z. Li, C. Wang, S. Katiyar, M. Rao, K. G. Allen, R. I. Glazer, C. Ge, P. Stanley, M. P. Lisanti, H. Rui and R. G. Pestell (2008). "ErbB2 induces Notch1 activity and function in breast cancer cells." Clin Transl Sci **1**(2): 107-115.

Lippman, M. E., K. A. Krueger, S. Eckert, A. Sashegyi, E. L. Walls, S. Jamal, J. A. Cauley and S. R. Cummings (2001). "Indicators of lifetime estrogen exposure: effect on breast cancer incidence and interaction with raloxifene therapy in the multiple outcomes of raloxifene evaluation study participants." J Clin Oncol **19**(12): 3111-3116.

Liu, X., G. W. Robinson, K. U. Wagner, L. Garrett, A. Wynshaw-Boris and L. Hennighausen (1997). "Stat5a is mandatory for adult mammary gland development and lactogenesis." Genes Dev **11**(2): 179-186.

Lonning, P. E. (2007). "Breast cancer prognostication and prediction: are we making progress?" Ann Oncol **18 Suppl 8**: viii3-7.

Lopez, J., L. Ogren, R. Verjan and F. Talamantes (1988). "Effects of perinatal exposure to a synthetic estrogen and progestin on mammary tumorigenesis in mice." Teratology **38**(2): 129-134.

Losa, G. A. and T. F. Nonnenmacher (1996). "Self-similarity and fractal irregularity in pathologic tissues." Mod Pathol **9**(3): 174-182.

Lu, P., M. D. Sternlicht and Z. Werb (2006). "Comparative mechanisms of branching morphogenesis in diverse systems." J Mammary Gland Biol Neoplasia **11**(3-4): 213-228.

Lu, P. and Z. Werb (2008). "Patterning mechanisms of branched organs." Science **322**(5907): 1506-1509.

Lydon, J. P. (2010). "Stem cells: Cues from steroid hormones." Nature **465**(7299): 695-696.

Lydon, J. P., F. J. DeMayo, C. R. Funk, S. K. Mani, A. R. Hughes, C. A. Montgomery, Jr., G. Shyamala, O. M. Conneely and B. W. O'Malley (1995). "Mice lacking progesterone receptor exhibit pleiotropic reproductive abnormalities." Genes Dev **9**(18): 2266-2278.

Mailleux, A. A., B. Spencer-Dene, C. Dillon, D. Ndiaye, C. Savona-Baron, N. Itoh, S. Kato, C. Dickson, J. P. Thiery and S. Bellusci (2002). "Role of FGF10/FGFR2b signaling during mammary gland development in the mouse embryo." Development **129**(1): 53-60.

Makarem, M., N. Kannan, L. V. Nguyen, D. J. Knapp, S. Balani, M. D. Prater, J. Stingl, A. Raouf, O. Nemirovsky, P. Eirew and C. J. Eaves (2013). "Developmental changes in the in vitro activated regenerative activity of primitive mammary epithelial cells." PLoS Biol **11**(8): e1001630.

Makarem, M., B. T. Spike, C. Dravis, N. Kannan, G. M. Wahl and C. J. Eaves (2013). "Stem cells and the developing mammary gland." J Mammary Gland Biol Neoplasia **18**(2): 209-219.

Mark, M., N. B. Ghyselinck and P. Chambon (2009). "Function of retinoic acid receptors during embryonic development." Nucl Recept Signal **7**: e002.

Markey, C. M., E. H. Luque, M. Munoz De Toro, C. Sonnenschein and A. M. Soto (2001). "In utero exposure to bisphenol A alters the development and tissue organization of the mouse mammary gland." Biol Reprod **65**(4): 1215-1223.

Marti, A., Z. Feng, H. J. Altermatt and R. Jaggi (1997). "Milk accumulation triggers apoptosis of mammary epithelial cells." Eur J Cell Biol **73**(2): 158-165.

McDermott, S. P. and M. S. Wicha (2010). "Breast tumors: of mice and women." Breast Cancer Res **12**(3): 108.

Meier-Abt, F., E. Milani, T. Roloff, H. Brinkhaus, S. Duss, D. S. Meyer, I. Klebba, P. J. Balwierz, E. van Nimwegen and M. Bentires-Alj (2013). "Parity induces differentiation and reduces Wnt/Notch signaling ratio and proliferation potential of basal stem/progenitor cells isolated from mouse mammary epithelium." Breast Cancer Res **15**(2): R36.

Mendes-Pereira, A. M., D. Sims, T. Dexter, K. Fenwick, I. Assiotis, I. Kozarewa, C. Mitsopoulos, J. Hakas, M. Zvelebil, C. J. Lord and A. Ashworth (2012).

"Genome-wide functional screen identifies a compendium of genes affecting sensitivity to tamoxifen." Proc Natl Acad Sci U S A **109**(8): 2730-2735.

Meng, X. L., D. Su, L. Wang, Y. Gao, Y. J. Hu, H. J. Yang and S. N. Xie (2012). "Low expression of stathmin in tumor predicts high response to neoadjuvant chemotherapy with docetaxel-containing regimens in locally advanced breast cancer." Genet Test Mol Biomarkers **16**(7): 689-694.

Miceli, C., A. Tejada, A. Castaneda and S. J. Mistry (2013). "Cell cycle inhibition therapy that targets stathmin in in vitro and in vivo models of breast cancer." Cancer Gene Ther.

Miller, L. D., J. Smeds, J. George, V. B. Vega, L. Vergara, A. Ploner, Y. Pawitan, P. Hall, S. Klaar, E. T. Liu and J. Bergh (2005). "An expression signature for p53 status in human breast cancer predicts mutation status, transcriptional effects, and patient survival." Proc Natl Acad Sci U S A **102**(38): 13550-13555.

Millour, J., D. Constantinidou, A. V. Stavropoulou, M. S. Wilson, S. S. Myatt, J. M. Kwok, K. Sivanandan, R. C. Coombes, R. H. Medema, J. Hartman, A. E. Lykkesfeldt and E. W. Lam (2010). "FOXM1 is a transcriptional target of ERalpha and has a critical role in breast cancer endocrine sensitivity and resistance." Oncogene **29**(20): 2983-2995.

Molyneux, G., F. C. Geyer, F. A. Magnay, A. McCarthy, H. Kendrick, R. Natrajan, A. Mackay, A. Grigoriadis, A. Tutt, A. Ashworth, J. S. Reis-Filho and M. J. Smalley (2010). "BRCA1 basal-like breast cancers originate from luminal

epithelial progenitors and not from basal stem cells." Cell Stem Cell **7**(3): 403-417.

Monks, J., D. Rosner, F. J. Geske, L. Lehman, L. Hanson, M. C. Neville and V. A. Fadok (2005). "Epithelial cells as phagocytes: apoptotic epithelial cells are engulfed by mammary alveolar epithelial cells and repress inflammatory mediator release." Cell Death Differ **12**(2): 107-114.

Mori, T., H. A. Bern, K. T. Mills and P. N. Young (1976). "Long-term effects of neonatal steroid exposure on mammary gland development and tumorigenesis in mice." J Natl Cancer Inst **57**(5): 1057-1062.

Mukherjee, S., S. G. Louie, M. Campbell, L. Esserman and G. Shyamala (2000). "Ductal growth is impeded in mammary glands of C-neu transgenic mice." Oncogene **19**(52): 5982-5987.

Muller, W. J., C. L. Arteaga, S. K. Muthuswamy, P. M. Siegel, M. A. Webster, R. D. Cardiff, K. S. Meise, F. Li, S. A. Halter and R. J. Coffey (1996). "Synergistic interaction of the Neu proto-oncogene product and transforming growth factor alpha in the mammary epithelium of transgenic mice." Mol Cell Biol **16**(10): 5726-5736.

Nakamura, T. and H. Hamada (2012). "Left-right patterning: conserved and divergent mechanisms." Development **139**(18): 3257-3262.

National Institutes of Health. (2002, April 28, 2002). "Stem Cell Basics: Introduction." Retrieved 8 Jan, 2015, from http://stemcells.nih.gov/info/basics/pages/basics1.aspx.

Nautiyal, J., J. H. Steel, M. R. Mane, O. Oduwole, A. Poliandri, X. Alexi, N. Wood, M. Poutanen, W. Zwart, J. Stingl and M. G. Parker (2013). "The transcriptional co-factor RIP140 regulates mammary gland development by promoting the generation of key mitogenic signals." Development **140**(5): 1079-1089.

Nezadal, M., O. Zemeskal and M. Buchnicek (2001). The box-counting: critical study, 4th conference on prediction, synergetic and more…. The Faculty of Management, Institute of Information Technologies, Faculty of Technology, Tomas Bata University in Zlin.

Ngan, E. S., Z. Q. Ma, S. S. Chua, F. J. DeMayo and S. Y. Tsai (2002). "Inducible expression of FGF-3 in mouse mammary gland." Proc Natl Acad Sci U S A **99**(17): 11187-11192.

Nyirenda, N., D. L. Farkas and V. K. Ramanujan (2011). "Preclinical evaluation of nuclear morphometry and tissue topology for breast carcinoma detection and margin assessment." Breast Cancer Res Treat **126**(2): 345-354.

Oakes, S. R., H. N. Hilton and C. J. Ormandy (2006). "The alveolar switch: coordinating the proliferative cues and cell fate decisions that drive the formation of lobuloalveoli from ductal epithelium." Breast Cancer Res **8**(2): 207.

Oakes, S. R., M. J. Naylor, M. L. Asselin-Labat, K. D. Blazek, M. Gardiner-Garden, H. N. Hilton, M. Kazlauskas, M. A. Pritchard, L. A. Chodosh, P. L. Pfeffer, G. J. Lindeman, J. E. Visvader and C. J. Ormandy (2008). "The Ets

transcription factor Elf5 specifies mammary alveolar cell fate." Genes Dev **22**(5): 581-586.

Okasha, M., P. McCarron, D. Gunnell and G. D. Smith (2003). "Exposures in childhood, adolescence and early adulthood and breast cancer risk: a systematic review of the literature." Breast Cancer Res Treat **78**(2): 223-276.

Olayioye, M. A., R. M. Neve, H. A. Lane and N. E. Hynes (2000). "The ErbB signaling network: receptor heterodimerization in development and cancer." EMBO J **19**(13): 3159-3167.

Park, J. P., A. Raafat, J. A. Feltracco, W. M. Blanding and B. W. Booth (2013). "Differential gene expression in nuclear label-retaining cells in the developing mouse mammary gland." Stem Cells Dev **22**(8): 1297-1306.

Patterson, K. D., T. A. Drysdale and P. A. Krieg (2000). "Embryonic origins of spleen asymmetry." Development **127**(1): 167-175.

Perkins, C. I., J. Hotes, B. A. Kohler and H. L. Howe (2004). "Association between breast cancer laterality and tumor location, United States, 1994-1998." Cancer Causes Control **15**(7): 637-645.

Persson, I. (2000). "Estrogens in the causation of breast, endometrial and ovarian cancers - evidence and hypotheses from epidemiological findings." J Steroid Biochem Mol Biol **74**(5): 357-364.

Pfefferle, A. D., B. T. Spike, G. M. Wahl and C. M. Perou (2015). "Luminal progenitor and fetal mammary stem cell expression features predict breast

tumor response to neoadjuvant chemotherapy." Breast Cancer Res Treat **149**(2): 425-437.

Polyak, K. and R. Kalluri (2010). "The role of the microenvironment in mammary gland development and cancer." Cold Spring Harb Perspect Biol **2**(11): a003244.

Prat, A. and C. M. Perou (2009). "Mammary development meets cancer genomics." Nat Med **15**(8): 842-844.

Propper, A. and L. Gomot (1967). "[Tissue interactions during organogenesis of the mammary gland in the rabbit embryo]." C R Acad Sci Hebd Seances Acad Sci D **264**(22): 2573-2575.

Propper, A. Y. (1978). "Wandering epithelial cells in the rabbit embryo milk line. A preliminary scanning electron microscope study." Dev Biol **67**(1): 225-231.

Raguso, G., A. Ancona, L. Chieppa, S. L'Abbate, M. L. Pepe, F. Mangieri, M. De Palo and R. M. Rangayyan (2010). "Application of fractal analysis to mammography." Conf Proc IEEE Eng Med Biol Soc **2010**: 3182-3185.

Rangayyan, R. M., S. Banik and J. E. Desautels (2010). "Computer-aided detection of architectural distortion in prior mammograms of interval cancer." J Digit Imaging **23**(5): 611-631.

Rangayyan, R. M., S. Banik and J. E. Desautels (2013). "Detection of architectural distortion in prior mammograms via analysis of oriented patterns." J Vis Exp(78).

Rashidnasab, A., P. Elangovan, M. Yip, O. Diaz, D. R. Dance, K. C. Young and K. Wells (2013). "Simulation and assessment of realistic breast lesions using fractal growth models." Phys Med Biol **58**(16): 5613-5627.

Raya, A. and J. C. Izpisua Belmonte (2006). "Left-right asymmetry in the vertebrate embryo: from early information to higher-level integration." Nat Rev Genet **7**(4): 283-293.

Regan, J. L., H. Kendrick, F. A. Magnay, V. Vafaizadeh, B. Groner and M. J. Smalley (2012). "c-Kit is required for growth and survival of the cells of origin of Brca1-mutation-associated breast cancer." Oncogene **31**(7): 869-883.

Reichman, M. E., S. Altekruse, C. I. Li, V. W. Chen, D. Deapen, M. Potts, X. C. Wu, D. Morrell, J. Hafterson, A. I. Phipps, L. C. Harlan, L. G. Ries and B. K. Edwards (2010). "Feasibility study for collection of HER2 data by National Cancer Institute (NCI) Surveillance, Epidemiology, and End Results (SEER) Program central cancer registries." Cancer Epidemiol Biomarkers Prev **19**(1): 144-147.

Richert, M. M., K. L. Schwertfeger, J. W. Ryder and S. M. Anderson (2000). "An atlas of mouse mammary gland development." J Mammary Gland Biol Neoplasia **5**(2): 227-241.

Rios, A. C., N. Y. Fu, G. J. Lindeman and J. E. Visvader (2014). "In situ identification of bipotent stem cells in the mammary gland." Nature **506**(7488): 322-327.

Robichaux, J. P., R. M. Hallett, J. W. Fuseler, J. A. Hassell and A. F. Ramsdell (2014). "Mammary glands exhibit molecular laterality and undergo left-right asymmetric ductal epithelial growth in MMTV-cNeu mice*." Oncogene.

Rogers, J. A. and J. W. Fuseler (2007). "Regulation of NF-kappaB activation and nuclear translocation by exogenous nitric oxide (NO) donors in TNF-alpha activated vascular endothelial cells." Nitric Oxide **16**(3): 379-391.

Roychoudhuri, R., V. Putcha and H. Moller (2006). "Cancer and laterality: a study of the five major paired organs (UK)." Cancer Causes Control **17**(5): 655-662.

Roychoudhuri, R., V. Putcha and H. Møller (2006). "Cancer and Laterality: A Study of The Five Major Paired Organs (UK)." Cancer Causes and Control **17**(5): 655-662.

Ruan, W., C. B. Newman and D. L. Kleinberg (1992). "Intact and amino-terminally shortened forms of insulin-like growth factor I induce mammary gland differentiation and development." Proc Natl Acad Sci U S A **89**(22): 10872-10876.

Saez, R. A., W. L. McGuire and G. M. Clark (1989). "Prognostic factors in breast cancer." Semin Surg Oncol **5**(2): 102-110.

Sakakura, T. (1991). "New aspects of stroma-parenchyma relations in mammary gland differentiation." Int Rev Cytol **125**: 165-202.

Sakakura, T., I. Kusano, M. Kusakabe, Y. Inaguma and Y. Nishizuka (1987). "Biology of mammary fat pad in fetal mouse: capacity to support

development of various fetal epithelia in vivo." Development **100**(3): 421-430.

Sakakura, T., Y. Nishizuka and C. J. Dawe (1976). "Mesenchyme-dependent morphogenesis and epithelium-specific cytodifferentiation in mouse mammary gland." Science **194**(4272): 1439-1441.

Sakakura, T., Y. Sakagami and Y. Nishizuka (1979). "Persistence of responsiveness of adult mouse mammary gland to induction by embryonic mesenchyme." Dev Biol **72**(2): 201-210.

Sakakura, T., Y. Sakagami and Y. Nishizuka (1982). "Dual origin of mesenchymal tissues participating in mouse mammary gland embryogenesis." Dev Biol **91**(1): 202-207.

Sale, S., D. Lafkas and S. Artavanis-Tsakonas (2013). "Notch2 genetic fate mapping reveals two previously unrecognized mammary epithelial lineages." Nat Cell Biol **15**(5): 451-460.

Saleh, F. and S. Abdeen (2007). "Pathobiological features of breast tumours in the State of Kuwait: a comprehensive analysis." J Carcinog **6**: 12.

Scaltriti, M., C. Verma, M. Guzman, J. Jimenez, J. L. Parra, K. Pedersen, D. J. Smith, S. Landolfi, S. Ramon y Cajal, J. Arribas and J. Baselga (2009). "Lapatinib, a HER2 tyrosine kinase inhibitor, induces stabilization and accumulation of HER2 and potentiates trastuzumab-dependent cell cytotoxicity." Oncogene **28**(6): 803-814.

Schaefer, C. F., K. Anthony, S. Krupa, J. Buchoff, M. Day, T. Hannay and K. H. Buetow (2009). "PID: the Pathway Interaction Database." Nucleic Acids Res **37**(Database issue): D674-679.

Sebastian, L. T., L. De Matteo, G. Shaw and M. B. Renfree (1998). "Mesotocin receptors during pregnancy, parturition and lactation in the tammar wallaby." Anim Reprod Sci **51**(1): 57-74.

Sell, S. (2010). "On the stem cell origin of cancer." Am J Pathol **176**(6): 2584-2494.

Shackleton, M., F. Vaillant, K. J. Simpson, J. Stingl, G. K. Smyth, M. L. Asselin-Labat, L. Wu, G. J. Lindeman and J. E. Visvader (2006). "Generation of a functional mammary gland from a single stem cell." Nature **439**(7072): 84-88.

Shaw, F. L., H. Harrison, K. Spence, M. P. Ablett, B. M. Simoes, G. Farnie and R. B. Clarke (2012). "A detailed mammosphere assay protocol for the quantification of breast stem cell activity." J Mammary Gland Biol Neoplasia **17**(2): 111-117.

Shehata, M., A. Teschendorff, G. Sharp, N. Novcic, A. Russell, S. Avril, M. Prater, P. Eirew, C. Caldas, C. J. Watson and J. Stingl (2012). "Phenotypic and functional characterization of the luminal cell hierarchy of the mammary gland." Breast Cancer Res **14**(5): R134.

Shiratori, H. and H. Hamada (2006). "The left-right axis in the mouse: from origin to morphology." Development **133**(11): 2095-2104.

Silberstein, G. B. (2001). "Postnatal mammary gland morphogenesis." Microsc Res Tech **52**(2): 155-162.

Simoes, B. M., M. Piva, O. Iriondo, V. Comaills, J. A. Lopez-Ruiz, I. Zabalza, J. A. Mieza, O. Acinas and M. D. Vivanco (2011). "Effects of estrogen on the proportion of stem cells in the breast." Breast Cancer Res Treat **129**(1): 23-35.

Smalley, M. and A. Ashworth (2003). "Stem cells and breast cancer: A field in transit." Nat Rev Cancer **3**(11): 832-844.

Smalley, M. J. (2010). "Isolation, culture and analysis of mouse mammary epithelial cells." Methods Mol Biol **633**: 139-170.

Smalley, M. J., H. Kendrick, J. M. Sheridan, J. L. Regan, M. D. Prater, G. J. Lindeman, C. J. Watson, J. E. Visvader and J. Stingl (2012). "Isolation of mouse mammary epithelial subpopulations: a comparison of leading methods." J Mammary Gland Biol Neoplasia **17**(2): 91-97.

Smalley, M. J., I. Titley and A. Ashworth (2005). "An improved definition of mouse mammary epithelial side population cells." Cytotherapy **7**(6): 497-508.

Smith, T. G., Jr., G. D. Lange and W. B. Marks (1996). "Fractal methods and results in cellular morphology--dimensions, lacunarity and multifractals." J Neurosci Methods **69**(2): 123-136.

Sopel, M. (2010). "The myoepithelial cell: its role in normal mammary glands and breast cancer." Folia Morphol (Warsz) **69**(1): 1-14.

Sotiriou, C. and L. Pusztai (2009). "Gene-expression signatures in breast cancer." N Engl J Med **360**(8): 790-800.

Spike, B. T., D. D. Engle, J. C. Lin, S. K. Cheung, J. La and G. M. Wahl (2012). "A mammary stem cell population identified and characterized in late

embryogenesis reveals similarities to human breast cancer." Cell Stem Cell **10**(2): 183-197.

Stalsberg, H. (1969). "The origin of heart asymmetry: right and left contributions to the early chick embryo heart." Dev Biol **19**(2): 109-127.

Sternlicht, M. D. (2006). "Key stages in mammary gland development: the cues that regulate ductal branching morphogenesis." Breast Cancer Res **8**(1): 201.

Sternlicht, M. D., H. Kouros-Mehr, P. Lu and Z. Werb (2006). "Hormonal and local control of mammary branching morphogenesis." Differentiation **74**(7): 365-381.

Stingl, J., P. Eirew, I. Ricketson, M. Shackleton, F. Vaillant, D. Choi, H. I. Li and C. J. Eaves (2006). "Purification and unique properties of mammary epithelial stem cells." Nature **439**(7079): 993-997.

Stull, M. A., M. M. Richert, A. V. Loladze and T. L. Wood (2002). "Requirement for IGF-I in epidermal growth factor-mediated cell cycle progression of mammary epithelial cells." Endocrinology **143**(5): 1872-1879.

Stull, M. A., A. M. Rowzee, A. V. Loladze and T. L. Wood (2004). "Growth factor regulation of cell cycle progression in mammary epithelial cells." J Mammary Gland Biol Neoplasia **9**(1): 15-26.

Su, D., S. M. Smith, M. Preti, P. Schwartz, T. J. Rutherford, G. Menato, S. Danese, S. Ma, H. Yu and D. Katsaros (2009). "Stathmin and tubulin expression and survival of ovarian cancer patients receiving platinum treatment with and without paclitaxel." Cancer **115**(11): 2453-2463.

Sucov, H. M., E. Dyson, C. L. Gumeringer, J. Price, K. R. Chien and R. M. Evans (1994). "RXR alpha mutant mice establish a genetic basis for vitamin A signaling in heart morphogenesis." Genes Dev **8**(9): 1007-1018.

Sullivan, A. C., J. P. Hunt and A. L. Oldenburg (2011). "Fractal analysis for classification of breast carcinoma in optical coherence tomography." J Biomed Opt **16**(6): 066010.

Tambasco, M., M. Eliasziw and A. M. Magliocco (2010). "Morphologic complexity of epithelial architecture for predicting invasive breast cancer survival." J Transl Med **8**: 140.

Tambasco, M. and A. M. Magliocco (2008). "Relationship between tumor grade and computed architectural complexity in breast cancer specimens." Hum Pathol **39**(5): 740-746.

Teh, M. T. (2012). "FOXM1 coming of age: time for translation into clinical benefits?" Front Oncol **2**: 146.

Troyer, K. L. and D. C. Lee (2001). "Regulation of mouse mammary gland development and tumorigenesis by the ERBB signaling network." J Mammary Gland Biol Neoplasia **6**(1): 7-21.

U.S. Food and Drug Administration (2012). "Tykerb (lapatinib) Prescribing Information February 2012."

Veltmaat, J. M., A. A. Mailleux, J. P. Thiery and S. Bellusci (2003). "Mouse embryonic mammogenesis as a model for the molecular regulation of pattern formation." Differentiation **71**(1): 1-17.

Veltmaat, J. M., A. F. Ramsdell and E. Sterneck (2013). "Positional variations in mammary gland development and cancer." J Mammary Gland Biol Neoplasia **18**(2): 179-188.

Veltmaat, J. M., F. Relaix, L. T. Le, K. Kratochwil, F. G. Sala, W. van Veelen, R. Rice, B. Spencer-Dene, A. A. Mailleux, D. P. Rice, J. P. Thiery and S. Bellusci (2006). "Gli3-mediated somitic Fgf10 expression gradients are required for the induction and patterning of mammary epithelium along the embryonic axes." Development **133**(12): 2325-2335.

Veltmaat, J. M., W. Van Veelen, J. P. Thiery and S. Bellusci (2004). "Identification of the mammary line in mouse by Wnt10b expression." Dev Dyn **229**(2): 349-356.

Vermot, J., J. Gallego Llamas, V. Fraulob, K. Niederreither, P. Chambon and P. Dolle (2005). "Retinoic acid controls the bilateral symmetry of somite formation in the mouse embryo." Science **308**(5721): 563-566.

Vilhais-Neto, G. C., M. Maruhashi, K. T. Smith, M. Vasseur-Cognet, A. S. Peterson, J. L. Workman and O. Pourquie (2010). "Rere controls retinoic acid signalling and somite bilateral symmetry." Nature **463**(7283): 953-957.

Visvader, J. E. (2009). "Keeping abreast of the mammary epithelial hierarchy and breast tumorigenesis." Genes Dev **23**(22): 2563-2577.

Visvader, J. E. (2011). "Cells of origin in cancer." Nature **469**(7330): 314-322.

Visvader, J. E. and G. H. Smith (2011). "Murine mammary epithelial stem cells: discovery, function, and current status." Cold Spring Harb Perspect Biol **3**(2).

Visvader, J. E. and J. Stingl (2014). "Mammary stem cells and the differentiation hierarchy: current status and perspectives." Genes Dev **28**(11): 1143-1158.

Wadia, P. R., L. N. Vandenberg, C. M. Schaeberle, B. S. Rubin, C. Sonnenschein and A. M. Soto (2007). "Perinatal bisphenol A exposure increases estrogen sensitivity of the mammary gland in diverse mouse strains." Environ Health Perspect **115**(4): 592-598.

Walker, B. E. (1984). "Tumors of female offspring of mice exposed prenatally to diethylstilbestrol." J Natl Cancer Inst **73**(1): 133-140.

Walker, B. E. (1990). "Tumors in female offspring of control and diethylstilbestrol-exposed mice fed high-fat diets." J Natl Cancer Inst **82**(1): 50-54.

Walter, J., R. J. and M. W. Berns (1986). Digital Image Processing and Analysis. Video Microscopy. S. Inoue. New York and London, Plenum Press**:** 327-392.

Wang, Y., J. G. Klijn, Y. Zhang, A. M. Sieuwerts, M. P. Look, F. Yang, D. Talantov, M. Timmermans, M. E. Meijer-van Gelder, J. Yu, T. Jatkoe, E. M. Berns, D. Atkins and J. A. Foekens (2005). "Gene-expression profiles to predict distant metastasis of lymph-node-negative primary breast cancer." Lancet **365**(9460): 671-679.

Wang, Y. A., K. Shen, Y. Wang and S. C. Brooks (2005). "Retinoic acid signaling is required for proper morphogenesis of mammary gland." Dev Dyn **234**(4): 892-899.

Wang, Z., Y. Li, A. Ahmad, A. S. Azmi, S. Banerjee, D. Kong and F. H. Sarkar (2010). "Targeting Notch signaling pathway to overcome drug resistance for cancer therapy." Biochim Biophys Acta **1806**(2): 258-267.

Warner, M. R. (1976). "Effect of various doses of estrogen to BALB/cCrgl neonatal female mice on mammary growth and branching at 5 weeks of age." Cell Tissue Kinet **9**(5): 429-438.

Warner, M. R. and R. L. Warner (1975). "Effects of age at carcinogen administration and exposure as neonates to 17beta-estradiol on subsequent gland-pair distribution of murine mammary dysplasias." J Natl Cancer Inst **54**(6): 1369-1372.

Warner, M. R., L. Yau and J. M. Rosen (1980). "Long term effects of perinatal injection of estrogen and progesterone on the morphological and biochemical development of the mammary gland." Endocrinology **106**(3): 823-832.

Watson, C. J. (2006). "Involution: apoptosis and tissue remodelling that convert the mammary gland from milk factory to a quiescent organ." Breast Cancer Res **8**(2): 203.

Watson, C. J. and W. T. Khaled (2008). "Mammary development in the embryo and adult: a journey of morphogenesis and commitment." Development **135**(6): 995-1003.

Weiss, H. A., S. S. Devesa and L. A. Brinton (1996). "Laterality of breast cancer in the United States." Cancer Causes Control **7**(5): 539-543.

Wilting, J. and M. Hagedorn (2011). "Left-right asymmetry in embryonic development and breast cancer: common molecular determinants?" Curr Med Chem **18**(36): 5519-5527.

Wood, E. R., A. T. Truesdale, O. B. McDonald, D. Yuan, A. Hassell, S. H. Dickerson, B. Ellis, C. Pennisi, E. Horne, K. Lackey, K. J. Alligood, D. W. Rusnak, T. M. Gilmer and L. Shewchuk (2004). "A unique structure for epidermal growth factor receptor bound to GW572016 (Lapatinib): relationships among protein conformation, inhibitor off-rate, and receptor activity in tumor cells." Cancer Res **64**(18): 6652-6659.

Yokoyama, T., N. G. Copeland, N. A. Jenkins, C. A. Montgomery, F. F. Elder and P. A. Overbeek (1993). "Reversal of left-right asymmetry: a situs inversus mutation." Science **260**(5108): 679-682.

Yoruk, O., M. Karasen, H. Timur, T. Erdem, S. Dane and U. Tan (2009). "Lateralizations of head-neck cancers are not associated with peripheral asymmetry of cell-mediated immunity." Int J Neurosci **119**(6): 815-820.

Zeeneldin, A. A., M. Ramadan, N. Elmashad, I. Fakhr, A. Diaa and E. Mosaad (2013). "Breast cancer laterality among Egyptian patients and its association with treatments and survival." J Egypt Natl Canc Inst **25**(4): 199-207.

Zeps, N., J. M. Bentel, J. M. Papadimitriou and H. J. Dawkins (1999). "Murine progesterone receptor expression in proliferating mammary epithelial cells during normal pubertal development and adult estrous cycle. Association with eralpha and erbeta status." J Histochem Cytochem **47**(10): 1323-1330.

Zeps, N., H. J. Dawkins, J. M. Papadimitriou, S. L. Redmond and M. I. Walters (1996). "Detection of a population of long-lived cells in mammary epithelium of the mouse." Cell Tissue Res **286**(3): 525-536.

Zhang, D., A. Pal, W. G. Bornmann, F. Yamasaki, F. J. Esteva, G. N. Hortobagyi, C. Bartholomeusz and N. T. Ueno (2008). "Activity of lapatinib is independent of EGFR expression level in HER2-overexpressing breast cancer cells." Mol Cancer Ther **7**(7): 1846-1850.

Zhao, S. and R. D. Fernald (2005). "Comprehensive algorithm for quantitative real-time polymerase chain reaction." J Comput Biol **12**(8): 1047-1064.

Zhao, X., G. K. Malhotra, H. Band and V. Band (2012). "Derivation of myoepithelial progenitor cells from bipotent mammary stem/progenitor cells." PLoS One **7**(4): e35338.

Zvelebil, M., E. Oliemuller, Q. Gao, O. Wansbury, A. Mackay, H. Kendrick, M. J. Smalley, J. S. Reis-Filho and B. A. Howard (2013). "Embryonic mammary signature subsets are activated in Brca1-/- and basal-like breast cancers." Breast Cancer Res **15**(2): R25.

BIOGRAPHY

Jacqulyne Robichaux earned her Bachelor of Science degree in Chemistry with a minor in mathematics from Nicholls State University in Thibodaux, Louisiana in 2010. She joined the doctoral program in biomedical science at the Medical University of South Carolina in 2010. Jacqulyne was a recipient of the dissertation scholarship award from the Southern Regional Education Board in 2014 and placed second at Perry Haluska Student research day for an oral PhD presentation in 2013. In addition, Jacqulyne has presented at a national Gordon Conference on mammary gland biology and published in *Oncogene* as well as *AntiCancer Research.* Jacqulyne's dissertation was supervised by Dr. Ann Ramsdell.